LATVIJAS UNIVERSITĀTE
ATOMFIZIKAS UN SPEKTROSKOPIJAS INSTITŪTS

Vanesa Lukinsone
(Inesa Feruļova)

IN VIVO ĀDAS AUTOFLUORESCENCES KINĒTIKA NEPĀRTRAUKTĀ UN IMPULSVEIDA LĀZERU IEROSMĒ

PROMOCIJAS DARBS

Doktora grāda iegūšanai fizikas nozarē
Apakšnozare: medicīniskā fizika

Rīga, 2017

Promocijas darbs izstrādāts Latvijas Universitātes Atomfizikas un spektroskopijas institūtā laika posmā no 2011. gada līdz 2016. gadam ar vairāku Latvijas un starptautisku projektu atbalstu.

Darbs sastāv no 5 nodaļām un literatūras saraksta.
Darba forma: disertācija.

Darba zinātniskais vadītājs: profesors *Dr. habil. phys.* **Jānis Spīgulis**

Darba recenzenti:

1. *Dr. habil. phys.* Ruvins Ferbers
2. *Dr. phys.* Aleksejs Kataševs
3. *Dr. rer. nat. Dr.-Ing. habil.* Jürgen Lademann

Promocijas darba aizstāvēšana notiks Latvijas Universitātes Fizikas, astronomijas un mehānikas zinātnes nozares specializētās promocijas padomes atklātajā sēdē 2017. gada 12. decembrī plkst 15.00 Rīgā, Zeļļu ielā 23, 213 auditorijā.

Ar promocijas darbu un tā kopsavilkumu var iepazīties Latvijas Universitātes Fizikas un matemātikas fakultātes bibliotēkā (Zeļļu ielā 23, Rīgā).

Promocijas padomes priekšsēdētājs: profesors *Dr. habil. phys.* **Ruvins Ferbers**

Promocijas padomes sekretāre: **Laureta Buševica**

ISBN 978-9934-18-283-9

ANOTĀCIJA

Darbā izstrādātas un eksperimentāli/klīniski aprobētas divas mērījumu iekārtas pigmentētu ādas jaunveidojumu fluorescentai diagnostikai un četras iekārtas autofluorescences (AF) fotoizbalēšanas ietekmes pētīšanai uz cilvēka ādas spektrālajiem parametriem, izmantojot nepārtrauktu un impulsveida lāzeru ierosmi.

Mērījumu iekārtas ar nepārtrauktu 532 nm ierosmi ādas pigmentēto jaunveidojumu punktveida mērījumiem un ar 405 nm ierosmi attēlošanas mērījumiem ir klīniski aprobētas uz vairāk kā 50 pacientiem. Piedāvāts jauns diagnostiskais kritērijs, kas ļauj atšķirt bazālo šūnu karcinomas jaunveidojumus no citām ādas patoloģijām.

Ādas AF mērījumi 405 nm un 470 nm lāzeru pikosekunžu impulsu ierosmē veikti ar $\sim 10^{-10}$s laika izšķirtspēju. AF kinētikas pētījumi apliecina fotoizbalēšanas ietekmi uz ādas fluorescences dzišanas laika komponentēm – pirmā no tām (τ_1) praktiski nemainās, otrā (τ_2) pieaug un trešā (τ_3) samazinās. Savukārt intradermālajos nēvusos novērota gan τ_2, gan τ_3 samazināšanās. Analīzes rezultātā secināts, ka fotoizbalēšanas procesam vairāk pakļauti nikotīnamīda adenīnedinukleotīda NAD(P)H fluorofori. Atrasta korelācija starp ādas un intradermāla nēvusa AF fotoizbalēšanas ātrumu un dzīves laika τ_1, τ_2, τ_3 komponenšu izmaiņām, ko iespējams pielietot klīniskajā diagnostikā.

Difūzās atstarošanas spektru kontakta un bezkontakta mērījumi apstiprina ādas oksihemoglobīna koncentrācijas pieaugumu fotoizbalēšanas procesā. Tas norāda uz iespējamu ādas iekaisumu zemas jaudas lāzerstarojuma ietekmē.

Atslēgvārdi: autofluorescences fotoizbalēšana, fluorescences dzīves laiks, difūza atstarošana, āda.

ABSTRACT

Two measuring devices for pigmented skin neoplasms diagnosis by fluorescence were developed and experimentally/clinically approbated and four devices for research of an autofluorescence (AF) photobleaching effect on spectral parameters of human skin using a continuous and pulsed laser excitation.

Measuring devices with continuous excitation of 532 nm for spot measurements of skin pigmented neoplasms, and 405 nm for imaging measurements have been clinically approbated on more than 50 patients. New diagnostic criterion that allows distinguishing basal cell carcinomas from other skin neoplasms has been proposed.

The skin AF measurements at the 405 nm and 470 nm picosecond pulse laser excitation were performed with time resolution $\sim 10^{-10}$ (s). AF kinetics studies confirm the influence of photobleaching on components of the skin autofluorescence decay time, the first of them τ_1 practically does not change, the second (τ_2) increases and the third (τ_3) decreases. On the other hand, the decrease of both τ_2 and τ_3 was observed in intradermal nevi. The results of the analysis show that the photobleaching process is more susceptible to nicotinamide adenine nucleotide NAD(P)H fluorophors. The correlation between skin and intradermal nevus in AF photobleaching speed and changes of lifetime components τ_1, τ_2, τ_3 was found, that can be used in clinical diagnosis.

Contact and contactless measurements of the diffuse reflectance spectra confirm the increase of skin oxyhemoglobin concentration during the photobleaching process. This indicates a possible inflammation of the skin due to the low-power laser radiation.

Keywords: autofluorescence photobleaching, fluorescences lifetime, diffuse reflectance, skin.

SAĪSINĀJUMI

AF – autofluorescence

BCC – pigmentēta bazālo šūnu karcinoma jeb bazalioma

FAD/$FADH_2$ – flavīna adenīna dinukleotīda oksidētā/reducētā forma (flavin adenine dinucleotide)

NADH/NAD^+ – nikotīnamīda adenīndinukleotīda reducētā/oksidētā forma (nicotinamide adenine dinucleotide)

NAD(P)H/$NAD(P)^+$ – nikotīnamīda adenīndinukleotīda fosfāta reducētā/oksidētā forma (nicotinamide adenine dinucleotide phosphate)

$\mathbf{N_G}$ – AF fotoizbalēšanas kinētikas parametrs, kur N – normēts parametrs un G – G (green (zaļais)) kanāls RGB kamerā

Oks – oksidēšana

Red – reducēšana

Redoks – oksidēšanās–reducēšanās ķīmiskās reakcijas

SPCImage – fluorescences kinētikas apstrādes programma no Backer&Hickl

$\boldsymbol{\tau_1}$ – dzīves laika 1. komponente / AF fotoizbalēšanas kinētikas ātrā komponente

$\boldsymbol{\tau_2}$ – dzīves laika 2. komponente / AF fotoizbalēšanas kinētikas lēnā komponente

$\boldsymbol{\tau_3}$ – dzīves laika 3. komponente

TCSPC – laikā korelēta atsevišķu fotonu skaitīšana (time-correlated single photon counting)

TRES – emisijas spektrs ar laika izšķirtspēju (time resolved emission spectra)

SATURA RĀDĪTĀJS

IEVADS

Āda ir viens no svarīgākajiem cilvēka orgāniem [1], un ādas patoloģiju savlaicīgai un precīzai diagnostikai ir liela nozīme veselības aprūpē. Lai dermatologu vizuālo, uz pieredzi balstīto patoloģiju novērtējumu papildinātu ar kvantitatīviem un objektīvi izmērāmiem kritērijiem, tiek attīstītas dažādas optiskās diagnostikas metodes, starp kurām nozīmīgu vietu ieņem ādas fluorescentā diagnostika [2]. Metodes pamatā ir ādas virskārtā esošo biomolekulu optiska ierosme (piemēram, ar lāzeru starojumu), kuras rezultātā šīs molekulas – t.s. ādas fluorofori – emitē tām raksturīgo fluorescento starojumu. Šī starojuma spektrāla un cita veida analīze sniedz papildus informāciju par ādas jaunveidojumu struktūru un potenciālo ļaundabību.

Pigmentētais nēvuss ir izplatītākais ādas jaunveidojums, kas var būt iedzimts vai arī veidoties dzīves laikā. Starp pigmentētiem jaunveidojumiem, kas veidojas dzīves laikā, var rasties ļaundabīgie veidojumi – tādi kā melanoma, bazālo šūnu karcinoma un plakanšūnu karcinoma. Agrīnā stadijā tie izskatās līdzīgi labdabīgiem pigmentētiem jaunveidojumiem, un ļaundabīgo veidojumu noteikšanai medicīnas praksē izmanto biopsiju – patoloģijas parauga izkniebšanu no ādas ar sekojošu histoloģisko analīzi, kas ir invazīva un metastazēšanās risku palielinoša metode. Tādēļ ir svarīgi izstrādāt neinvazīvas diagnostiskas metodes un ierīces, kas būtu ērti un viegli pielietojamas klīniskajā praksē. Ādas optiskajā diagnostikā noderīgas ir metodes, kas balstītas uz fluorescences spektrālo un intensitātes parametru noteikšanu [3–8].

Problēmu rada tas, ka dzīvas ādas flurescencei piemīt t.s. fotoizbalēšanas īpašība – emisijas spektru intensitāte pie nemainīgas ierosmes jaudas pakāpeniski samazinās. Šī parādība ir pētīta vairāku autoru darbos [9–13] un ir noskaidrots, ka ādas autofluorescences (AF) intensitāte un fotoizbalēšanas ātrums dažādiem jaunveidojumiem atšķiras [10]. AF fotoizbalēšana ir novērota kā pie stacionāras, tā arī pie impulsveida optiskās ierosmes [10, 14], bet bieži netiek ņemta vērā, kas var radīt kļūdas mērījumos un pat novest pie neprecīzas diagnozes.

AF fotoizbalēšanas mehānisms pagaidām nav pietiekoši izpētīts – nav zināms, kādi ādas fluorofori un hromofori piedalās fotoizbalēšanas procesā pie dažādiem ierosmes viļņu garumiem un kāpēc dažādiem jaunveidojumiem fotoizbalēšanas ātrumi atšķiras [4, 10]. Nav pietiekoši labi izpētīts, kādus procesus ādā izraisa lāzara apstarošana un kāda ir tās ietekme uz fluoroforiem.Līdz šim nav veikti kompleksi in-vivo ādas AF pētījumi ar laika izšķirtspēju gan stacionārā, gan impulsu ierosmē, kas varētu sniegt plašāku informāciju par autofluorescences fotoizbalēšanas ietekmi gan uz veselu ādu, gan uz ādas jaunveidojumiem.

Darba mērķis – izpētīt ādas un jaunveidojumu *in vivo* autofluorescences kinētiku nepārtrauktā un impulsveida lāzeru ierosmē, lai noskaidrotu kinētisko parametru izmantošanas iespējas ādas diagnostikā.

Darba uzdevumi:

1. Izstrādāt metodiku un mēriekārtas ādas autofluorescences emisijas un fotoizbalēšanas kinētikas pētīšanai.
2. Noteikt ādas un jaunveidojumu autofluorescences kinētiskos parametrus un to izmaiņas fotoizbalēšanas ietekmē.
3. Iegūt autofluorescences dzīves laiku un fotoizbalēšanas ātrumu sadalījuma attēlus no iepriekš neapstarotiem un apstarotiem cilvēka ādas apgabaliem. Noskaidrot, vai pastāv korelācija starp ādas autofluorescences dzīves laiku un fotoizbalēšanas ātrumu.
4. Izpētīt ādas difūzās atstarošanas spektrālās izmaiņas atkarībā no lāzera apstarošanas viļņu garuma un jaudas blīvuma.
5. Sniegt secinājumus par kinētisko parametru izmantošanas iespējām ādas jaunveidojumu diagnostikā.

Darba novitāte:

- Pirmo reizi piedāvāta AF kinētikas parametru kartēšana pigmentētu jaunveidojumu diagnostikai, izmantojot RGB viedtālruņa kameru ar izstrādāto papildierīci AF ierosmei.
- Pirmo reizi pētīta fotoizbalēšanas ietekme uz ādas un pigmentēta jaunveidojuma AF spektrāliem parametriem, izmantojot spektroskopiju ar laika izšķirtspēju. Atrasta korelācija starp ādas un intradermāla nēvusa AF kinētiskiem parametriem.
- Pirmo reizi eksperimentāli pierādīts, ka AF fotoizbalēšanas procesā pieaug oksihemoglobīna koncentrācija ādā.

Promocijas darba struktūra

Promocijas darbs sastāv no 5 nodaļām, kuras ir iekļautas 2 tabulas, 43 attēli un izmantoti 102 literatūras avoti. Darba kopējais apjoms ir 135 lappuses, no kurām pielikums (deviņas publikācijas) ir 60 lappuses.

1. nodaļā aprakstīta ādas uzbūve un optiskās īpašības.
2. nodaļā sniegts pārskats par ādas AF fotoizbalēšanas pētījumiem citu valstu laboratorijās un aprakstītas ierīces ādas jaunveidojumu diagnostikai ar AF fotoizbalēšanas metodēm.

3. nodaļā sniegts pārskats par ādas fluoroforu pētījumiem citu valstu laboratorijās un aprakstīti ādas autofluorescences dzīves laiku pētījumi un AF fotoizbalēšanas ietekme uz ādu.
4. nodaļā sniegts pārskats par ādas optisko īpašību pētījumiem. Aprakstīta lāzera apstarošanas ietekme uz oksihemoglobīna koncentrāciju ādā. Fotona lidojuma laiks caur ādu un nēvusu atkarība no viļņa garuma.
5. nodaļā sniegts rezultātu kopsavilkums, apkopoti secinājumi un formulētas aizstāvamās tēzes.

1. CILVĒKA ĀDAS UZBŪVE UN OPTISKĀS ĪPAŠĪBAS

1.1. Ādas uzbūve

Āda ir ķermeņa daudzfunkcionāls ārējais apvalks, kas pasargā dziļāk gulošos audus no ārējiem kaitīgiem faktoriem. Tajā atrodas matu saknes, tauku un sviedru dziedzeri, ādā var deponēties līdz litram asiņu. Āda piedalās vielmaiņā, ūdens, vitamīnu un sāļu maiņā, termoregulācijas procesos. Caur ādu kopā ar ūdeni izdalās hlorīdu, pienskābes, slāpekli saturošas vielas [1].

Šķērsgriezumā āda sastāv no trim pamatslāņiem (1.1. attēls):

- epidermas (biezums: 0,05–1,50 mm),
- dermas (biezums: 0,5–5,0 mm),
- hipodermas (biezums: 1–6 mm, atkarībā no lokācijas vietas).

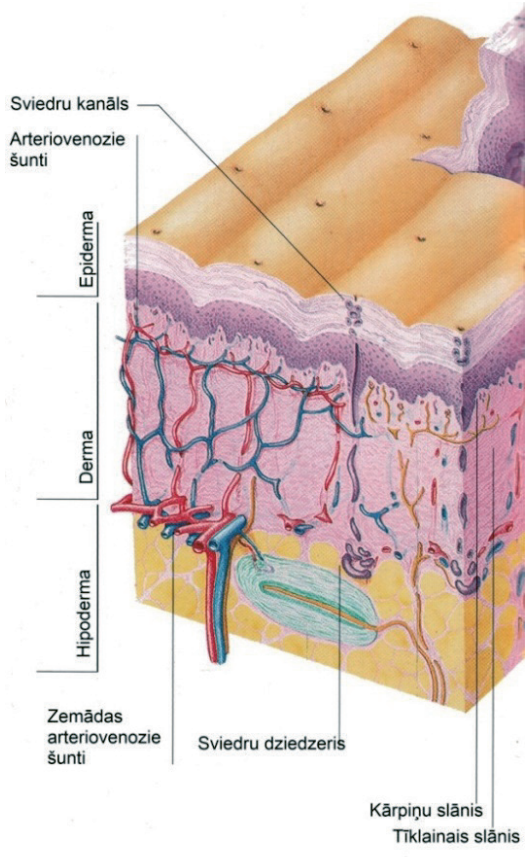

1.1. att. Ādas uzbūve [15].

Epidermā galvenās šūnas ir keratinocīti, kas ražo keratīna olbaltumvielas. Epiderma sadalās četros slāņos (1.2. attēls, [15]):

1) Raga slānis (*stratum corneum*) – šūnās ir ragvielas (keratīns un gaisa pūslīši), tās pastāvīgi atdalās un nomainās ar jaunām šūnām, kuras nāk no dziļākiem slāņiem. Raga slānis ir pēdējais nobriešanas posms keratinocītiem. Tas sastāv no poligonālām lokšņu šūnām bez kodola. Uz pēdām un plaukstām šūnu kārta ir biezāka, salīdzinot ar citām ķermeņa vietām. Šūnas kopā satur lipīdu līme, kas rodas granulu membrānu pārklājumā. Raga slānis ir elastīgs un var absorbēt ūdeni trīs reizes vairāk par savu svaru, bet, kad izžūst, lokanība un elastība pazūd [1, 15].
2) Graudainais slānis (*stratum granulosum*) – šūnas kļūst plakanas, veido 3–4 šūnu kārtas. Dotajā slānī enzīmi izraisa kodola un organoīdu degradāciju. Šūnu citoplazmā ir bazofilās granulas – keratohialīna graudiņi, kas var pilnīgi pārklāt kodolu [1, 15].
3) Dzeloņainais slānis (*stratum spinosum*) – sastāv no atdalītām keratinocīta šūnām, kuras tur nonāk no bazālā slāņa, migrējot uz augšējo slāni pa poligonālām šūnu kārtām, kuras saista desmosomas un notur šūnas 20 nm attālumā. Langerhansa šūnas, kas ir cieši saistītas ar imūnsistēmu, pārsvarā atrodas šajā slānī. Dzeloņainajā slānī šūnas var mitotiski dalīties (augt) [1, 15].
4) Bazālais slānis (*stratum basale*) – galvenokārt sastāv no keratinocītiem, kuri mitotiski dalās, to pamatfunkcija ir sintezēt pretmikrobu peptīdus un nodrošināt pretbaktēriju aizsardzību. Melanocītu šūnas bazālajā slānī ir 5–10%, to pamatfunkcija ir sintezēt melanīnu; melanīna absorbcijas spektrs parādīts 1.12. attēlā.

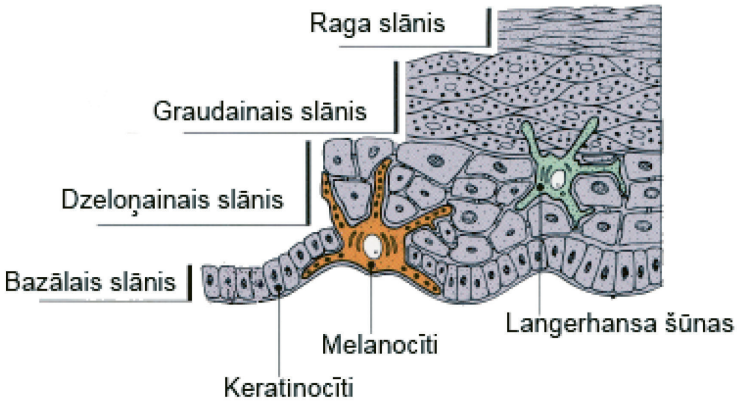

1.2. att. Epidermas uzbūve [15].

Derma sastāv no diviem slāņiem [1, 15]:

1) Kārpiņu slānis – irdeni nenoformēti saistaudi, tajos atrodas daudz šūnu un kapilāru;
2) Tīklainais slānis – blīvi nenoformēti saistaudi, tajos ir kolagēna šķiedras, matu saknes, sviedru un tauku dziedzeri.

Hipoderma – saistaudos ir daudz taukšūnu, kas ir organisma tauku depo un nodrošina organisma siltuma regulāciju [1].

1.2. Ādas asinsrite

Uz dermas un hipodermas robežas atrodas dziļais ādas arteriālo asinsvadu tīkls. Tā atzari baro matu folikulus un taukšūnas, sviedru un tauku dziedzerus. No šī tīkla artērijas iet caur dermu un uz robežas ar kārpiņu slāni sadalās arteriolās, kas veido virspusējo ādas arteriālo asinsvadu tīklu. No šī tīkla sākas atzarojumi, kas veido kapilāru tīklu kārpiņu slānī. Pēc kapilāriem sākas vēnulas, arī tās veido dziļo un virspusējo tīklus [1].

1.3. Pigmentēti ādas jaunveidojumi jeb nēvusi

Dzimumzīme (jeb nēvuss kā medicīniskais nosaukums) ir visbiežāk sastopamais labdabīgais jaunveidojums. Nēvusi var būt gan iedzimti, gan veidojušies dzīves laikā. Visbiežāk sastopamo nēvusu sastāvā ir palielināta labdabīgo melanocītu šūnu koncentrācija (1.1. tabula). Iemesli nēvusu attīstībai joprojām nav zināmi, daudzās ģimenēs tā ir iedzimta īpašība. Uzskata, ka melanocītu nēvusi rodas no melanocītu šūnām, kas migrē uz epidermu no nervu cekula embrionālās attīstības laikā.

1.1. tabula. Klīniska nēvusa klasifikācija [15].

Grupa	Nosaukums	Apraksts
Melanocītu	Iedzimtie nēvusi (Congenital)	Parādās uzreiz pēc piedzimšanas. Parasti izmērs ir lielāks par 10 mm, krāsa mainās no gaiši brūnas līdz melnai. Biežāk izliekti, ar augošiem matiem. Pastāv neliels risks (līdz 5%), ka attīstīsies ļaundabīga melanoma.
	Robežnēvusi (Junction)	Izskatās kā plankumi, izmērs līdz 10 mm, krāsa no gaišas līdz tumši brūnai. Pēc formas ovāli vai apaļi (1.3. attēls).
	Intradermālie nēvusi (Intradermal)	Pēc izskata izliekti, var būt ādas krāsā vai pigmentēti (1.3. attēls).
	Kombinētie nēvusi (Compound)	Biežāk pēc izmēra mazāki par 10 mm, ar gludu virsmu un dažādu pigmentāciju (1.3. attēls).
	Špica nēvusi (Spitz)	Cieti, sarkanbrūni noapaļoti mezgliņi. Sākotnējā izaugsme var būt strauja. Histoloģiski – proliferatīvās nēvusu šūnas un paplašinātie dermālie kapilāri.
	Halo nēvusi (Halo)	Oreola veida nēvusi. Apkārt nēvusam ir baltas krāsas oreols, kas izveidojas antimelanocītu autoimūnā uzbrukuma dēļ, kura rezultātā tiek iznīcinātas nēvusa šūnas.
	Displastiskie nēvusi	Mēdz būt ar nepastāvīgu formu un krāsu.
Epidermālie	Kārpveidīgie nēvusi (Warty neavus)	Pigmentētie, bieži lineārie. Pārsvarā mazi, dažreiz mēdz būt plaši. Šos nēvusus izgriež, ja jaunveidojums atrodas uz galvas, jo tie var pārvērties par ļaundabīgo jaunveidojumu.

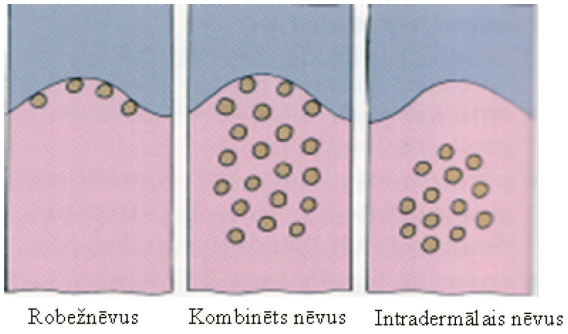

1.3. att. Melanocītu nēvusu veidi. Vieta, kur izvietojas melanocītu nēvusa šūnas, nosaka tā veidu: šūnas izvietotas uz dermas-epidermas robežas – robežnēvuss; dermā – intradermālais nēvuss; abos slāņos – kombinētais nēvuss [15].

1.4. Pigmentēto bazālo šūnu karcinoma jeb bazalioma (BCC)

Bazalioma ir visizplatītākais ļaundabīgais jaunveidojums. Tā rodas ādā no epidermas bazālā slāņa šūnām, tām pārvietojoties uz dermu un hipodermu (1.4. attēls). Bazalioma var sākt veidoties:

- UVB (290–320 nm) starojuma ietekmē, kas rada mutācijas gēnos.
- Rentgena un jonizējoša starojuma ietekmē.
- Ģenētiskas iedzimtības dēļ (bazālā nēvusa sindroms).

Klīniski bazaliomas iedala: čūlojošā, nodulārā, virspusējā, sklerozējošā un pigmentētā karcinoma. Bazalioma ir lēni augošs, agresīvs, ļaundabīgs jaunveidojums bez metastāzēm [16–18].

1.5. Plakanšūnu karcinoma

Plakanšūnu karcinoma ir ļaundabīgs jaunveidojums, kas rodas ādā no keratinocītiem, parasti pēc saules apdeguma (1.4. attēls). Veido metastāzes. Iemesli plakanšūnu veidošanai:

- Hroniski fotoķīmiski bojājumi, kas rodas saules starojuma ietekmē un uzkrājas visā dzīves garumā.
- Rentgena un jonizējoša starojuma ietekmē.
- Termiski apdegumi.
- Smēķēšana (parādās uz lūpam).
- Rūpnieciski kancerogēnie izmeši.
- Ģenētiski mantota patoloģija [15, 19, 20].

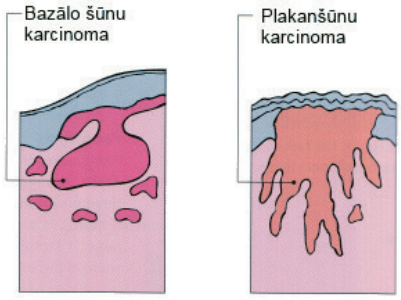

1.4. att. Bazālo šūnu un plakanšūnu karcinoma [15].

1.6. Melanoma

Melanoma ir ļaundabīgs jaunveidojums, kas attīstās divos virzienos – horizontāli un vertikāli. Sākuma stadijā epidermā izplešas horizontāli, pārejot dermā, sāk augt vertikāli un veidot metastāzes. Sākuma stadijā, kad jaunveidojums attīstās tikai epidermā, tas neveido metastāzes (1.5. attēls). Melanomas rašanas iemesli nav zināmi, viens pieņēmums ir, ka tās rodas īslaicīga, bet intensīva UV starojuma ietekmē. 30% melanomu izmeklēšanas gadījumos tika konstatēts, ka tā attīstījās melanocītu nēvusa vietā.

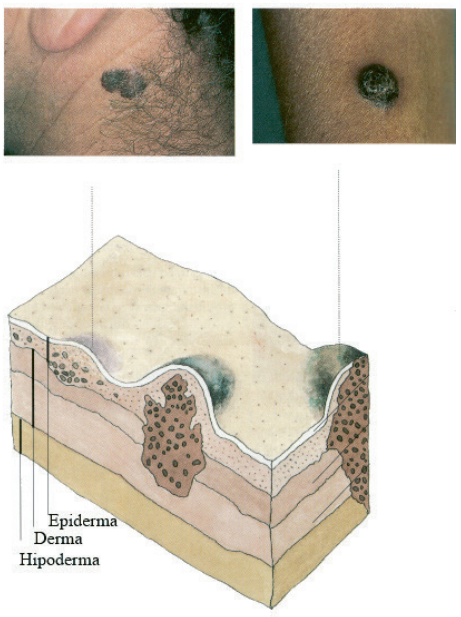

1.5. att. Melanomas vertikāla attīstība [15].

Melanomas klasifikācijai izmanto *Klarka* (1.6. attēls) un *Breslova* (1.7. attēls) *klasifikācijas metodi.* Klarka klasifikācijas metode pamatojas uz jaunveidojuma dziļumu anatomiskajos līmeņos:

I līmenis – jaunveidojums ir sākuma stadijā, attīstās epidermā;
II līmenis – jaunveidojums iespiežas papillārajā dermas slānī;
III līmenis – jaunveidojums aizņem visu papillāro dermas slāni;
IV līmenis – jaunveidojums iespiežas retikulārajā dermas slānī;
V līmenis – jaunveidojums iespiežas zemādā.

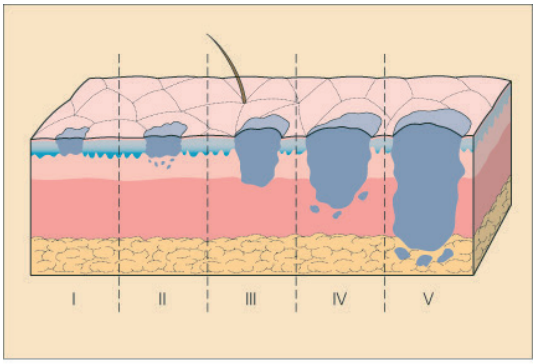

Rigel et al: Cancer of the Skin © 2005 Elsevier Inc.

1.6. att. Klarka klasifikācija [19].

Breslova klasifikācijas metode pamatojas uz metrisko dziļumu, ko mēra no graudainā epidermas šūnu slāņa līdz dziļākai melanomas šūnai [15, 19, 20].

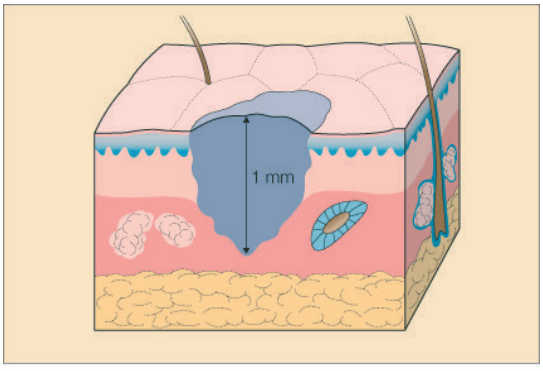

Rigel et al: Cancer of the Skin © 2005 Elsevier Inc.

1.7. att. Breslova klasifikācija [19].

1.7. Optiskā starojuma mijiedarbība ar ādu

Lāzera starojums, kā arī nekoherenta gaisma var absorbēties, reflektēt, izkliedzdēties un/vai reemitēt (audu fluorescence) bioloģiskajā vidē (1.8. attēls); katrs process sniedz informāciju par vides mikro- un makrostruktūru, to sastāvdaļu kustību un formu. Lāzera starojums ar mērenu intensitāti rada nespecifisku termisko, bet ar lielu intensitāti – destruktīvo (sabrukšanas) iedarbību uz ādu ļoti mazos apjomos (t.sk. šūnās vai pat to daļās) [21].

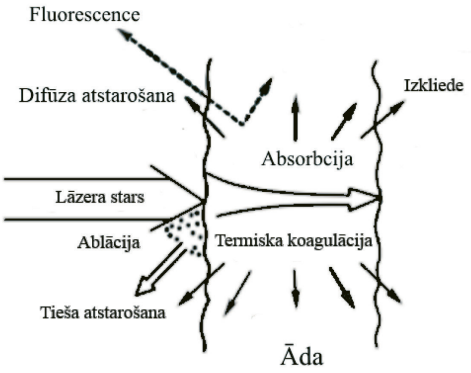

1.8. att. Lāzera stara mijiedarbības veidi ar ādu [17].

Redzamā un ultravioletā gaisma var ietekmēt audus fotobioķīmiski. Gaismas starojums diapazonā no ultravioletā (UV) līdz infrasarkanajam (IS) būtiski ietekmē ādu salīdzinājumā ar īso rentgena starojumu, γ-starojumu un starojumu radio diapazonā, kas saistīts ar gaismas un molekulu daudzveidīgajiem mijiedarbības procesiem (disociāciju, elektronu ierosmi, svārstību vai rotācijas ierosmi). Fotoni ar mazu enerģiju (tāls IS un terahercu starojums) var izraisīt selektīvu iedarbību uz dažām biomolekulām un to izveidotajiem savienojumiem ar apkārtējo vidi. Piemēram, var ierosināt makromolekulas rotācijas līmeņus, molekulas mehāniskās svārstības vai akustiskās svārstības šūnu membrānā. Pārsvarā iedarbība ir nespecifiska un pāriet termiskajā enerģijā. Rentgena starojumam un starojumam ar īsāku viļņa garumu piemīt tik liela enerģija, ka ar vienādu efektivitāti var jonizēt molekulu, kas ietilpst sarežģīti organizētā bioloģiskā matērijā, tādēļ mijiedarbība ar molekulām nav atkarīga no molekulas ķīmiskās dabas.

Procesus, kuri raksturo lāzera starojuma mijiedarbību ar ādu, var sadalīt trīs grupās. Pirmajā grupā ietilpst procesi, kas neizraisa izmaiņas bioobjektos, otrajā – fotoķīmiskie un termiskie procesi, un trešajā – fotosabrukšanas procesi (ablācija, foto koagulācija).

Tā kā iedarbība notiek uz dzīvas ādas, tad jāievēro ne tikai lāzera stara fizikāli-ķīmisko mijiedarbību ar audiem, bet arī tā ietekmi uz dzīvo audu funkcionēšanu, ko nosaka objekta homeostāzes pakāpe. Homeostāzes pakāpe ir evolūcijas attīstības funkcija un ir viszemākā bioloģiskām molekulām un visaugstākā mugurkaulniekiem (mugurkaulu dzīvniekiem). Mazas jaudas (< 200 mW/cm^2) starojums neiniciē organisma adaptācijas mehānismu un neietekmē homeostāzi. Pie nelielām jaudām (200 mW/cm^2 – 10 W/cm^2) tiek ierosināta tikai lokāla homeostāze, bet ne visos pētījumos tā tika novērota. Intensitātes palielināšana stimulē adoptācijas un regulācijas mehānismus dzīvajā ādā, kas pilnībā atjauno šo sistēmu, ja starojuma intensitāte nav pārāk liela. Turpinot palielināt intensitāti, mehānismi nespēj pilnība atjaunot biosistēmu un rodas daļēji neatgriezeniski procesi. Lielas intensitātes (> 10 W/cm^2) gadījumā destruktīvie procesi ir tik nopietni, ka sistēmu vairs nevar uzskatīt par "dzīvu". Rezultātus neietekmē biosistēmas regulējošie mehānismi, jo tā nav "dzīva", un tās sastāvs un īpašības ir nemainīgas jau kopš tā brīža, kad tās dzīvības mehānisms tika izbeigts.

Tāpēc pie salīdzinoši mazām intensitātēm ir iespēja ar gaismu pētīt procesus dzīvajā ādā, saglabājot tās struktūru. Interesi rada ļoti mazas (<< 200 mW/cm^2) intensitātes rajons, kas dod iespēju izmantot jutīgas pētījumu metodes, kur starojuma intensitāte neizraisa dzīvas matērijas homeostāzi pat lokālā līmenī, kas var ietekmēt rezultātus [21–23].

1.8. Fluorescence

Optiskā atomu un molekulu ierosme notiek ar fotonu absorbciju. Ierosinot ar monohromatisku starojumu, atomu sistēmai var nodot noteiktu enerģijas devu $\hbar\nu$, ($\hbar$ ($6.626 \cdot 10^{-34}\, J \cdot s$) – Planka konstante un ν – frekvence). Absorbcijas spektru nosaka molekulas pārejas enerģija starp pamata stāvokli un ierosinātiem stāvokļiem, bet emisijas spektru – starp relaksēto ierosmes stāvokli uz pamata stāvokli (1.9. attēls). Dotās sistēmas absorbcijas un emisijas spektru raksturo gan kā spektrālo līniju vai joslu kopumu, gan kā intensitātes sadalījumu spektrā. Emisijas intensitāte ir atkarīga no pārejas varbūtības un no enerģijas līmeņa apdzīvotības (atomux skaita enerģētiskajā līmenī). Ar pārejas varbūtību saistīts vēl viens no svarīgākajiem ierosinātu stāvokļu raksturlielumiem – tā *dzīves laiks* (detalizētāk aprakstīts 1.12. nodaļā), kas raksturo starošanas ilgumu pēc ierosmes pārtraukuma.

Izstarošanu ar īsu (~10^{-9} s) emisijas laiku sauc par fluorescenci, ar ilgāku emisijas laiku > 10^{-6} s – par fosforescenci [24].

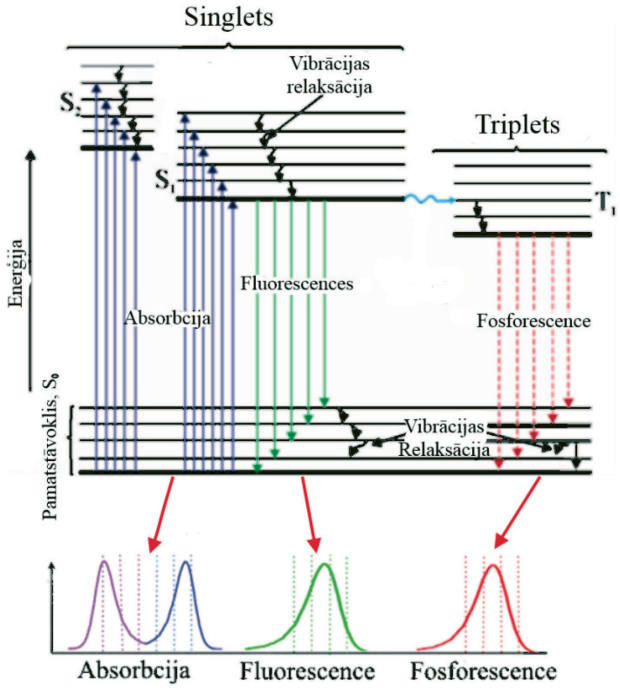

1.9. att. Jablonska diagramma, fluorescences spektra formēšanas [25].

Ādas absorbcijas un emisijas spektrus nosaka galvenie ādas hromofori un fluorofori, kuru absorbcijas un emisijas spektri parādīti 1.10. attēlā [26].

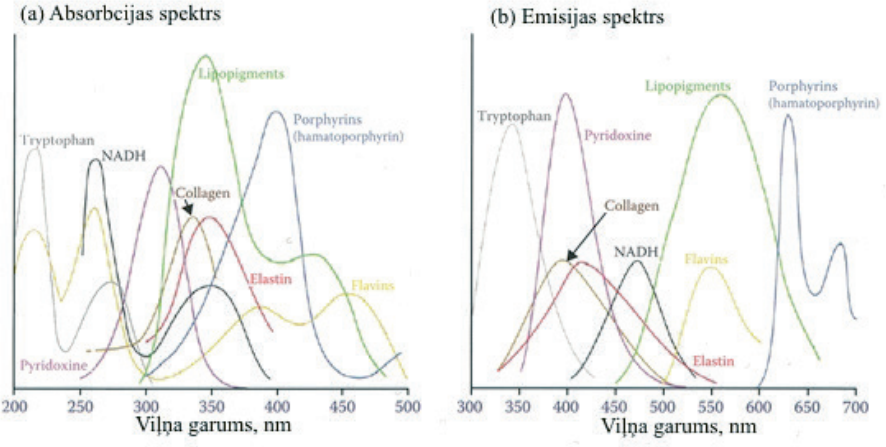

1.10. att. Endogeno fluoroforu absorbcijas un emisijas spektri [26].

1.9. Ādas fluorofori

NAD(P)H (*NADH – nikotīnamīda adenīndinukleotīda reducētā forma*, un *NADPH – nikotīnamīda adenīndinukleotīda fosfāta reducētā forma*), $FADH_2$ (*flavīna adenīna dinukleotīda reducētā forma*), skābeklis un adenozīna trifosfāts (ATP) ir galvenās biomolekulas oksidatīvās fosforilēšanas vielmaiņas procesā (1.11. attēls) [27, 28].

NADH un NADPH emisijas spektri pārklājas, un atšķirt tos spektrāli nav iespējams. Šo molekulu fluorescenci apzīmē ar NAD(P)H.

NADH pārnes elektronus caur kompleksu I uz elpošanas ķēdi, tajā laikā kompleksā II caur $FADH_2$ ienāk sukcināti. Elektroni ceļo pa elpošanas ķēdi ar secīgam oksidēšanas–reducēšanas reakcijām pie kompleksiem I – IV, kas nodrošina brīvās enerģijas daudzumu ATP sintēzei kompleksā V.

NADPH ir vēl viena molekula, kas atrodas šūnā. Atšķirībā no NADH, kas pārnes elektronus, NADPH ir nepieciešama antioksidatīvajos procesos [26].

Mitohondriju autofluorescence zilā spektrāla diapazonā ir attiecināta uz NAD(P)H [29–32], savukārt dzeltens/zaļš spektrālais diapazons ir attiecināts uz oksidētiem flavoproteīniem (FAD) [30, 33–35], ja ierosināts ar ultravioletā vai redzamā diapazona gaismu. NAD(P)H fluorescē reducētā forma, bet oksidētā forma ne. Turpretim FAD fluorescē oksidētā forma, bet ne reducētā forma ($FADH_2$). Šo iemeslu dēļ NAD(P)H un FAD ir plaši izmantots, lai novērtētu vielmaiņas oksidatīvo stāvokli šūnās un audos.

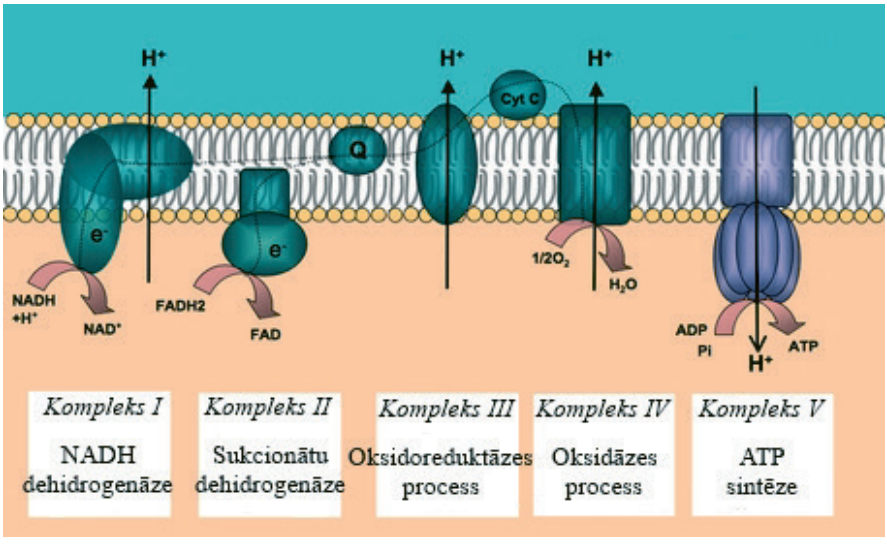

1.11. att. Oksidatīvā fosforilēšana [36].

Flavīns ir koenzīms, kas piedalās visos oksidēšanas-reducēšanas vielmaiņas procesos. Pazīstamākās no flavīniem ir divas molekulas: flavīna adenīna dinukleotīds (FAD) un flavīna mononukleotīds (FMN), kas ir atvasinājumi no riboflavīna (vitamīna B2). Lielākā daļa no flavīniem bioloģiskajās sistēmās ir saistīti ar olbaltumvielām, kur tie darbojas kā kofaktori un ir zināmi kā flavoproteīni un flavoenzīmi. FAD, kā elektronu transportēšanas grupa, ir nepieciešama oksidoreduktāzei [26]. Flavīnam absorbcijas maksimums ir pie 450 nm un fluorescences emisijas maksimums ir pie 520–530 nm, paradīts 1.10. attēlā.

Lipīdi ir visai daudzveidīga bioorganisko vielu grupa. Pie lipīdiem pieder: taukskābes, tauki, eļļas, vaski, terpēni, fosfolipīdi, steroīdi. Lipīdi ietilpst ikvienas šūnas membrānas struktūras sastāvā. Lielākā daļa no lipīdiem nefluorescē, kā fluorescējoša grupa atzīmējami lipopigmenti, kas sastāv no diviem cieši saistītiem lipīdiem: lipofuscīns (tumšie tauki) un vaskveidīgie neironu lipofuscīni (vasks), kas ar vecumu uzkrājas organismā. Lipīdu absorbcijas maksimums ir pie 360–421 nm, emisijas maksimums ir pie 540–650 nm, kā parādīts 1.10. attēlā [26].

Lipofuscīns – dzeltens / brūns autofluorescējošs pigments, pazīstams kā vecuma pigments, uz ādas izpaužas kā vecuma plankumi, sastāv no lipīdu un pēctranslācijas proteīnu modifikācijas sajaukuma. Lipofuscīns ir granulviedīgs, slikti šķīstošs un reaktīvs. Pigmentēto granulu diametrs var sasniegt 5 μm.

Melanīns jeb melnais ādas pigments nosaka ādas, kā arī acu un matu krāsu. Pigments atrodas galvenokārt epidermā [1, 15]. Melanīns ir dominējošais endogēnais pigments, kas pasargā ķermeni no saules nelabvēlīgās ietekmes – tas absorbē no ultravioletā 300 nm līdz tuvajam infrasarkanajam 800 nm starojumam [37]. Melanīna fluorescences dzīves laiks cilvēkā ādā, to ierosinot ar UV/redzamo diapazonu un novērojot pie 440 nm, 520 nm, 575 nm, var būt 0.2 ns, 1.9 ns, 7.9 ns [26, 38].

Kolagēns ir galvenais strukturālais proteīns, kas veido dzīvnieku un cilvēku saistaudus (kauli, derma utt.) un nodrošina to izturību un elastību. Tas sastāda 25–35% no ķermeņa kopējā proteīnu daudzuma. Kolagēna šķiedras ir saistītas kopā un stabilizētas ar krustveida kovalentām saitēm. Samazinoties kolagēna krustveida saitēm, palielinās otras harmonikas signāls un samazinās fluorescences dzīves laiks. Kolagēnam absorbcijas maksimums ir pie 325 nm un emisijas maksimums ir pie 400 nm (1.10. attēls). Tam ir relatīvi ilgs fluorescences dzīves laiks no 2 ns šķidrumā līdz 8,9 ns pulverī. Ar vienfotonu ierosmi kolagēna absorbcijas un emisijas spektrs sakrīt ar elastīna spektru, un tos ir grūti atšķirt. Lai tos atšķirtu, izmanto divfotonu ierosmi (760 nm) – ar otro harmonikas ģenerāciju kolagēns fluorescē sarkanajā diapazonā (620–750 nm).

Elastīns ir strukturālais fluorescējošais proteīns saistaudos, kura galvenā funkcija ir nodrošināt audu elastību. Absorbcijas maksimums ir pie 325 nm un

fluorescējošā emisija – pie 400 nm (1.10. attēls). Izmantojot laika izšķirtspējas spektroskopiju, var izšķirt elastīnu no kolagēna, jo elastīnam fluorescences dzīves laiks (0,2 – 2,5 ns) ir mazāks nekā kolagēnam [26].

1.10. Ādas absorbenti

Spēcīgākie absorbenti ādā redzamajā spektra daļā ir melanīns (sk. "*Ādas fluorofori*"), asinis – hemoglobīns [39, 40]. Dermālajā slānī asinis aizņem 2–7% tilpuma daļas. Hemoglobīna koncentrācija ir 143–173 g/L. Hemoglobīna absorbciju nosaka piesaistītā skābekļa daudzums – atkarībā no skābekļa daudzuma hemoglobīns tiek iedalīts divos tipos – oksihemoglobīnā un deoksihemoglobīnā. Ādas optiskās īpašības nosaka melanīna, oksihemoglobīna un deoksihemoglobīna absorbcija spektrs intervālā 250–800 nm (1.12. attēls). Oksihemoglobīna absorbcijas pīķi ir pie 415 nm, 542 nm un 577 nm, deoksihemoglobīna – pie 433 nm un 556 nm [41–45].

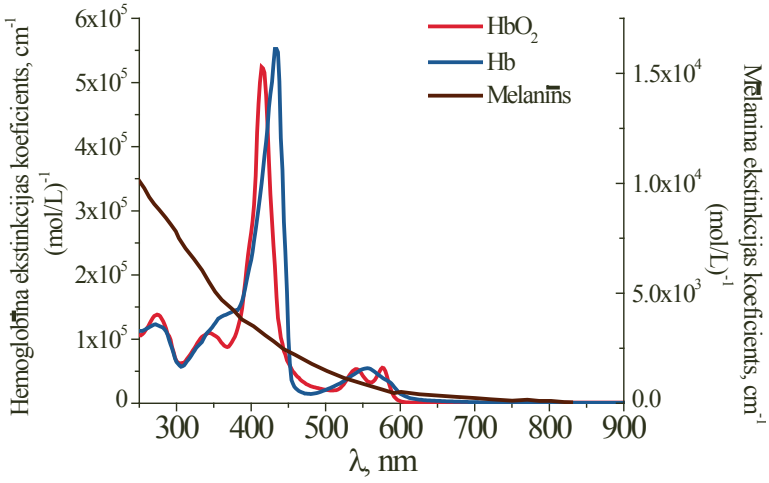

1.12. att. Melanīna, oksihemoglobīna un deoksihemoglobīna molāro ekstinkcijas koeficientu izmaiņas spektra intervālā 250 – 900 nm [46, 47].

1.11. Autofluorescences fotoizbalēšana

Ādas fluorescenci var iedalīt divās kategorijās:

1. endogēnā fluorescence, jeb autofluorescence (AF);
2. eksogēnā fluorescence.

Endogēnā fluorescence – pašu audu fluorescence jeb autofluorescence, to var izmantot diagnostiskas nolūkos.

Eksogēnā fluorescence – audos mākslīgi ievadīto vielu fluorescence, ko izmanto diagnostikā vai terapijā.

Par AF fotoizbalēšanu sauc procesu, kad ilgstošā, nepārtrauktā vai impulsu optiskā ierosmē notiek AF intensitātes samazināšanās. Tā shematiski parādīta 1.12. attēlā.

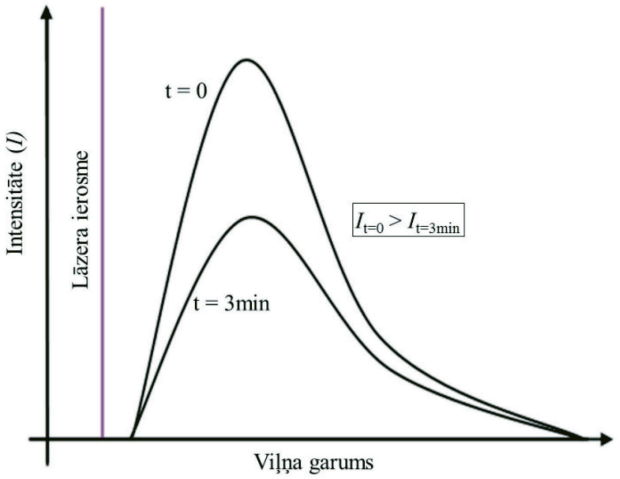

1.12. att. Fluorescences fotoizbalēšana nepārtrauktā lāzera ierosmē [11].

1.12. Fluorescences dzīves laiks

Ar pārejas varbūtību ir saistīts vēl viens svarīgs ierosinātu stāvokļu raksturlielums – *dzīves laiks*, kas raksturo starošanas ilgumu pēc ierosmes pārtraukuma [24]. Dzīves laiks ir atkarīgs no spontānās izstarošanas varbūtības A_{ik}.

$$A_{ik} = \frac{Z_{ik}^{(sp)}}{N_i}. \quad (1)$$

A_{ik} – pastāvīgs proporcionalitātes koeficients,

$Z_{ik}^{(sp)}$ – spontāni izstarotu fotonu skaits laika vienībā,

N_i – ierosināto daļiņu skaits augšējā (ierosinātajā) līmenī.

Laika momentā $t = 0$ ierosinātā enerģijas līmeņa apdzīvotība E_i ir vienāda ar N_{i0} un turpmāka ierosināšana netiek veikta. N_i skaita samazināšanos $(dN_i)_k$ spontānās pārējas dēļ $E_i \rightarrow E_k$ laika vienībā no t līdz $t + dt$ raksturo vienādojums:

$$-(dN_i)_k = Z_{ik}^{sp} dt = A_{ik} N_i dt. \quad (2)$$

N_i – līmeņa E_i apdzīvotība laika momentā t.

$$A_{ik} = -\frac{(dN_i)_k}{N_i dt}. \quad (3)$$

Spontānās pārejas varbūtība ir vienāda ar ierosināto daļiņu skaita relatīvo samazināšanos laika vienībā. Vienādojums (3) attiecas uz vienu noteiktu parēju. Pilnā spontānās pārejas varbūtība no līmeņa E_i uz visiem līmeņiem E_k, ir vienāda ar visu pāreju varbūtību A_{ik} summu .

$$A_i = \sum_k A_{ik} = -\frac{dN_i}{N_i dt}. \quad (4)$$

No vienādojuma (4) seko:

$$-dN_i = A_i N_i dt. \quad (5)$$

Atrisinot vienādojumu (5), iegūstam likumu, kas raksturo ierosināto daļiņu skaita samazināšanos laikā:

$$N_i = A_{i0} e^{-A_i t}. \quad (6)$$

Dažādām daļiņām laiks, ko tās pavada ierosinātā stāvoklī, atšķiras, tādēļ ierosināta stāvokļa dzīves laiku var izteikt kā vidējo ilgumu, kad daļiņas atrodas ierosinātā stāvoklī. Dzīves laiku var izteikt, izmantojot A_i:

$$\tau_i = \frac{1}{A_i} = \frac{1}{\sum_k A_{ik}}. \quad (7)$$

Tādējādi τ ir apgrieztais lielums pilnai spontānas izstarošanas varbūtībai. Tas ir laiks, kurā ierosinātu daļiņu skaits samazinās e reizes (kad $t = \tau$) [24]:

$$\frac{N_i}{N_{i0}} = \frac{1}{e} = \frac{1}{2.718} = 0.368. \quad (8)$$

Izolētu atomu līmeņu dzīves laikus nosaka, tos ierosinot ar īsiem optiskiem impulsiem un sekojot fluorescences intensitātes izmaiņām laikā [24]. Līdzīgi var izsekot daudz sarežģītāku atomu un molekulu sistēmu fluorescences kinētikai, izmantojot augšminēto dzīves laika definīciju. Tomēr jāsaprot, ka vairāku sarežģītu biomolekulu sistēmā, tai skaitā cilvēka ādā, fluorescences emisijā var piedalīties dažādu molekulu dažādi ierosinātie līmeņi, līdz ar to fluorescences dzišana laikā var notikt vienlaikus ar dažādiem ātrumiem. Citiem vārdiem, intensitātes laika atkarība šādās situācijās var būt multi-eksponenciāla, un katrai no šīm eksponentēm atbilst sava dzīves laika τ komponente, kas raksturo attiecīgo fluoroforu.

2. JAUNVEIDOJUMU AUTOFLUORESCENCES FOTOIZBALĒŠANAS PĒTĪJUMI NEPĀRTRAUKTĀ IEROSMĒ

2.1. Literatūras pārskats par agrākiem autofluorescences fotoizbalēšanas pētījumiem

Literatūrā fotoizbalēšana aplūkota divos aspektos: 1) mērot eksogēno fluorescenci, fluoroforu autofluorescenci uzskata kā fona troksni un to fotoizbalē [48–50]. 2) ilgstošākā mērījumā autofluorescences intensitāte samazinās jeb fotoizbalē [51–56].

AF fotoizbalēšana nav neatgriezenisks process, ar laiku bioobjektu emisijas spēja atjaunojas. Metodi ar nosaukumu FRAP (fluorescence recovery after photobleaching) jeb fluorescences atjaunošanos pēc fotoizbalēšanas izmanto, piemēram, šūnu/molekulu migrācijas pētīšanā [57–61].

H. Zeng u. c. [9, 14] ādas AF un fotoizbalēšanu sāka pētīt 1993. gadā, to optiski ierosinot tuvā ultravioletā un redzamā spektra diapazonā. AF ierosmei spektra diapazonā 200 – 1100 nm izmantoja ksenona lampu. Pētījumiem tika izvelēti 350nm, 370 nm, 380 nm, 390 nm, 430 nm, 470 nm ierosmes viļņa garumi, to izdalīšanai izmantojot monohromatoru. Mērījumu gaitā tika konstatēts, ka AF intensitāte un tās dzišanas kinētika ir atkarīga no ierosmes intensitātes (jeb jaudas blīvuma) un ierosināšanas viļņa garuma – jo lielāka ierosmes intensitāte, jo lielāka arī AF intensitāte un straujāk notiek fotoizbalēšana, turklāt AF intensitāte straujāk dziest, ja tā tiek ierosināta ar lielākiem viļņa garumiem. Ādas AF intensitāte pilnīgi atjaunojās 6 dienu laikā. H. Zeng piedāvāja AF fotoizbalēšanas kinētiku analizēt ar dubult-eksponenciālo aproksimāciju (9) (2.1. attēls), pamatojoties uz to, ka pirmā (τ_1) – ātrākā – komponente atbilst ādas augšējā slāņa fluorescencei un otra (τ_2) – lēnākā – komponente – dziļāko slāņu fluorescencei:

$$I(t) = a \cdot e^{-\frac{t}{\tau_1}} + b \cdot e^{-\frac{t}{\tau_2}} + A. \qquad (9)$$

Parametri *a, b, A,* τ_1 un τ_2 apraksta ādas AF intensitātes fotoizbalēšanas procesu laikā *t*.

A. A. Stratoņikovs u. c. 2001. gadā [12] pētīja ādas AF fotoizbalēšanas kinētiku pie 532 nm, 633 nm un 670 nm lāzeru ierosmes viļņa garumiem. Tika konstatēts, ka AF piedalās vairāki fluorofori ar dažādiem fotoizbalēšanas ātrumiem un AF intensitāte fotoizbalēšanas procesā krīt vidēji par 30%. Ādas jaunveidojumiem AF fotoizbalēšanas laiks izrādījās lielāks, nekā veselai ādai.

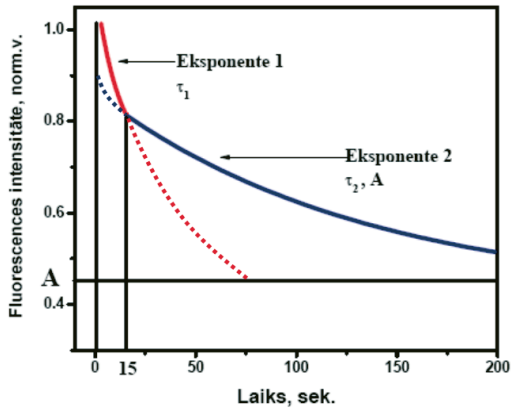

2.1. att. Autofluorescences fotoizbalēšanas kinētika:
τ_1 – ātrā un τ_2 – lēnā dzišanas fāze, A – fona līmenis [10, 11].

A. Lihačovs u. c. 2011. gadā [13] pētīja fotoizbalēšanas kinētiku no pigmentētiem ādas jaunveidojumiem, ierosinot autofluorescenci ar 532 nm. Veicot klīniskos mērījumus, tika uzkrāta datu bāze ar mērījumu rezultātiem. Analizējot fotoizbalēšanas kinētiku ar dubult-eksponenciālo aproksimāciju, tika novērots, ka fotoizbalēšanas ātrums pigmentētiem jaunveidojumiem atšķiras savā starpā. Pētījumi tika turpināti, izmantojot citu ierosmes viļņa garumu un izstrādājot fotoizbalēšanas ātrumu kartēšanas metodes.

E. K. Borisova [3] pētīja *in vivo* autofluorescenci no normālas ādas un jaunveidojumiem, ierosinātu ar 405 nm lāzera viļņa garumu. Rezultāti rāda, ka bazālo šūnu karcinomai (BCC) autofluorescence ir vājāka, nekā normālai ādai, bet plakanšūnu karcinomai ir augstāka. Vēlā stadijā bazālo šūnu karcinomas autofluorescencei sarkanajā spektra diapazonā paradās maksimums, kas saistīts ar endogēno porfirīnu uzkrāšanos.

M. E. Darvin u. c. 2017. gadā publicēja darbu [62] par ādas autofluorescences fotoizbalēšanas pētījumiem pie vairākiem lāzeru ierosmes viļņa garumiem (325 nm, 473 nm, 633 nm, 785 nm). Autori konstatēja, ka AF dzišanas ātrums ir atkarīgs no ierosmes viļņa garuma: jo īsāks ierosmes viļņa garums, jo procentuāli mazāk samazinās autofluorescences intensitāte fotoizbalēšanas procesā salīdzinājumā ar lielākiem ierosmes viļņa garumiem. Ierosinot autofluorescenci ar 325 nm viļņa garumu, autofluorescences intensitāte pēc 315 sekundēm samazinājās par 18–29%, ar 473 nm – par 39–54%, ar 633 nm – par 36–60%, ar 785 nm – par 50–80%. Tika secināts, ka AF fotoizbalēšanas procesā pie lielākiem ierosmes viļņa garumiem piedalās mazāk ādas fluoroforu.

2.2. Komerciālās ierīces ādas fluorescentai diagnostikai

VELscope – mutes dobuma vēža diagnostikas ierīce. Autofluorescenci ierosina ar LED 400–460 nm diapazonā (violeti-zilais diapazons) un vizuāli novēro 500–550 nm diapazonā (zaļais diapazons). Veseliem audiem AF intensitāte ir lielāka salīdzinājumā ar audzēju AF intensitāti [63].

FotoFinder – veidots bazālo šūnu karcinomas diagnostikai, bet nav derīgs melanomas diagnostikai. Ierīce aprīkota ar violeto LED gredzenu pirms kameras, starp kameru un LED gredzenu ievietot filtrs, kas nelaiž cauri LED apgaismojumu. Mērījumi notiek, uzsmērējot fotosensibilizatoru, kas uzkarājas jaunveidojumā (bazālo šūnu karcinomā) un fluorescē sarkanajā (620–750 nm) diapazonā, ierosinot ar violeto (380–450 nm) LED. FotoFinder dod iespēju novērot reālā laikā, kā arī fotografēt jaunveidojumu. Šī metode dod iespēju noteikt jaunveidojuma robežas [64].

Wood lamp – UV (365 nm) ierosme. Novēro AF caur palielinošo lēcu, kas pārklāta ar filtru un nelaiž cauri UV gaismu. Diagnostika balstās uz AF intensitātes vizuālu novērtēšanu [65].

OBSERV – kosmētiskai ādas diagnostikai. Nosaka ādas mitrumu, aknes, rozācijas, kolagēna trūkumu, saules apdegumus utt., ierosinot fluorescenci pie 365 nm un novērojot emisiju pie 405 nm. Diagnostika balstās uz AF intensitātes vizuālu novērtēšanu [66].

2.3. Ierīce autofluorescences dzišanas kinētikas mērījumiem ar punktveida metodi

Darbā izstrādātā punktveida mērījumu prototipa ierīce sastāv no:

- diožu lāzera – DPSS, Huanic DD532-10-3, ar jaudas blīvumu 32 mW/cm^2;
- fotodiodes – PicoLog 1216, OPT101;
- filtriem – Semrock BLP01-532R un Eksma OG570/KG3.

Mērījumu ierīce shematiski attēlota 2.2. attēlā. AF ierosmei izmantots nepārtraukta starojuma 532 nm zemjaudas diožu lāzers (~8.3 mW). Lāzers uzstādīts 45° leņķī pret ādas virsmu. Kombinācija no diviem filtriem pirms fotodiodes paralēli ādas virsmai atrodas 3mm attālumā no tās un nodrošina caurlaidību spektrālajā diapazonā no 550 nm līdz 650 nm. Fotodiode AF reģistrēšanai ar iebūvētu pastiprinātāju ir savienota ar datoru. PicoLog programma nodrošina mērījumu vadību un datu saglabāšanu. Autofluorescences fotoizbalēšana ādai un jaunveidojumiem tiek reģistrēta 30 sekundes. Iegūtie rezultāti apstrādāti ar dubult-eksponenciālo aproksimāciju (9) un analizēti pēc AF kinētikas parametriem un AF intensitātes vērtībām. Prototipa ierīces konstrukcija nodrošina apkārtējās gaismas izolāciju mērījumu laikā, samazinot fona troksni.

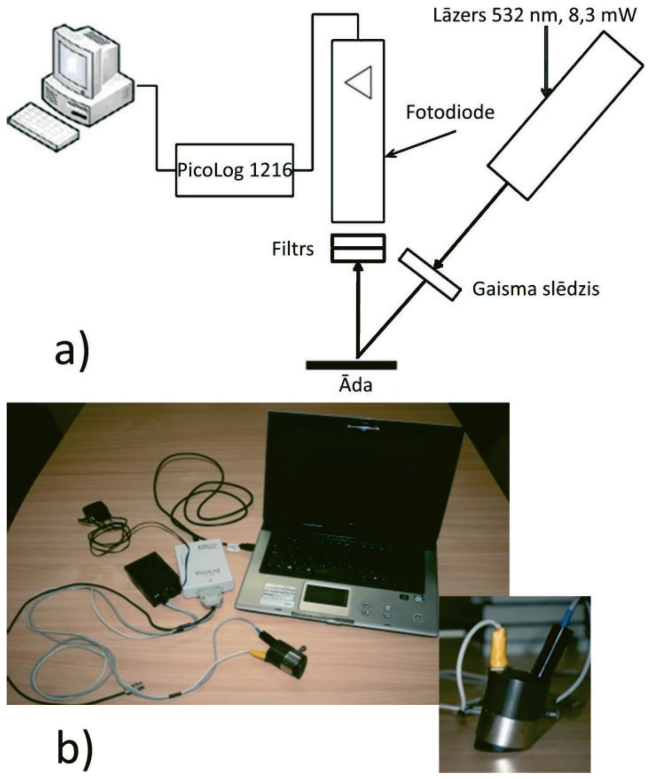

2.2. att. a) shematiski attēlota mērījumu ierīce; b) prototipa ierīces izskats.

Mērījumi ar šo ierīci tika veikti uz 51 ādas jaunveidojumu Rīgas Lāzerplastikas klīnikā ar ētikas komisijas atļauju, ievērojot lāzeru drošības nosacījumus [67]. AF fotoizbalēšanas kinētika apstrādāta ar dubult-eksponenciālo aproksimāciju (9), tās rezultāti ilustrēti 2.3. attēlā.

Mērījumu rezultāti rāda, ka sākotnējā AF intensitāte no ādas vienmēr ir lielāka nekā no pigmentētiem jaunveidojumiem un, jo lielāka pigmentācija, jo zemāka AF intensitāte. Savukārt τ_1 (fotoizbalēšanas ātruma 1.komponente) vienmēr ir lielāka pigmentētiem jaunveidojumiem.

Attiecība starp sākotnējo intensitāti no ādas un no mazāk pigmentēta jaunveidojuma $\left(\frac{I_{norm.ādas}}{I_{pig.pataloģija}}\right)$ ir 1,2–1,7, savukārt vairāk pigmentētam jaunveidojumam attiecība ir 2,3–4,8. Klīnisko mērījumu rezultāti ir publicēti [*IX*] žurnālā.

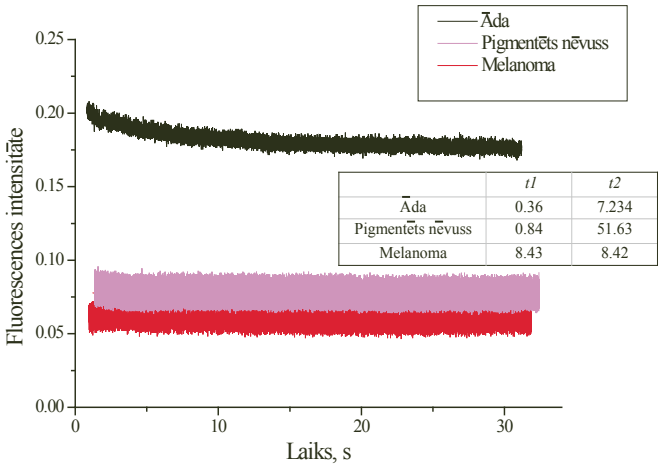

2.3. att. Autofluorescences fotoizbalēšanas kinētikas līknes un fotoizbalēšanas parametri τ_1(t1)un τ_2(t2).

2.4. Ierīce ādas autofluorescences parametriskai kartēšanai ar viedtālruni

AF fotoizbalēšanas kinētikas parametriskās kartēšanas ierīce (2.4. att.) sastāv no:

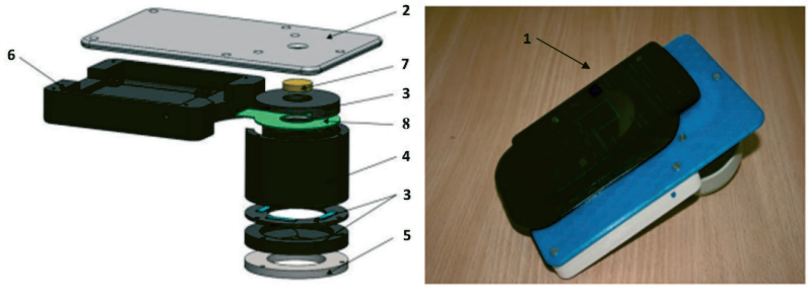

2.4. att. Prototipa ierīce ādas AF ierosmei un fotoizbalēšanas parametra kartēšanai ar viedtālruni: a – uzbūves shēma, b – ārējais izskats komplektā ar viedtālruni.

1. Viedtālruņa – uzņem un apstrādā attēlus, Samsung Galaxy Note 3 ar integrētu kameru CMOS RGB 13MP;
2. Atbalsta plāksnes ar apaļu atveri viedtālruņa kamerai – noklāta ar lipīgu, nesmērējošu virsmu (Grippy Pad), kas nodrošina ērtu telefona piestiprināšanu pie ierīces;
3. Distancera – savieno un atbalsta ierīces elementus;

4. Ekranējoša cilindra – nodrošina fiksētu attālumu līdz pētāmai virsmai, lai uzņemtu asus attēlus;
5. Silikona gredzena – nodrošina ciešu kontaktu ar pētāmo virsmu;
6. Korpusa – nodrošina vietu baterijām un elektronikas elementiem;
7. Gaismas filtra – absorbē violeto ierosmes starojumu, laiž cauri ādas AF starojumu;
8. 405 nm gaismas diožu gredzena – nodrošina AF ierosmi, 405 nm LED, Engin LZ1-00UA00-U8
9. Balto LED diožu gredzena – nodrošina balto apgaismojumu, lai nofokusētu kameru uz jaunveidojuma [68].

AF intensitātes reģistrēšanai izmantota viedtālruņa RGB kamera. AF ierosināta ar 405 nm LED (joslas pusplatums 30 nm; jaudas blīvums 20 mW/cm^2). Laboratorijā tika optimizēta fluorescences ierosmes LED (405 nm) intensitāte. Veikta korpusa modificēšana un programmatūras pielāgošana ērtākai lietošanai. LED intensitāte rediģēta atbilstoši viedtālruņa kameras jutības diapazonam, kā arī kadru maiņas frekvencēm [68]. Attēli iegūti ar uzstādījumiem: ISO–100, baltā balanss – dienas gaisma (daylight), fokuss – manuāli, ekspozīcijas laiks – 200 ms. Ādas un jaunveidojumu emisijas spektrs atrodas diapazonā no 450 nm līdz 700 nm, ar maksimumu 510 – 530 nm spektra zaļajā daļā jeb uztvērēja G (green (zaļā)) kanālā. LEDi izvietoti cilindrā radiāli apkārt kamerai. Attālums starp kameru un ādas virsmu – 6,0 cm, apgaismotais laukums ~12 cm^2 (jeb aplis 4 cm diametrā). Filtrs ar caurlaidību no 515 nm (pakāpes filtrs) ievietots pirms kameras, lai izvairītos no izkliedētā LED apgaismojuma. AF intensitātes reģistrēšana notiek pirmajā sekundē un pēc nepārtrauktas ierosmes divdesmitajā sekundē. Iegūtais attēlu masīvs tika sadalīts pa RGB kanāliem, un G kanālā katrā pikselī, izmantojot AF intensitātes vērtības, tika aprēķinātas parametriskās kartes:

$$N_G = \frac{[I_{t_0} - I_t]}{I_{t_0}}, \tag{10}$$

kur N_G – attēlo autofluorescences intensitātes dzišanas parametru katrā pikselī (vai pikseļu grupā), G indekss nozīme G (green (zaļais)) kanālu. Publikacijā [*II*] šis parametrs apzīmēts kā N(C), kur C ir viens no RGB kanāliem;

I_{t_0} – autofluorescences intensitāte sākuma momentā;

I_t – autofluorescences intensitāte beigu momentā (pēc 20 sekundēm).

Datu apstrāde veikta MATLAB® vidē [69].

Viedtālruņa ierīces prototipa aprobācijai tika veikti klīniskie mērījumi Latvijas Onkoloģijas centrā ar Ētikas komisijas atļauju, ievērojot drošības nosacījumus [67]. Mērījumi veikti 50 pacientiem ar 150 ādas jaunveidojumiem. Analīzei izvēlēti

13 BCC jaunveidojumi un 1 īpašs nehomogēns (trīsdaļīgs) nēvuss. Desmit no BCC jaunveidojumiem bija homogēni pigmentēti un trīs čūlojoši.

2.5. attēlā parādīts BCC jaunveidojuma attēls baltā apgaismojumā (a), autofluorescences intensitātes attēls (b) un parametriskās kartēšanas attēls G-kanālā (c). G-kanāla attēlā, pateicoties izteiktam kontrastam starp audzēju un ādu, ir labi redzamas audzēja robežas. Analizējot iegūtos datus 10 BCC jaunveidojumiem (diagnoze apstiprināta ar histoloģiju), tika novērots, ka BCC jaunveidojumu AF intensitāte vienmēr ir zemāka un vienmērīgi sadalīta, salīdzinot ar apkārtējo ādu un citiem jaunveidojumiem, bet fotoizbalēšanas parametra N_G vērtība ir lielāka, salīdzinot ar ādu.

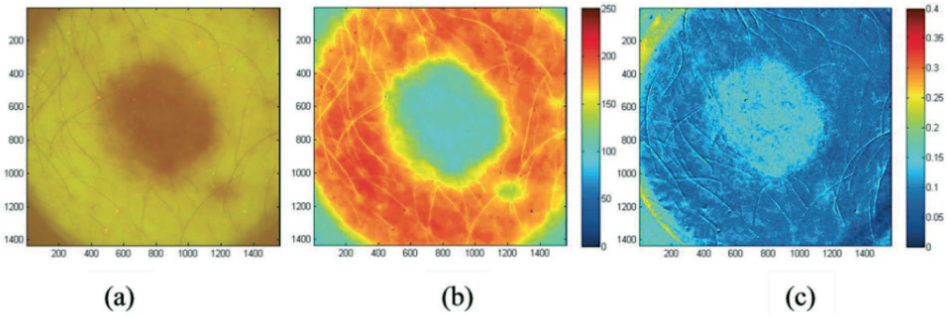

2.5. att. BCC jaunveidojums. (a) attēls, kass uzņemts baltā apgaismojumā,
(b) autofluorescences intensitātes attēls G-kanālā,
(c) parametra N_G sadalījuma karte G-kanālam.

2.6. attēlā ilustrēts čūlojošs BCC jaunveidojums. Autofluorescences intensitāte ir augstāka čūlojošā audzēja centrā, salīdzinot ar apkārtējo pigmentēto laukumu. Pigmentetā laukumā AF ir vienmērīgi sadalīta. Savukārt N_G parametra vērtība G-kanālā ir lielāka pigmentētajam laukumam salīdzinājumā ar ādu un čūlojošo zonu.

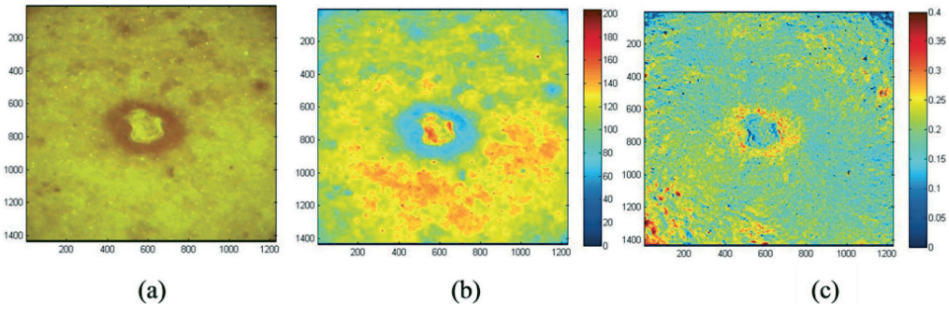

2.6. att. Čūlojoša BCC jaunveidojums. (a) attēls, kas uzņemts baltā apgaismojumā,
(b) autofluorescences intensitātes attēls G-kanālā,
(c) parametra N_G sadalījuma karte G-kanālam.

Klīnisko mērījumu gaitā tika iegūti attēli no netipiska nēvusa, kas sākotnēji tika klasificēts kā melanoma. Parametra N_G sadalījuma karte G-kanālā uzrādīja trīs zonas ar atšķirīgām parametra vērtībām. Vēlāk histoloģija apstiprināja, ka šis nēvuss tiešām sastāv no trim nēvusiem: lejasdaļā – robežnēvuss ar lielāko N_G parametra vērtību, vidusdaļā – displastisks nēvuss un augšdaļā – intradermāls nēvuss (2.7. attēls). Vizuāli šīs trīs zonas atšķirt nebija iespējams.

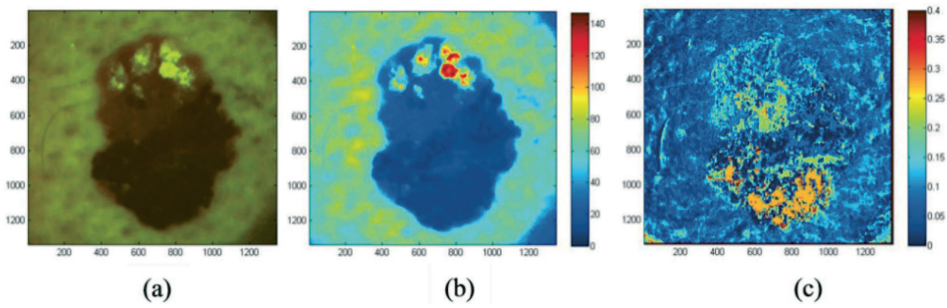

2.7. att. Netipisks nēvuss, apakšējā daļā – robežnēvuss; vidējā daļā – displastisks nēvuss; augšējā daļā – intradermāls nēvuss. (a) attēls, kas uzņemts baltā apgaismojumā, (b) autofluorescences intensitātes attēls G-kanālā, (c) parametra N_G sadalījuma karte G-kanālam.

2.5. Secinājumi par autofluorescences pētījumiem nepārtrauktā ierosmē

Punktveida AF detektora prototipa (ar 532 nm ierosmi) klīniskā aprobācija sniedza datus par AF intensitātes vērtībām no pigmentētiem jaunveidojumiem un ādas. Ņemot vērā iepriekšējos mērījumus, tika izstrādāts viedtālruņa prototips AF fotoizbalēšanas kinētikas parametra kartēšanai un algoritms pigmentēto jaunveidojumu diagnostikai. AF un parametra kartēšana paver jaunas iespējas ādas pataloģiju diagnostikai, klīniski apstiprinot BCC atšķirības no citiem pigmentētiem jaunveidojumiem. Rezultāti no netipiskā trīsdaļīgā nēvusa apliecina potenciālo iespēju bezkontakta ceļā pēc AF fotoizbalēšanas kinētikas datiem atšķirt dažādus pigmentētos jaunveidojumus. Turpinot darbu šajā virzienā, nepieciešams uzkrāt statistiski reprezentatīvu datu bāzi ar pigmentēto ādas jaunveidojumu AF un fotoizbalēšanas ātruma digitāliem attēliem. Klīnisko mērījumu rezultāti ir publicēti [*II*].

3. ĀDAS UN JAUNVEIDOJUMU AUTOFLUORESCENCES PĒTĪJUMI IMPULSU IEROSMĒ

Šajā sadaļā tiek apskatīti rezultāti, kas iegūti, izmantojot fluorescences spektroskopiju ar augstu laika izšķirtspēju. Rezultāti apkopoti par AF dzīves laika vērtībām pirms un pēc fotoizbalēšanas. AF kinētika analizēta ar TRES apstrādes metodi, datus normējot pēc fluorescences signālu maksimuma. Sniegti arī iegūtie AF dzīves laika x-y sadalījuma attēli, raksturota korelācija starp AF dzīves laika un AF fotoizbalēšanas ātruma parametriem, salīdzinot ādu un intradermālo nēvusu.

3.1. Pārskāts par ādas fluorofori un to pētīšanas metodes

Autofluorescenci no audiem un šūnām var raksturot ar spektra formu, emisijas intensitāti un izspīdēšanas laiku. Pētot dažādus fluorescences parametrus, rodas iespēja iegūt vairāk informācijas par bioloģiskiem audiem un fizioloģiskām transformācijām tajos [70, 71].

Aizvien vairāk pētījumu tiek veikti, lai noskaidrotu korelāciju starp fluorescences dzīves laikiem vai fluorescences spektriem un bioloģiskajām patoloģijām ar pielietojumu iespējām diagnostikā. Apvienojot fluorescences pētīšanas metodes ar sarežģītu digitālo datu analīzi, var ievērojami uzlabot mūsu zināšanas par dažāda veida izmaiņām dzīvajos audos.

Mūsdienu komerciālās tehnoloģijas ļauj pētīt fluorescenci ar dzīves laiku līdz nanosekunžu desmitdaļām. Piemēram, Becker&Hickl un PicoQuant piedāvā iekārtas ar iespējām pētīt fluorescences dzīves laiku ar punktveida makro vai mikro attēlošanas metodēm vienlaicīgi pie dažādiem viļņa garumiem redzamajā un tuvajā infrasarkanajā diapazona [38, 72–74].

Liela uzmanība pievērsta NAD(P)H (NADH un NADPH reducētā forma) un FAD (oksidētā forma) endogeno fluoroforu pētījumiem. NADH un FAD fluorofori iesaistās šūnas metabolisma procesā, nodrošinot oksidēšanās-reducēšanās reakcijas šūnu membrānā. [75–78]

O.Warburg u. c. [79, 80] 1956. gadā publicēja rezultātus par NAD(P)H un FAD fluoroforiem. NAD(P)H fluorescē reducētā un nefluorescē oksidētā formā, FAD fluorescē oksidētā un nefluorescē reducētā formā (kad reducējas līdz $FADH_2$). Mainoties fluorescences intensitātei no NADH un FAD, mainās *redoks* stāvoklis audos. *Redoks* atkarības koeficients rāda oksidēto vai reducēto stāvokli audos. Veselo audu šūnās ir vairāk oksidatīvais metabolisms, bet vēža audzēju šūnās – reducētais metabolisms. NADH un FAD fluorescenci ierosina ar tuvo ultravioleto

starojumu (350 nm – 375 nm), novēro NAD(P)H fluorescenci zilajā spektra rajonā 450 nm – 475 nm un FAD – zaļajā spektra rajonā 530 nm – 550 nm, kā parādīts 1.10. attēlā. [26, 29, 30].

NAD(P)H fluorescences dzīves laiks ir atkarīgs no mikrovides, it īpaši no viskozitātes un polaritātes. Relatīvi plaši tika izpētīts "brīvs" NAD(P)H (free NAD(P)H) *in vitro* [81], izmantojot divu eksponentu aproksimāciju fluorescences dzišanas līknēm. Šodien vispārīgi atzīts, ka īso dzīves laiku (0,4 ns) var izmantot kā indikatoru "brīvām" NAD(P)H molekulām šūnās un audos [6, 7, 76, 77].

Vairākus endogenos fluoroforus ādā pētījis K. Konig u. c. 2003. gadā [38], izmantojot divfotonu ierosmi. Pētījumu iekārta apvieno TCSPC sistēmu ar multifotonu mikroskopu, ierosme veikta ar 80 MHz impulsu lāzeri diapazonā no 750 nm līdz 850 nm. Pētījuma rezultātā iegūti dati par ādas NAD(P)H, flavīna, melanīna un lipofuscīna AF dzīves laiku (3.1.tabula).

3.1. tab. Endogeno fluoroforu ierosmes un emisijas viļņu garumi un autofluorescences dzīves laiki [38].

Fluorofori	Ierosmes viļņa garums (nm)	Emisija (nm)	Fluorescences dzīves laiks (ns)
NAD(P)H	340	450–470	0,3 (saistīts ar proteīnu: 2)
Flavīns	370, 450	530	5,2 (saistīts ar proteīnu: < 1)
Melanīns	UV/redzamais	440, 520, 575	0,2/1,9/7,9
Lipofuscins	UV/redzamais	570–590	Multi-eksponenciāls

Apkopotā literatūra [81] parāda, ka dzīves laikā vērtības τ vienam un tam pašam fluoroforam atšķiras atkarībā no atrašanās vietas audos, *in vivo* vai *in vitro* mērījumu veida, kā arī no ierosmes un detektēšanas viļņa garuma [82–89].

3.2. Fluorescences dzīves laika mērījumu iekārtas shēma un darbības princips

AF fotoizbalēšanas ietekme uz ādas fluoroforu spektrāliem parametriem tika pētīta, izmantojot fluorescences spektroskopiju ar laika izšķirtspēju ~10^{-10}s redzamajā spektra diapazonā. Mērījumi tika veikti ar TCSPC (Time-correlated single photon counting) reģistrēšanas sistēmu, AF ierosināta ar 405 nm un 470 nm pikosekunžu lāzeriem. AF ierosme veikta 3 minūtes nepārtrauktā režīmā. Ādas autofluorescences dzīves laika mērījumi veikti ar divām metodēm: punktveida un attēlošanas metodi. Eksperimentālā iekārta shematiski attēlota 3.1. attēlā.

Eksperimentālā mērījumu iekārta sastāv no:

- TCSPC (Time-correlated single photon counting): SPC – 150, Becker&Hickl;
- optisko šķiedru Y-veida kūļa, katras optiskās šķiedras serdeņa diametrs 200 μm;
- lāzeriem – PicoQuant, LDH-D-C-405 (impulsa pusplatums 59 ps); LDH-D-C-470 (impulsa pusplatums 73ps);
- detektora – fotoelektronu pavairotāja PMC-100-4, Becker&Hickl;
- monohromatora.

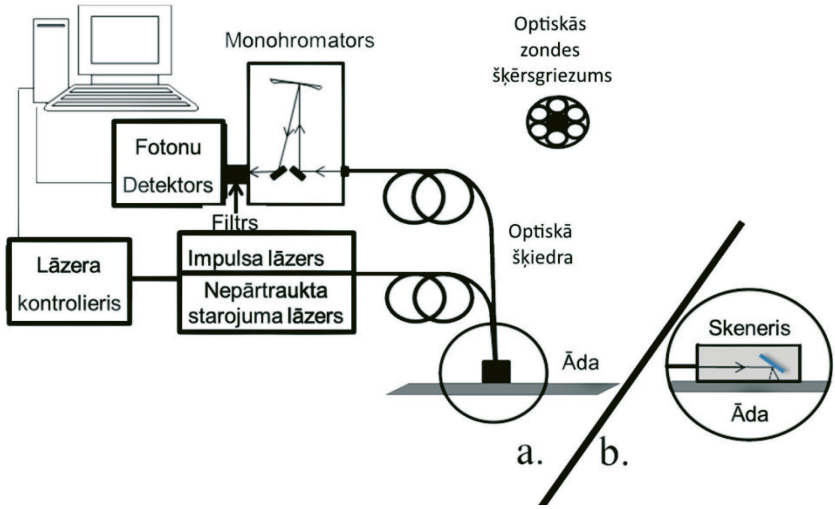

3.1. att. Fluorescences dzīves laiku mērījumu iekārtas shēma:
a – punktveida metodei ar optiskās šķiedras zondi, b – x-y attēlošanai ar spoguļu skeneru

TCSPC sistēmas darbības princips balstās uz viena fotona reģistrēšanu periodā starp lāzera impulsiem un laika noteikšanu starp fotona reģistrācijas brīdi un ierosinošo lāzera impulsu. Detektors (fotolektronu pavairotājs jeb FEP), uztverot fotonu, pastiprina to un padod elektronisko impulsu uz diskriminatoru. FEP izejas elektronisko impulsu amplitūda ir mainīga, tāpēc sistēmā tiek izmantots CFD (*Constant Fraction Discriminator*), kas dubulto impulsa signāla amplitūdu, invertē to, apgriežot uz negatīvo pusi pa y asi, aizkavē un tad summē ar sākotnējo impulsu. Iegūtā impulsa krustošanās laiku ar x asi pieņem par starta (vai stop) signālu, padodot tālāk uz TAC (*time-to-amplitude converter*). TAC ģenerē elektrisko spriegumu, kas ir proporcionāls laikam starp lāzera impulsu un fotona detektēšanas momentu. Pienākot starta signālam, elektriskā strāva sāk uzlādēt kondensatoru un pārtrauc uzlādēt pēc stop impulsa pienākšanas. ADC (*Analog-to Digital Converter*), nolasot elektrisko spriegumu no TAC, pārvērš to ciparu formātā (3.2. attēls). Katrs

reģistrētais fotons nonāk atmiņas kartē un par "1" palielina skaitli atbilstošajā "kastītē" laika intervālu masīvā. Pēc daudziem impulsiem, savācot pietiekamu statistiku, reģistrētos vienfotonu signālus summē laikā atkarīgu, integrētu signālu formā (3.3. attēls) [90–93].

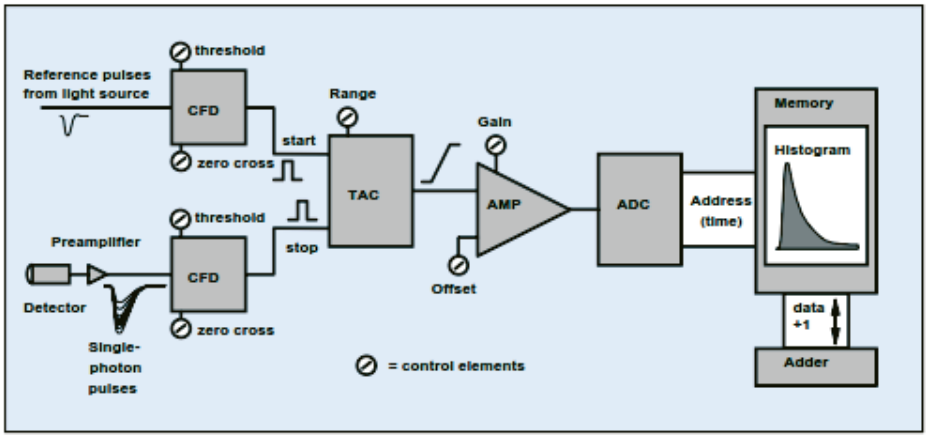

3.2. att. TCSPC mēriekārtas klasiska arhitektūra [93].

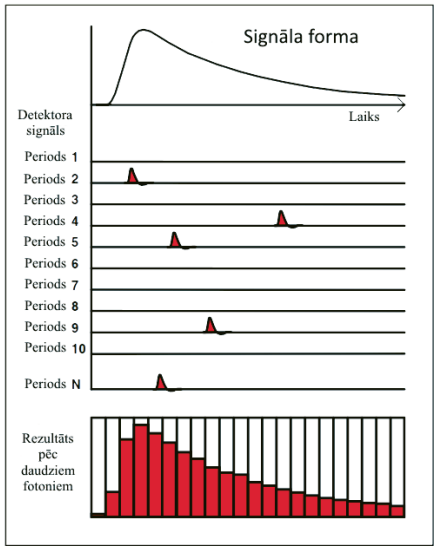

3.3. att. TCSPC reģistrēšanas princips [93].

3.3. Ādas autofluorescences dzīves laika punktveida mērījumi

Šajā daļā AF dzīves laika mērījumi *in vivo* no ādas virsmas tika veikti spektrālajā diapazonā no 440 nm līdz 600 nm ar soli 10 nm, ierosinot ar 405 nm pikosekunžu impulsu lāzeri, un spektrālajā diapazonā no 510–600 nm ar soli 10 nm, ierosinot ar 470 nm pikosekunžu impulsu lāzeri. Mērījumi no intradermāla nēvusa veikti tikai ar 405 nm lāzera ierosmi spektrālajā diapazonā 460–610 nm. AF tika reģistrēta pirms un pēc fotoizbalēšanas. Fotoizbalēšana veikta 3 min, pārslēdzot 405 nm vai 470 nm lāzeri no impulsa uz nepārtraukto starojuma režīmu ar jaudas blīvumu 40 mW/cm^2 (lāzera drošības standarts < 200 mW/cm^2 [70]). Mērījumu iekārta shematiski paradīta 3.1.(a). attēlā. Zondes iekšpusē ir apvienotas septiņas optiskās šķiedras, kas nostiprinātas 3 mm attālumā no ādas virsmas; sešas šķiedras ir savienotas ar monohromatoru un viena ar lāzeri. Monohromatora izejā ir pieslēgts detektors PMC-100-4 (fotoelektronu pavairotājs), kas savienots ar TCSPC SPC-150 karti sinhronizācijai, datu reģistrēšanai, saglabāšanai un apstrādei.

Iegūtie dati tika analizēti ar trīskāršo eksponenciālo aproksimāciju, izmantojot SPCImage programmu no Backer&Hickl iekārtas:

$$f(t) = a_1 e^{-t/\tau_1} + a_2 e^{-t/\tau_2} + a_3 e^{-t/\tau_3}, \quad (11)$$

kur $f(t)$ – multi-eksponenciāla funkcija, a – amplitūda, t – laiks, τ – fluorescences dzīves laiks. Programma saglabā fluorescences dzīves laika komponentes τ_1, τ_2, τ_3, to amplitūdas a_1, a_2, a_3 un AF kinētiku. Datu apstrādē tika izmantota triju eksponentu aproksimācija, jo tā, salīdzinot ar divu eksponentu aproksimāciju, deva labāku sakritību ar mērījumu rezultātiem [*VI, VII*].

Publikācijās [*IV, V*], ir aprakstīti AF dzīves laika kinētikas mērījumi. Kas veikti ik pa 10 sekundēm, nepārtraucot fotoizbalēšanas procesu (3 minūtes). Mērījumu laikā tika iegūts datu masīvs ar dzīves laika kinētiku un AF intensitātes dilšanu fotoizbalēšanas laikā. Apstrādei izvelēti AF dzīves laika kinētikas mērījumi pie fiksētiem laika intervāla masīviem (skat. 3.2. sadaļu un 3.3. attēlu). Rezultāti parādīja, ka pie dažādiem laika intervāliem AF intensitātes dilšana notiek ar atšķirīgu ātrumu, kas deva priekšstatu par fluorofora sadalījuma izmaiņām fotoizbalēšanas procesā. Turpmākam pētījumam tika izvelēta TRES metodika fluoroforu sadalījuma noteikšanai.

AF kinētikas dati tika analizēti, izmantojot TRES (time resolved emission spectra) apstrādes metodi. TRES analīzes metode pēta, kā mainās spektra forma dzišanas laikā pēc ierosmes pārtraukuma jeb pēta emisijas spektra evolūciju laikā. Atkarībā no tā, cik daudz fluoroforu ar dažādiem dzīves laikiem un spektra formām iesaistās procesā, izmainās spektra forma laikā. TRES iegūšanas princips parādīts 3.4. attēlā, kur uz abscisu ass atlikts viļņa garums (λ), uz ordinātu ass – intensitāte (I) [94].

Šajā darbā ar TRES iegūtie spektri tika normēti pēc intensitātes maksimuma un prezentēti kā *normētie TRES spektri*.

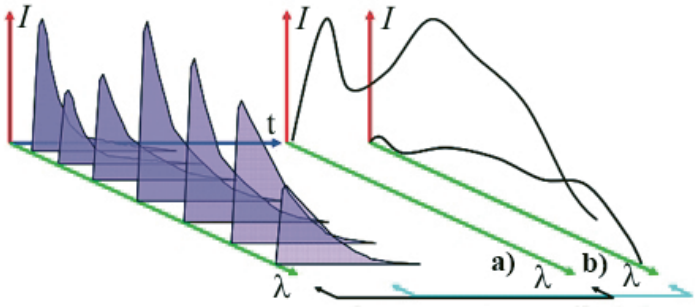

3.4. att. TRES metodes shēma.

3.4. Ādas autofluorescences dzīves laika attēlošana

Eksperimentālā iekārta ādas AF dzīves laika attēlošanas mērījumiem shematiski ilustrēta 3.1. (b). attēlā, kur optiskā šķiedra ir savienota ar x-y skeneri. AF, ierosināta ar 405 nm vai 470 nm impulsu lāzeri, tiek reģistrēta pie 550 nm viļņa garuma. Fotoizbalēšana tika nodrošināta, pārslēdzot lāzeru no impulsu uz nepārtrauktu starojuma režīmu ar jaudas blīvumu 40 mW/cm^2. Apstarots ādas apgabals 2–3 mm diametrā, skenēšanas virsma 1 cm^2. Attēla apstrāde veikta ar SPCImage programmu no Becker&Hickl [93]. Datu analīzei izvēlēta trīskārša eksponenciāla aproksimācija.

Tika uzņemti attēli pirms un pēc fotoizbalēšanas no ādas un intradermāla nēvusa. AF ierosināta ar 405 nm impulsa lāzeri un reģistrēta pie 550 nm. Mērījumi veikti, piestiprinot skeneri noteiktā ādas vietā. Fotoizbalēšanas nodrošināšanai nepārtraukti skenēta virsma līdz 5 minūtēm ar 405 nm nepārtraukta starojuma lāzeri pie jaudas blīvuma 40 mW/cm^2. Dati tika apstrādāti SPCImage programmā, un tika saglabāta informācija par fluorescences dzīves laika komponentēm un fluorescences intensitāti katrā pikselī (3.5. attēls.) Dati tika analizēti ar trīskāršo eksponenciālo aproksimāciju (11).

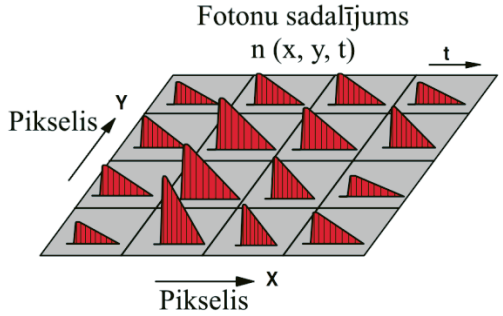

3.5. att. Fluorescences dzīves laika kinētika, katrā pikselī [93].

3.5. Autofluorescences dzīves laika mērījumi, ierosinot ar 405 nm pikosekunžu impulsa lāzeri pirms un pēc fotoizbalēšanas

Ādas AF dzīves laika mērījumi tika veikti spektra diapazonā 440–600 nm, ierosinot ar 405 nm impulsa lāzeri, pirms un pēc fotoizbalēšanas. Eksperimenta gaitā mērījumu diapazons tika sadalīts divās daļās, 440–500 nm un 510–600 nm, un mērījumi katrā spektra daļā tika veikti atsevišķi. Ādas AF dzīves laiku spektrālais sadalījums ilustrēts 3.6. un 3.7. attēlā, salīdzinot τ vērtības pirms un pēc AF fotoizbalēšanas spektra diapazonā 440–500 nm 3.6. attēlā un 510–600 nm 3.7. attēlā. Ādai "ātrās" komponentes τ_1 vērtība praktiski nemainījās, bet AF dzīves laika komponente τ_2 palielinājās no 5,0 ns līdz 7,5 ns spektra diapazonā 530–570 nm 3.7. attēlā. Novērota arī komponentes τ_3 samazināšanās no 10,5 ns līdz 7,5 ns diapazonā 530–600 nm. Ņemot vērā literatūras datus [81], tika pieņemts, ka ādai dzīves laika komponente τ_1 (0,3–2,0 ns) atbilst NAD(P)H fluoroforiem, τ_2 (~ 5,2 ns) – flavīnu grupai un τ_3 (> 7,0 ns) – lipopigmentiem un/vai melanīnam [26, 38, 81]. Diapazonā 440–510 nm ievērojamas AF dzīves laika komponenšu vērtību izmaiņas nav novērotas 3.6. attēlā.

Mērījumi tika turpināti arī pēc publikācijas [*III, IV, V, VI, VII*] un apstrādāti ar uzlabotu algoritmu programmā SPCImage, kas deva iespēju konstatēt autofluorescences dzīves laika izmaiņas ne tikai komponentei τ_3, bet arī komponentei τ_2.

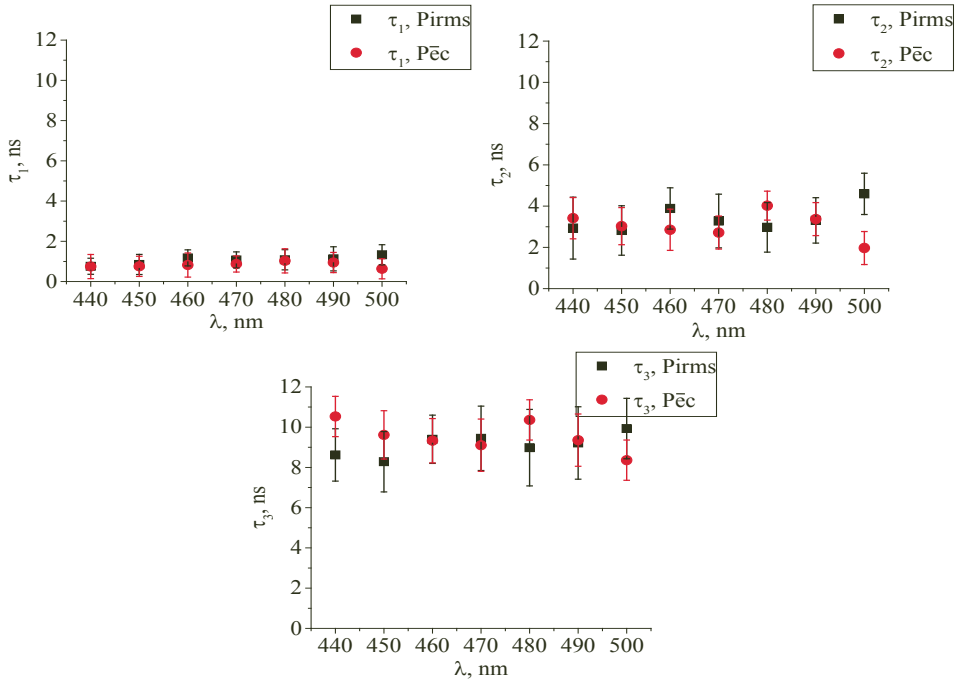

3.6. att. Ādas autofluorescences dzīves laika τ_1, τ_2, τ_3 komponenšu vērtības pirms un pēc ādas fotoizbalēšanas *in vivo* mērījumiem diapazonā 440–500 nm, ierosinot ar 405 nm pikosekunžu impulsu lāzeri.

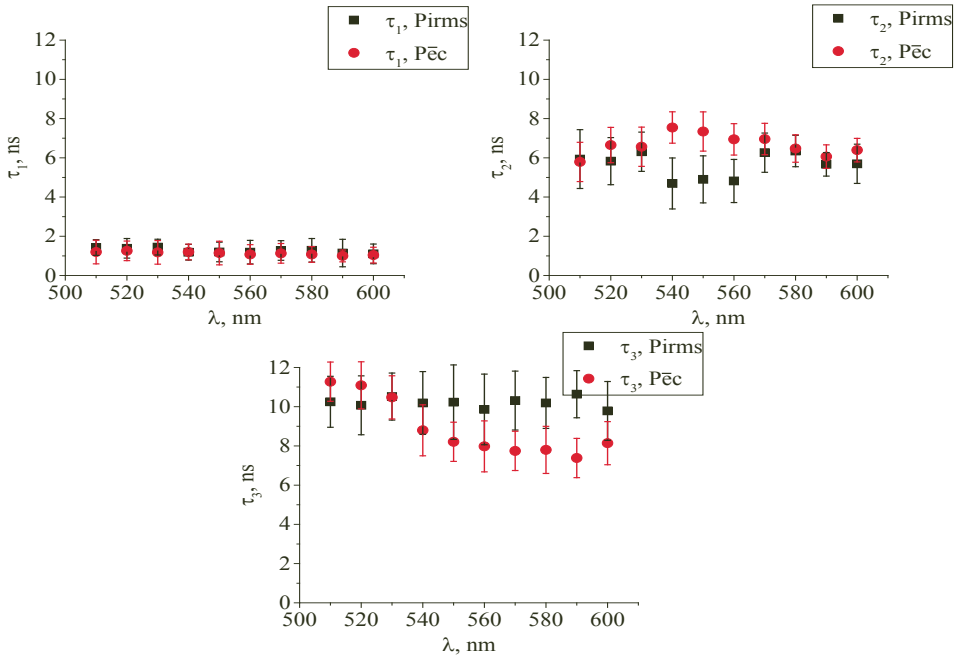

3.7. att. Ādas autofluorescences dzīves laika τ_1, τ_2, τ_3 komponenšu vērtības pirms un pēc ādas fotoizbalēšanas *in vivo* mērījumiem diapazonā 510–600 nm, ierosinot ar 405 nm pikosekunžu impulsu lāzeri.

Intradermāla nēvusa fluorescences dzīves laiki, kas uzņemti diapazonā 460–620 nm, ir ilustrēti 3.8. attēlā, salīdzinot τ vērtības pirms un pēc 3 minūšu autofluorescences fotoizbalēšanas. Tika novērota autofluorescences dzīves laika samazināšanās komponentēm τ_2 un τ_3 spektrālā diapazonā 480–620 nm. Līdzīgi kā ādai, "ātrā" dzīves laika komponente τ_1 šajā spektra rajonā praktiski nemainījās.

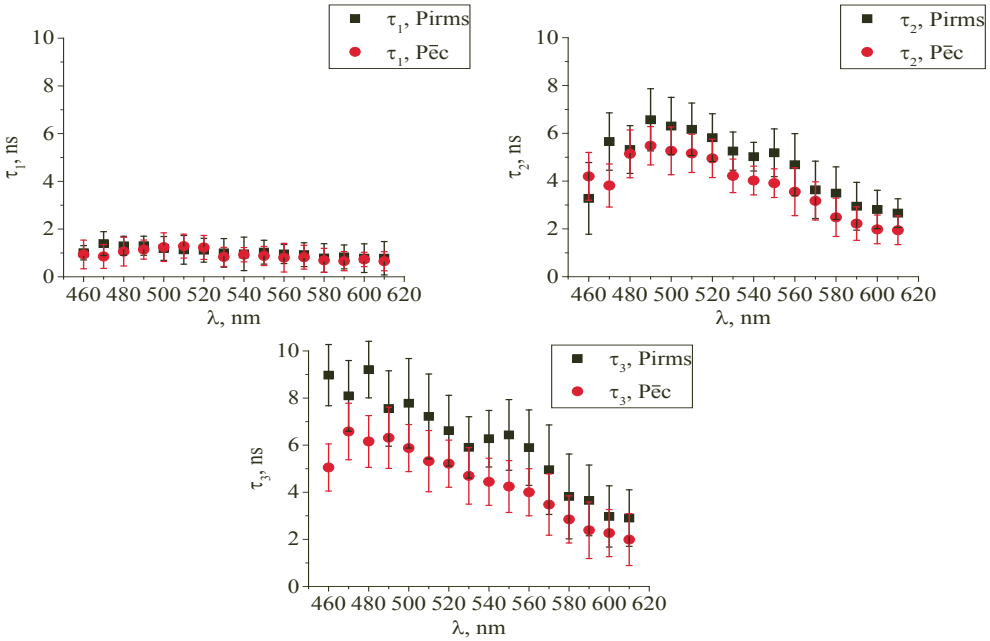

3.8. att. Intradermāla nēvusa autofluorescences dzīves laika τ_1, τ_2, τ_3 komponenšu vērtības pirms un pēc fotoizbalēšanas spektra diapazonā 460–610 nm, ierosinot ar 405 nm pikosekunžu impulsu lāzeri.

TRES apstrādes metodei tika atlasīti un pēc maksimumiem normēti ādas dati pie 1 ns, 5 ns, 10 ns, 15 ns, un 20 ns, spektrālajā diapazonā 430–510 nm (3.9. attēls) un 510–600 nm (3.10. attēls), no intradermāla nēvusa – spektrālajā diapazonā 460–610 nm (3.11. attēls). Ādas fluroforu emisijas spektros (1.10. attēls) NAD(P)H maksimums atrodas pie 460 nm, bet flavīnu grupai, lipopigmentiem un melanīnam diapazonā 550–600 nm. Varam secināt, ka ādai pēc fotoizbalēšanas notiek emisijas maksimumu nobīde no NAD(P)H uz flavīnu un lipopigmentu emisijas maksimuma pusi laika intervālos, sākot no 5 ns (3.9. attēls). Normētie TRES spektri no intradermāla nēvusa parādīti 3.11. attēlā. Ir novērojamas spektra kontūra izmaiņas, bet izteiktas maksimuma nobīdes nav novērotas.

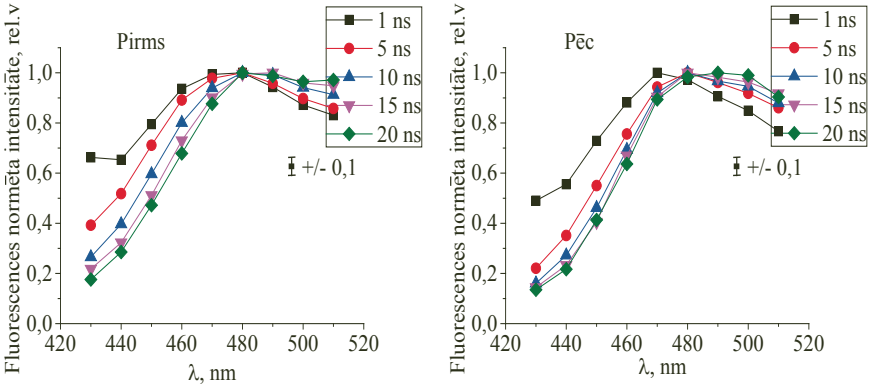

3.9. att. Normētie TRES spektri no ādas diapazonā 430–510 nm, ierosinot ar 405 nm pikosekunžu impulsu lāzeri.

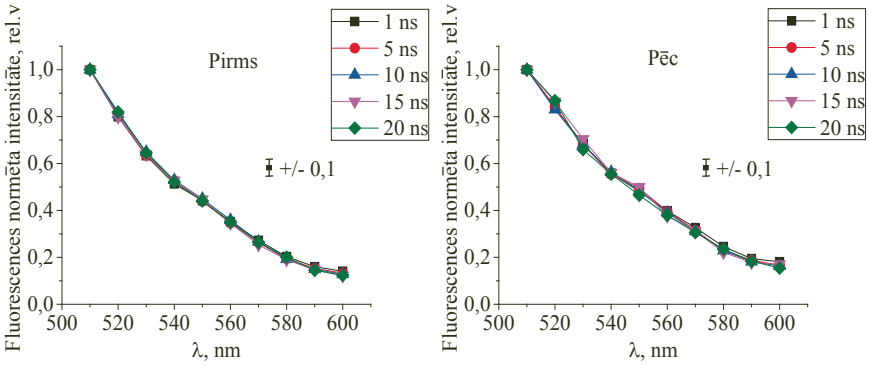

3.10. att. Normētie TRES spektri no ādas diapazonā 510–600 nm, ierosinot ar 405 nm pikosekunžu impulsu lāzeri.

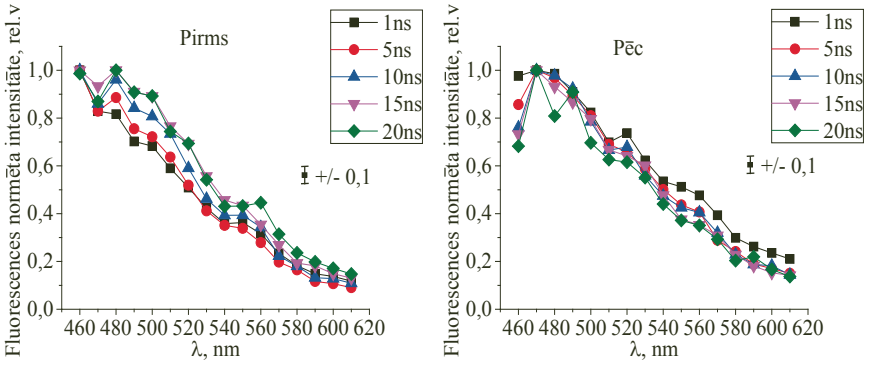

3.11. att. Normētie TRES spektri no intradermāla nēvusa diapazonā 460 – 610 nm, ierosinot ar 405 nm pikosekunžu impulsu lāzeri.

3.6. Autofluorescences dzīves laika mērījumi, ierosinot ar 470 nm pikosekunžu impulsu lāzeri pirms un pēc fotoizbalēšanas

Autofluorescences dzīves laika mērījumi ar 470 nm pikosekunžu impulsu lāzera ierosmi tika izmantoti, lai pārbaudītu dzīves laika komponentes τ_2 izmaiņas pēc fotoizbalēšanas. Ņemot vērā, ka τ_2 teorētiski atbilst flavīnu grupai, kuru var ierosināt arī ar 470 nm lāzeri, tika atkārtots eksperiments dzīves laika mērījumiem diapazonā 510–600 nm. Autofluorescences dzīves laika komponenšu vērtību spektrālās atkarības grafiski parādītas 3.12. attēlā, kur redzama sagaidāmā tendence τ_2 pieaugšanai no 3 ns līdz 6 ns spektra diapazonā 530–550 nm.

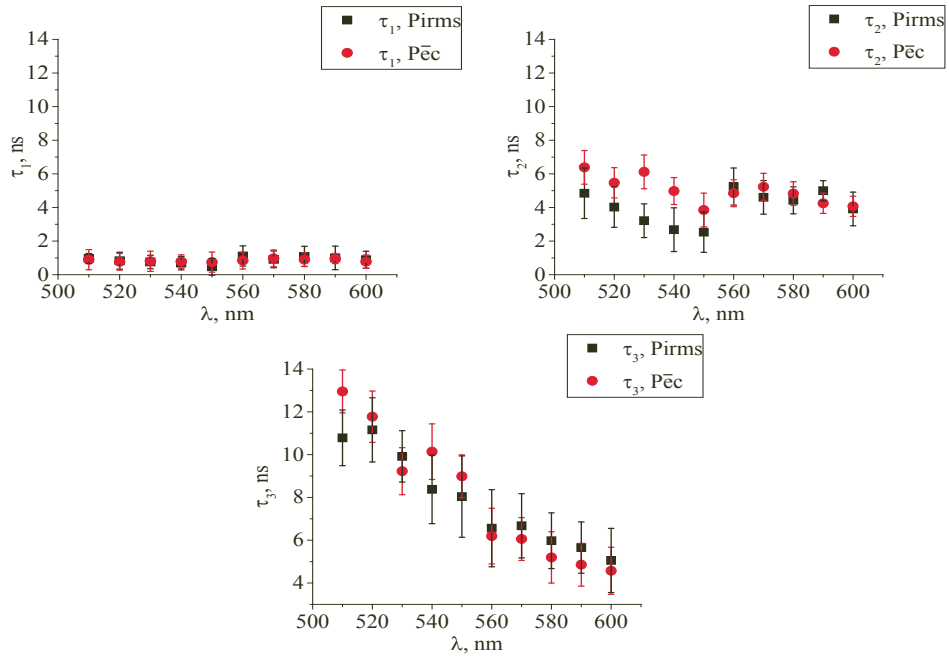

3.12. att. Ādas AF dzīves laika τ_1, τ_2, τ_3 komponenšu vērtības pirms un pēc fotoizbalēšanas *in vivo* mērījumos spektra diapazonā 510–600 nm, ierosinot ar 470 nm pikosekunžu impulsu lāzeri.

TRES apstrādes metodei tika atlasīti un pēc maksimumiem normēti ādas dati pie 1 ns, 5 ns, 10 ns, 15 ns, un 20 ns, spektra diapazonā 510–600 nm, ierosinot ar 470 pikosekunžu impulsu lāzeri (3.13. attēls). Nav novērojamas spektra kontūra izmaiņas. Spektra maksimums atrodas ārpus pētāmā diapazona, tāpēc novērot tā nobīdi nav iespējams.

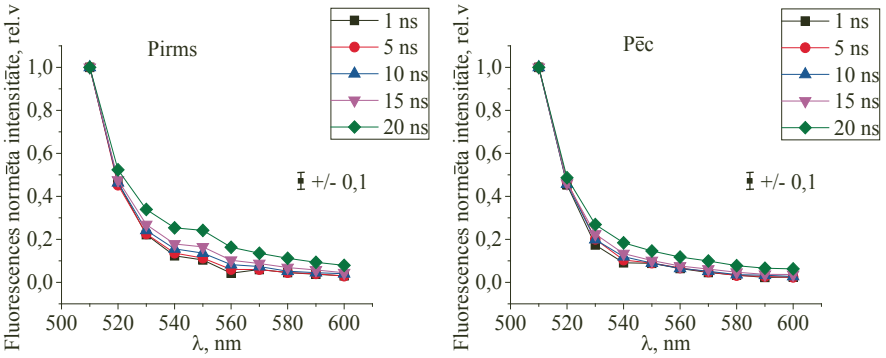

3.13. att. Normētie TRES spektri no ādas diapazonā 510–600 nm, ierosinot ar 470 nm pikosekunžu impulsu lāzeri.

3.7. Ādas autofluorescences dzīves laika komponenšu virsmas sadalījuma attēlošana

3.14. un 3.15. attēlā parādīti rezultāti ādas AF dzīves laika sadalījuma attēlošanas mērījumiem ar skeneri, ierosinot ar 405 nm (3.14. attēls) un 470 nm (3.15. attēls) pikosekunžu impulsu lāzeriem, AF reģistrēta pie 550 nm. Viļņa garums AF reģistrēšanai izvēlēts, lai nodrošinātu salīdzinājumu ar iepriekšējiem mērījumiem, ierosinot AF ar 405 nm un 470 nm. Rezultāti apliecina, ka AF dzīves laika komponentes τ_2 vērtība pēc fotoizbalēšanas pieaug. 3.14. un 3.15. attēlā pirmajā kolonnā ir attēlota ādas AF dzīves laika komponenšu vērtību sadalījuma attēls, otrajā kolonnā – AF dzīves laika komponenšu vērtības histogramma pirms fotoizbalēšanas (analīzei izvēlēts neapstarots ādas apgabals), trešajā kolonnā – AF dzīves laika komponenšu vērtības histogramma pēc apstarošanas (analīzei izvēlēts apstarots ādas apgabals). Attēlā ādas apstarotais (fotoizbalētais) apgabals parādās kā tumšāks laukums. Apstrāde tika veikta ar trīskāršo eksponenciālo aproksimāciju, katram τ_1, τ_2, τ_3 sadalījumam izveidots atsevišķs attēls.

	Ādas autofluorescences dzīves laiku parametru sadalījuma attēli, ierosinot ar 405 nm un reģistrējot AF pie 550 nm	Parametru vērtība neapstarotā laukumā	Parametru vērtība apstarotā laukumā
τ_1	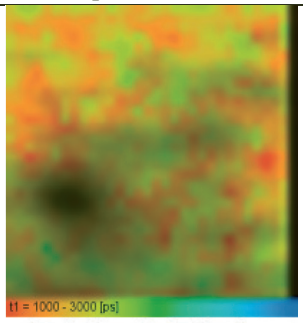	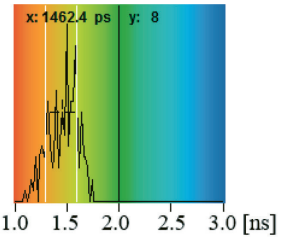	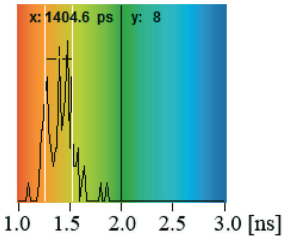
τ_2	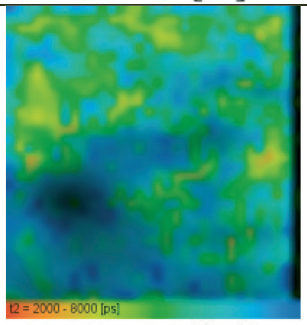	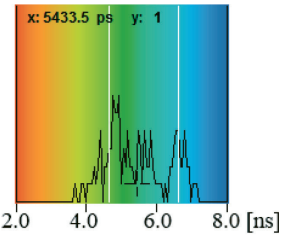	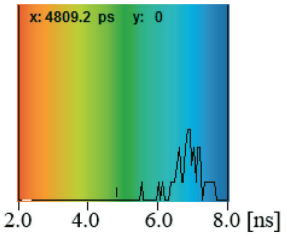
τ_3	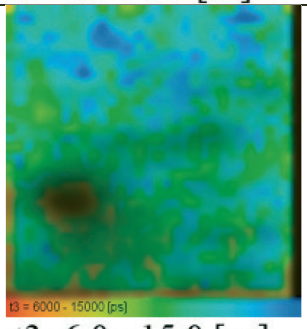	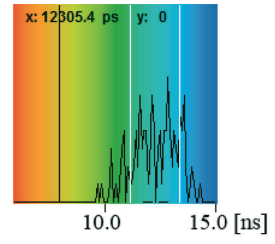	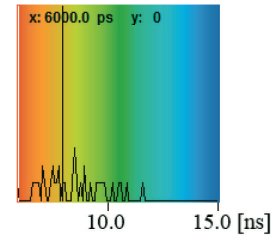

3.14. attēls. Ādas autofluorescences dzīves laika τ_1, τ_2, τ_3 komponenšu vērtību sadalījuma attēli (pirmā kolonna) un vērtību sadalījuma izmaiņas pirms (otrā kolonna) un pēc (trešā kolonna) fotoizbalēšanas. AF reģistrēta pie 550 nm, ierosinot ar 405 nm pikosekunžu impulsu lāzeri.

	Ādas autofluorescences dzīves laiku parametru sadalījuma attēli, ierosinot ar 470 nm un reģistrējot AF pie 550 nm	Parametru vērtība neapstarotā laukumā	Parametru vērtība apstarotā laukumā
τ_1	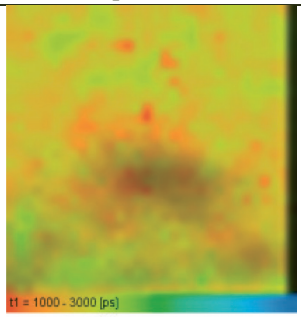 t1=1.0 - 3.0 [ns]	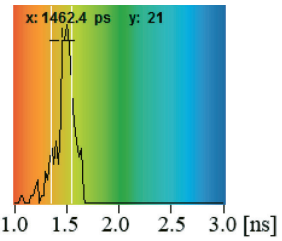	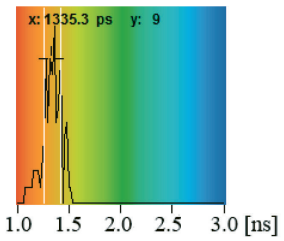
τ_2	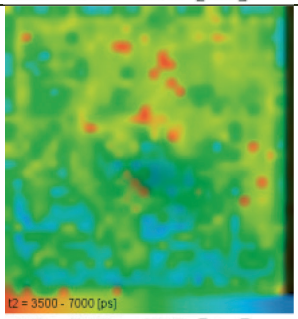 t2=3.5 - 7.0 [ns]	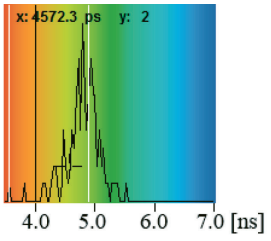	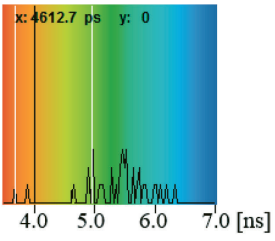
τ_3	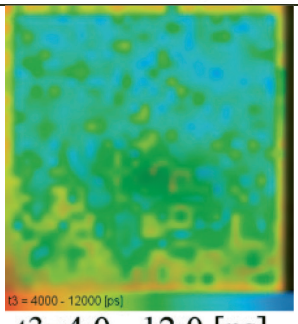 t3=4.0 - 12.0 [ns]	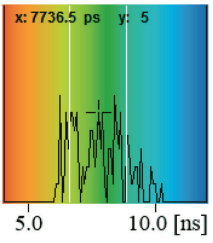	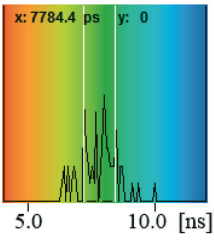

3.15. attēls. Ādas autofluorescences dzīves laika τ_1, τ_2, τ_3 komponenšu vērtību sadalījuma attēli (pirmā kolonna) un vērtību sadalījuma izmaiņas pirms (otrā kolonna) un pēc (trešā kolonna) fotoizbalēšanas. AF reģistrēta pie 550 nm, ierosinot ar 470 nm pikosekunžu impulsu lāzeri.

Rezultāti parādīja sagaidāmās AF dzīves laiku izmaiņas pēc fotoizbalēšanas: fluorescences dzīves laika komponente τ_2 pieaug un τ_3 samazinās pie ierosmes ar 405 nm pikosekunžu impulsa lāzeri un veicot fotobalēšanu ar nepārtraukta starojuma 405 nm lāzeri (3.14. attēls). Ierosinot ar 470 nm pikosekunžu impulsu lāzeri un veicot fotobalēšanu ar 470 nm nepārtraukta starojuma lāzeri, τ_2 pieaug, reģistrējot fluorescenci pie 550 nm (3.15. attēls).

Kā jau minēts, autofluorescences dzīves laika komponente τ_2 teorētiski atbilst flavīnu fluoroforu grupai, bet τ_3 lipopigmentiem un/vai melanīnam.

3.8. Korelācija starp dzīves laika komponentēm un autofluorescences intensitāti no ādas un intradermāla nēvusa

3.16. attēlā katrs grafiks atbilst vienai AF dzīves laika komponentei (τ_1, τ_2, τ_3), kur uz ordinātu ass atlikta komponentes vērtības starpība pirms un pēc fotoizbalēšanas $\Delta\tau = \tau_{pirms} - \tau_{pēc}$, uz abscisu ass atlikta autofluorescences intensitātes procentuālā izmaiņa pēc fotoizbalēšanas $\Delta I(\%) = \left(\frac{I_{pirms} - I_{pēc}}{I_{pirms}}\right) \cdot 100\%$.

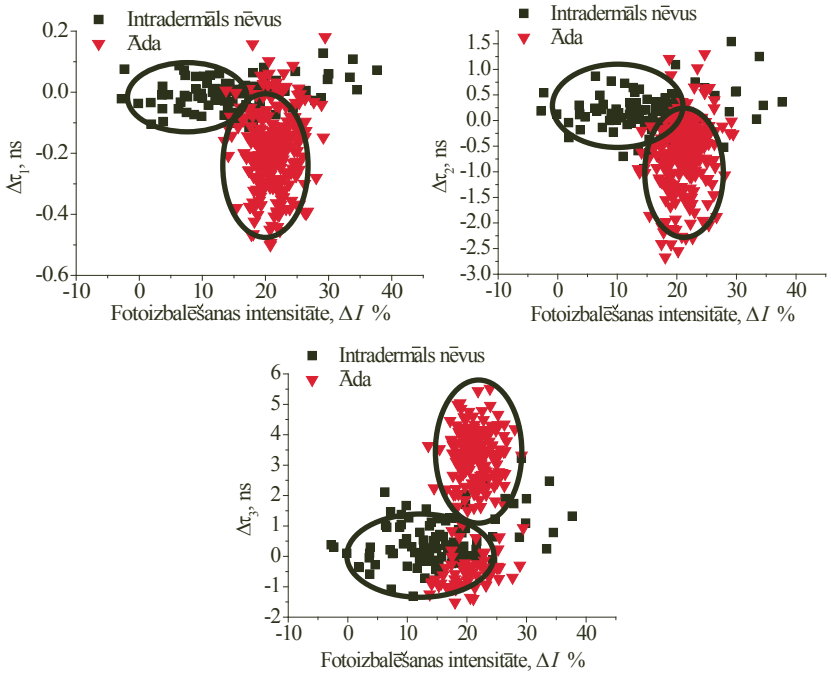

3.16. att. Korelācijas grafiki AF dzīves laikam un intensitātes samazinājumam pēc fotoizbalēšanas no ādas un intradermāla nēvusa.

Fotoizbalēšanas laikā ādas AF intensitāte samazinās par ~20 %, intradermāla nēvusa intensitātes samazinājums ir diapazonā 0 – 40 %. Savukārt dzīves laika komponentes izmaiņa $\Delta\tau_1$ ādai svārstās zem 0,5 ns, bet intradermālam nēvusam vērtības ir ap 0; $\Delta\tau_2$ ādai – līdz 3,0 ns, nēvusam svārstās ap 0,0 ± 1,0 ns; $\Delta\tau_3$ ādai – sasniedz 5,0 ns, nēvusam svārstības ir no 0,0 līdz 2,0 ns. τ noteikšanas kļūda ir 0,5 ns.

3.9. Secinājumi par autofluorescences pētījumiem impulsu ierosmē

Eksperimentālie rezultāti apliecina fotoizbalēšanas ietekmi uz ādas un intradermālā nēvusa AF spektrālajiem un kinētiskajiem parametriem. Uz ādas τ_2, kas atbilst flavīnu grupai, novērota AF dzīves laika palielināšanās no 5,0 ns līdz 7,5 ns spektra diapazonā 530 – 570 nm; τ_3, kas atbilst lipopigmentiem un/vai melanīnam, novērota AF dzīves laika samazināšanās no 10,5 nm līdz 7,5 ns spektra diapazonā 530 – 600 nm. FAD AF dzīves laika palielināšanās novērota ieplūstošām vēža šūnām [26, 95].

Normētie TRES spektri sniedz priekšstatu par ādas fluoroforu AF intensitātes izmaiņām fotoizbalēšanas laikā. Pirms fotoizbalēšanas dominē NAD(P)H fluoroforu AF intensitāte, pēc fotoizbalēšanas tiek novērota intensitātes maksimuma nobīde uz lielāka viļņa garuma spektra pusi, tādējādi var secināt, ka fotoizbalēšanas efekta ietekmē visvairāk samazinās NAD(P)H koncentrācija ādas šūnā. NAD(P)H koncentrācijas samazināšanās izraisa oksidatīvo stresu. Oksidatīvajā stresā rodas brīvie radikāļi, kas var izraisīt šūnas nāvi, vai radīt vēža šūnas, ja regulējošie mehānismi nepaspēj atjaunot šūnas *redoks* procesu. NAD(P)H AF samazināšanās attiecībā pret FAD novārota šūnās, kas atrodas blakus ļaundabīgam veidojumam [96].

Korelācijas rezultāti (3.16 att.) apliecina potenciālas iespējas izmantot doto metodi ādas jaunveidojumu diagnostikai.

4. ĀDAS DIFŪZĀS ATSTAROŠANAS MĒRĪJUMI

4.1. Literatūras pārskats par ādas optiskas īpašības pētījumiem

Pētot ādas optiskās īpašības, galvenā uzmanība tiek pievērsta tās spēcīgākajiem absorbentiem – hemoglobīnu un melanīnu. Absorbcijas spektri paradīti 1.12. attēlā.

N. Kollias u. c. 2001. gadā [40] pētīja ādas izkliedes īpašības atkarībā no melanīna koncentrācijas. Novērota oksihemoglobīna un melanīna absorbcija difūzās atstarošanas spektrā. Pētījuma laikā melanīna koncentrāciju palielināja ar UVB (280–315 nm) apstarošanu un secināja, ka izkliedes efektivitāte ir nedaudz lielāka pie lielākas melanīna koncentrācijas.

J. Lesiņš u. c. 2011. gadā [97], pētot ādas autofluorescences spektrus pēc neilgas apstarošanas ar 405 nm lāzeri, tajos novēroja oksihemoglobīna absorbcijas pīķus pie 542 nm un 577 nm. 4.1. attēlā fluorescences spektri ir pārveidoti attiecībā:

$$I(I_0, \lambda) = \frac{\Delta I}{I_0} = \frac{I(\lambda)_{t=0} - I(\lambda)_{t=5min}}{I(\lambda)_{t=0}}, \text{ kur} \qquad (12)$$

I_0 – sākuma fluorescences intensitāte,

I – fluorescences intensitāte pēc apstarošanas.

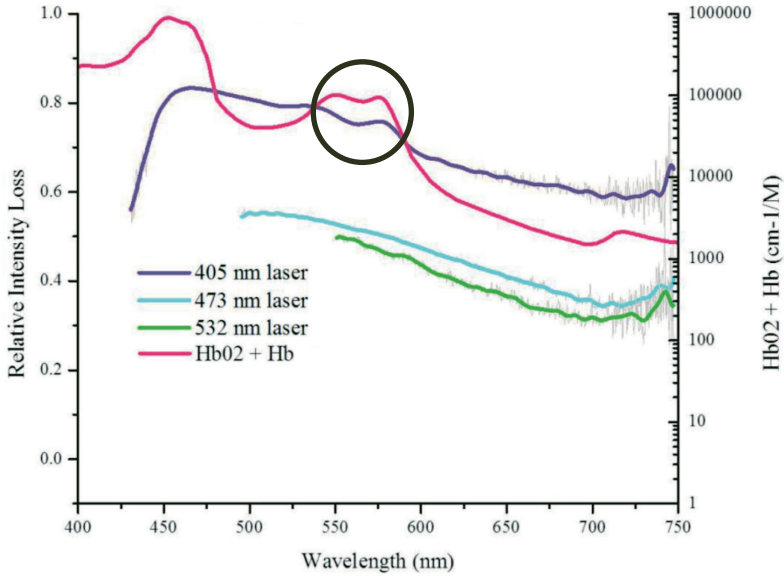

4.1. att. AF intensitāte pārveidota, izmantojot attiecību (12), fluorescence ierosināta ar 405 nm, 473 nm, 532 nm viļņa garumu un rezultāti salīdzināti ar oksihemoglobīna absorbcijas spektru.

Yu. P. Siničkins u. c. 2014. gadā [98] pētīja āda izkliedes un absorbcijas īpašības oklūzijas laikā ar difūzas atstarošanas metodi diapazonā no 500 nm līdz 900 nm. Tika secināts ka, samazinoties oksihemoglobīna koncentrācijai, izmainās ādas izkliedes un absorbcijas īpašības.

Ādai un jaunveidojumiem ir atšķirīgs fluoroforu/hromoforu sastāvs un to blīvums, kas var ietekmēt gaismas iespiešanās dziļumu un difūzi atstaroto fotonu izkliedes ceļu ādas struktūrās. Lai to novērtētu, ar iepriekš aprakstīto iekārtu tika veikti ādas difūzās atstarošanas kinētikas (TOF – *time of flight*) mērījumi pie fiksētiem viļņu garumiem, līdzīgi kā Lundas grupas pētnieku darbos [99, 100].

4.2. Iekārtas ādas difūzās atstarošanas mērījumiem

Kontakta metodes iekārta sastāv no (4.2. attēls):

- Baltās gaismas avota – halogēna lampas, AvaLight-HAL, Avantes BV, NL;
- Spektra detektora – divkanālu spektrometra AvaSpec-2048-2, 2048 pikseļu CCD kamera ar spektrālo jutību no 200 nm līdz 1100 nm, izšķirtspēja 2.1 nm, Avantes BV, NL;

Lāzeriem:

- 405 nm, MBL-III-405 nm – 50 mW, CNI, Ķīna ;
  darbības režīms: nepārtraukts;
  maksimālā izejas jauda: 70 mW.
- 473 nm, MBL-III-473 nm – 30 mW, CNI, Ķīna;
  darbības režīms: nepārtraukts;
  maksimālā izejas jauda: 70 mW.
- 532nm BremLas, Series GL-V6, NE 60825 (Vācija);
  darbības režīms: nepārtraukts;
  maksimālā izejas jauda: 60 mW.

Optiskās zondes – trīs optiskās šķiedras, kas apvienotas vienā galā, 3 mm attālumā no ādas virsmas.

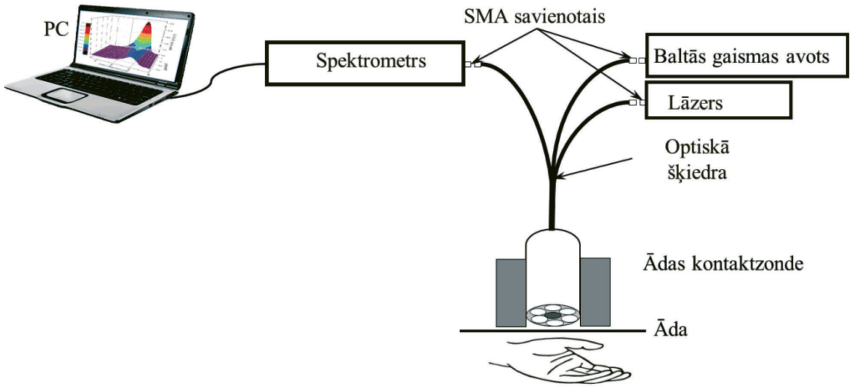

4.2. att. Kontakta metodes eksperimentālās iekārtas shēma.

4.2. attēlā shematiski parādīta kontakta metodes eksperimentālā iekārta. Difūzās atstarošanas spektrs tika reģistrēts pirms apstarošanas (tas tika izmantots kā reference) un pēc 60 sekunžu apstarošanas. Apstarošana tika veikta ar vienu no nepārtraukta starojuma lāzeriem (405 nm, 473 nm vai 510 nm) ar jaudas blīvumu no 20 mW/cm^2 līdz 120 mW/cm^2. Katram nākamajam mērījumam izvēlēta jauna, neapstarota ādas virsma.

Difūzās atstarošanas intensitātes spektri pirms un pēc apstarošanas pārveidoti optiskā blīvuma spektros, izmantojot formulu:

$$OD = -log_{10}\left(\frac{I}{I_0}\right), \text{ kur} \qquad (13)$$

I – difūzās atstarošanas intensitāte pēc apstarošanas,
I_0 – intensitāte pirms apstarošanas.

Bezkontakta metodes iekārta sastāv no (4.3. attēls):

- baltās gaismas avota – halogēna lampu gredzena;
- spektra detektora – Nuance 2.4 multispektrālās kameras, Cambridge Research & Instrumentation, Inc., USA (1392 × 1040 pikseļi), mērījumu spektra intervāls 450 nm – 950 nm.

Lāzeriem:

- 405 nm MBL-III-405 nm – 50 mW, CNI, Ķīna;
  darbības režīms: nepārtraukts;
  maksimālā izejas jauda: 70 mW.
- 473 nm MBL-III-473 nm – 30 mW, CNI, Ķīna;
  darbības režīms: nepārtraukts;
  maksimālā izejas jauda: 70 mW.

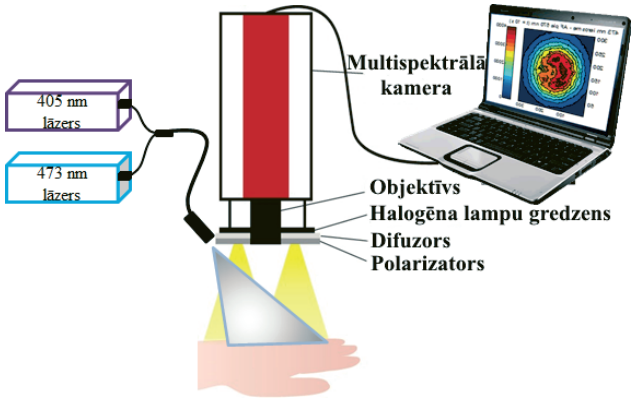

4.3. att. Bezkontakta metodes eksperimentālās iekārtas shēma.

Difūzās atstarošanas spektrs tika reģistrēts 20 cm attālumā no ādas virsmas ar attēlošanas iekārtu, kas paradīta 4.3. attēlā. Difuzors un polarizators tika izvietoti aiz halogēnās lampasgredzena, polarizējot gaismu ortogonālā virzienā attiecībā pret multispektrālajā kamerā iebūvēto polarizatoru, tādējādi no virsmas tieši atstarotā gaisma, kas nemainīja savu polarizācijas plakni, netika detektēta. Kamera ar iebūvētu šķidro kristālu filtru uzņem spektrālos attēlus intervālā 450 nm – 750 nm, ar soli 10 nm, katrā attēlā izšķirtspēja 0.75 × 0.75 mm atbilst vienam pikselim. Viens spektrālo attēlu masīvs I_0 kā reference uzņemts pirms apstarošanas un otrs spektrālo attēlu masīvs I – pēc apstarošanas. Ādas apstarošana tika veikta 60 sekundes ar vienu no izvēlētiem nepārtraukta starojuma lāzeriem ar jaudas blīvumu 532 nm starojumam – 120 mW/cm^2, 473 nm – 100mW/cm^2, 405 nm – 70 mW/cm^2. *CRi Nuance* programma datu apstrādei iegūtos attēlu masīvus pārvērš optiskā blīvuma kartēs, izmatojot formulu (13).

Fotona lidojuma laika eksperimentālā mērījumu iekārta sastāv no (3.1. attēls):

- TCSPC (Time-correlated single photon counting): SPC – 150, Becker&Hickl;
- Optisko šķiedru Y-veida kūļa, katras optiskās šķiedras serdeņa diametrs 200 μm;
- Lāzeriem – PicoQuant, LDH-D-C-405 (impulsa pusplatums 59 ps); LDH-D-C-510 (impulsa pusplatums 107 ps);
- Detektora – fotoelektronu pavairotāja PMC-100-4, Becker&Hickl;
- Monohromatora.

Pikosekunžu lāzeru difūzā atstarošana no *in vivo* ādas tika reģistrēta caur monohromatoru, kas uzstādīts uz tā paša viļņa garuma kā lāzers (3.1. attēls). Monohromators tika izmantots kā filtrs. lai izvairītos no audu AF reģistrācijas. Optiskās šķiedras zonde, kuras gals atradās 3 mm attālumā no ādas virsmas, bija

cieši nostiprināta perpendikulāri āda virsmai. Mērījumi veikti no ādas un pigmentētiem nēvusiem, iegūtie difūzi atstarotie lāzera impulsi tika salīdzināti pēc impulsa maksimumiem. Apstarošanai izmantoti 405 nm un 510 nm pikosekunžu impulsu lāzeri, novērtētais vidējais starojuma iespiešanās dziļumu ādā pie 405 nm ir ~ 0.1 mm un ~ 0.4 mm – pie 510 nm [101]. Mērījuma kļūdu (~6 ps) nosaka iekārtas uzstādījumi. Mērījumu rezultātu apstrādei tika reģistrēti ~ 100000 fotonu, kas aizņēma laiku no vienas sekundes līdz pat minūtei, atkarībā no ādas un nēvusa pigmentācijas pakāpes. Lāzera jaudas blīvums apstarošanai nepārsniedza atļauto dozu, mērījumi veikti ar Ētikas Komitejas atļauju. Pētījumā piedalījās 10 brīvprātīgie, vecuma no 22 līdz 30 gadiem, ar II ādas tipu [102].

4.3. Difūzās atstarošanas mērījumu rezultāti

Mērījumi ar kontakta metodi tika veikti laboratorijas apstākļos uz 10 brīvprātīgiem ar II un III ādas tipu [102]. 4.4. attēlā sniegtie rezultāti parāda, ka, pārvēršot difūzās atstarošanas spektrus optiskajā blīvumā, pēc apstarošanas novērojami pīķi pie 540 nm un 570 nm, kas atbilst oksihemoglobīna absorbcijas maksimumiem. Mērījumi tika veikti pie dažādiem lāzera jaudas blīvumiem. Viszemākais jaudas blīvums izraisīja minimālas izmaiņas difūzas atstarošanas spektrā. Vislielākais jaudas blīvums tika izvēlēts 532 nm lāzeram, iekļaujoties drošības standartos atļautajās apstarošanas devas robežās, 405 nm un 473 nm lāzeram maksimālās intensitātes izvēlētas pēc pacienta jutības pret apstarošanu.

Absorbcijas efektivitāte ir atkarīga no izvēlētā viļņa garuma. Kā redzams grafikos, pēc lāzera apstarošanas ar 532 nm absorbcija ir zemāka, nekā apstarojot ar 473 nm un 405 nm. Visintensīvāk tā ir izteikta 405 nm lāzera apstarošanas gadījumā. Oksihemoglobīna absorbciju ietekmē arī lāzera apstarošanas jaudas blīvums.

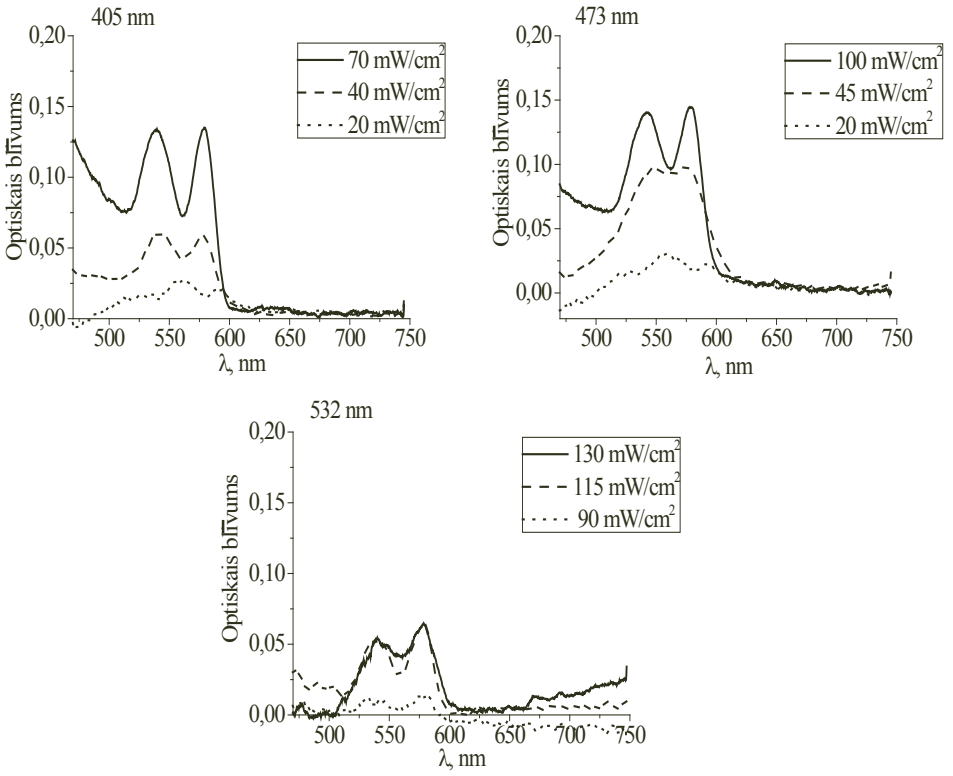

4.4. att. Kontakta metodes rezultāti cilvēka ādas optiskā blīvuma spektra izmaiņām pēc apstarošanas ar 405 nm, 473 nm un 532 nm nepārtraukta starojuma lāzeriem pie jaudas blīvumiem 20–130 mW/cm^2.

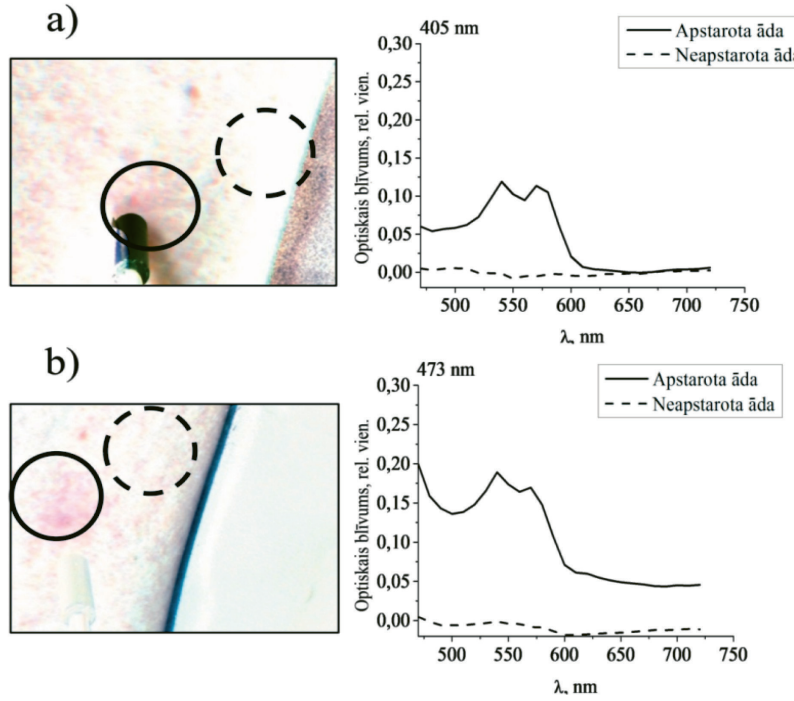

4.5. att. Bezkontakta metodes rezultāti: cilvēka ādas optiskā blīvuma izmaiņas pēc apstarošanas ar 405 nm (a) un 473 nm (b) nepārtraukta lāzera staru ar jaudas blīvumu 70–130 mW/cm^2.

Bezkontakta attēlošanas metode tika izstrādāta punktveida kontakta metodes rezultātu pārbaudei. Kontakta zondes piespiešana varēja izraisīt oklūziju ādas kapilāros lāzera apstarošanas laikā, kas tika izslēgts, reģistrācijai izmantojot multispektrālās attēlošanas kameru. 4.5. attēlā ir parādīti rezultāti pēc 405 nm un 473 nm lāzera apstarošanas, pa kreisi ir multispektrālās kameras attēls pie viļņu garumiem 450–750 nm un pa labi – optiskā blīvuma spektrālais sadalījums norādītajā apstarojuma vietā.

Fotona lidojuma laika mērījumu rezultātos ir konstatēta laika nobīde starp impulsu pīķiem kas atbilst veselai ādai un pigmentētam nēvusam. Pie 405 nm impulsa lāzera starpība svārstās no 19–58 ps. Izejot cauri veselas ādas slāņiem, fotona lidojuma laiks ir lielāks salīdzinājumā ar nēvusu, kas grafiski ir parādīts 4.6. attēlā. Pie 510 nm ierosmes un atbildes impulsu nobīde svārstās no 19–39 ps, kas atspoguļots 4.7. attēlā. 4.8. attēlā ir parādīts laika diapazons, kurā atšķiras fotona TOF, izkliedējoties veselā ādā un nēvusā pie dažādiem viļņa garumiem.

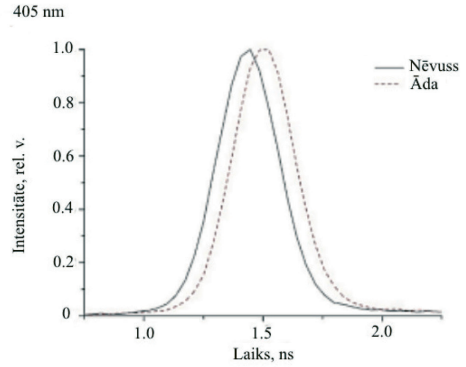

4.6. att. Diffūzi atstaroti 405 nm lāzera impulsi no ādas un nēvusa.

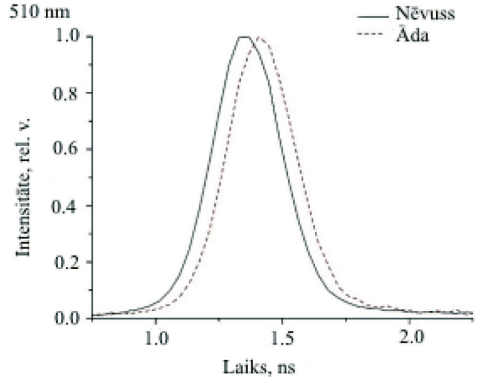

4.7. att. Diffūzi atstaroti 510 nm lāzera impulsi no ādas un nēvusa.

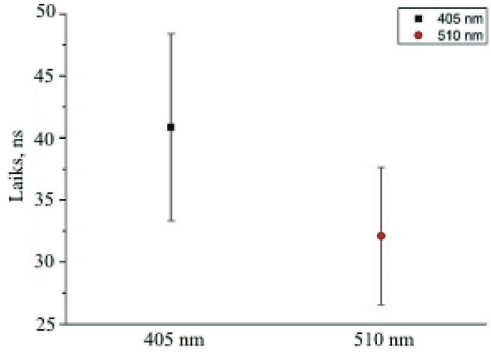

4.8. att. Laika starpība fotonu lidojumam caur ādu un nēvusu pie 405 nm un 510 nm.

4.5. Secinājumi par ādas difūzas atstarošanas mērījumiem

Mērījuma rezultāti parāda, ka pēc nepārtrauktas lāzera in vivo apstarošanas, ādas difūzās atstarošanas spektrā parādās oksihemoglobīna absorbcijas pazīmes. Bezkontakta metode apstiprina, ka šo efektu neietekmē kontakta zondes piespiešana lāzera apstarošanas laikā, kas varēja radīt oklūziju no piespiešanas un izraisīt asins pieplūdumu pētījuma vietā pēc zondes atlaišanas. Oksihemoglobīna absorbcija ir atkarīga no lāzera jaudas blīvuma un apstarošanai izvēlētā viļņa garuma. Rezultāti liecina, ka ilgstoša lāzera apstarošana var ietekmēt mērījuma rezultātus un optiskajā diagnostikā izraisīt kļūdainu diagnozi. Neskatoties uz Eiropas lāzeru drošības standartiem [67] jāņem vērā apstarošanas viļņa garums un apstarošanas laiks. Oksihemoglobīna koncentrācijas palielinājumam var būt dažādi cēloņi:

- apstarošanas laikā cilvēka imūnsistēmas procesi izraisa asins pieplūdumu apstarotajam ādas apgabalam;
- optiskā apstarošana izraisa termisko efektu, kas paplašina kapilārus un palielina asins pieplūdumu, lai izvairītos no audu pārkarsēšanas;
- fotoinducēts ādas eritēmas (iekaisuma) process, līdzīgs saules apdegumam.

Eksperimentā iegūtie dati liecina par atšķirīgo fotona lidojuma laiku ādā un nēvusā, kā arī atšķirība ir novērota pie dažādiem viļņa garumiem. Vidējā vērtību starpība, fotonam izejot caur ādu un nēvusu, ir 41 ps pie 405 nm, un 32 ps pie 510nm. Šī metode ir viegli pielietojama mērījumu veikšanai, jo aizņem maz laika, no sekundes līdz minūtei pie ļoti pigmentētiem jaunveidojumiem. Tādos jaunveidojumos ir liela melanīna koncentrācija, kas absorbē gaismu pie izvelētajiem viļņu garumiem un fotonu uzkrāšana aizņem vairāk laiku. Turpinot pielietot TOF mērījuma metodi, izmantojot citus viļņa garumus, var uzkrāt datu bāzi ne tikai ar ādas jaunveidojumiem, bet arī ar citām pataloģijām. Eksperimenta rezultāti publicēti [*I*] žurnalā.

5. REZULTĀTU KOPSAVILKUMS, SECINĀJUMI UN AIZSTĀVAMĀS TĒZES

Promocijas darbā apskatīti AF kinētikas pielietojumi diagnostikā un pētījumi fotoizbalēšanas ietekmei uz ādas fluoroforiem. Izstrādātas divas ierīces ādas jaunveidojuma *in vivo* diagnostikai, kas balstās uz fotoizbalēšanas efektu, un četras iekārtas *in vivo* pētījumiem AF fotoizbalēšanas ietekmei uz ādas fluoroforiem. Mērierīces, izejot klīnisko aprobāciju, pierādīja pielietojumu iespējas, izmantot AF intensitātes un fotoizbalēšanas kinētikas mērījumus jaunveidojumu diagnostikai. Darba gaita ir aprakstīta nodaļā "Ādas jaunveidojumu autofluorescences foto-izbalēšanas pētījumi nepārtrauktā ierosmē" un nozīmīgākie rezultāti pēc klīniskas aprobācijas un datu apkopojuma ir sekojoši:

- Punktveida ierīce sniedza datus par AF intensitātes vērtībām no pigmentētiem jaunveidojumiem un ādas. Jo lielāka pigmentācija, jo zemāka intensitāte.
- Klīniski apstiprināta iespēja atšķirt BCC jaunveidojumus no pārējiem pigmentētiem jaunveidojumiem, izmantojot N_G parametru. Novērots, ka BCC jaunveidojumiem AF intensitāte ir zemāk un vienmērīgāk sadalīta, nekā ādai un citiem pigmentētiem jaunveidojumiem (2.5., 2.6. attēls).
- Pierādīta iespēja bezkontakta ceļā konstatēt vairākus atšķirīgus patoloģiju veidus vienā ādas jaunveidojumā (netipiska vizuāli viendabīga nēvusa gadījums, 2.7. att.).

Mēriekārtas *in vivo* AF kinētikas ar laika izšķirtspēju pētījumi ir aprakstīti nodaļa "Ādas un jaunveidojumu autofluorescences pētījumi impulsu ierosmē". Darba gaitā tika izstrādātas un eksperimentāli aprobētas 4 metodes pētīšanai un datu analīzei: fluorescences dzīves laika mērījumi ar punktveida un attēlošanas metodi, iegūto datu analīze ar TRES apstrādes metodi un dzīves laiku – fotoizbalēšanas ātruma korelācijas metodi. Eksperimentāli pierādīts, ka AF fotoizbalēšana ietekmē veselās ādas un intradermālā nēvusa fluorescences dzīves laika komponenšu vērtības. Pēc maksimuma normētie TRES spektri sniedza priekšstatu par AF fotoizbalēšanas ietekmi uz ādas fluoroforu sadalījumu. Novērota atšķirīga korelācija starp AF dzīves laika komponentēm un intensitātes izmaiņām pēc fotoizbalēšanas ādai un intradermālam nēvusam (3.16. attēls), kas dod potenciālu iespēju pigmentētu jaunveidojumu diagnostikā. Šī pētījuma nozīmīgākie rezultāti:

- Ierosinot veselās ādas AF ar 405 nm impulsu lāzeri un veicot fotoizbalē-šanu ar 405 nm nepārtraukta starojuma zemjaudas lāzeri (40 mW/cm^2),

dzīves laika komponentes τ_2 vērtība pieaug spektra diapazonā 530–570 nm (3.7. attēls), kas atbilst flavīna emisijai (1.10. attēls), savukārt dzīves laika komponentes τ_3 vērtība samazinās spektra diapazonā 530–600 nm (3.7. attēls), kas atbilst lipopigmenta emisijai (1.10. attēls). Analizējot intradermālo nēvusu AF, novērota dzīves laika τ_2 un τ_3 komponenšu vērtību samazināšanās visā spektra diapazonā 460–610 nm (3.8. attēls).

- Ierosinot veselās ādas AF ar 470 nm impulsu lāzeri un veicot fotoizbalēšanu ar 470 nm nepārtraukta starojuma zemjaudas lāzeri (40 mW/cm^2), dzīves laika komponentes τ_2 vērtība pieaug spektra diapazonā 510–550 nm (3.12. attēls), kas atbilst flavīna emisijai (1.10. attēls).
- Analizējot iegūtus datus ar TRES apstrādes metode un normējot pēc signālu maksimuma, tika novērots, ka pie 405 nm ierosmes viļņu garumiem ādas AF spektrā dominē NAD(P)H emisija, bet pēc fotoizbalēšanas notiek šī fluorofora koncentrācijas samazināšanās un AF maksimuma nobīde uz flavīna/lipopigmentu emisijas pusi.

Balstoties uz pētījumiem citu valstu laboratorijās [26, 38, 81] τ_2 atbilst flavīnu grupai, kurā ietilpst FAD, kas iesaistās šūnas metabolismā. FAD AF dzīves laika palielināšanās novērota metastatiskam šūnām [26, 95]. NAD(P)H koncentrācijas samazināšanās, kas novērota TRES analīzē, izraisa oksidatīvo stresu. Oksidatīvā stresā rodas brīvie radikāļi, kas var izraisīt šūnas nāvi, ja regulējošie mehānismi nepaspēj atjaunot šūnas *redoks* stāvokli. Kā arī NAD(P)H AF samazināšanās attiecībā pret FAD novērota šūnās, kas atrodas blakus ļaundabīgam veidojumam [96]. Apkopojot iegūtus rezultātus, var secināt, ka fotoizbalēšana destruktīvi ietekmē ādas šūnas.

Ar divām metodēm – kontakta un bezkontakta – konstatēts ādas oksihemoglobīna koncentrācijas pieaugums pēc lāzerapstarošanas ar jaudas blīvumiem, kādi izraisa AF fotoizbalēšanu. Novērots, ka pie ierosmes ar īsākiem lāzera viļņa garumiem relatīvā oksihemoglobīna absorbcija ir lielāka, ne kā pie ierosmes ar lielākiem viļņa garumiem. Oksihemoglobīna absorbcijas pieaugums ādā ir proporcionāls apstarošanas jaudas blīvumam. Asins pieplūdumam lāzera apstarotajā ādas vietā var būt kāds no šiem iemesliem:

- Apstarošanas laikā tiek fotoinducēti ādas audi vai hromofori, tādēļ cilvēka imūnsistēma reaģē, izsaucot asins pieplūdumu apstarotajā vietā.
- Lāzera apstarošana izraisa termisko efektu un cilvēka aizsardzības mehānisms (imunitātes sistēma) atver kapilārus un palielina asins pieplūdumu, lai izvairītos no audu pārkaršanas.
- Notiek ādas fotoiekaisuma (eritēmas) process, līdzīgs saules apdegumam.

Darbā iegūti rezultāti liecina par fluorescences un fotoizbalēšanas klīniskajiem pielietojumiem – tādiem kā jaunveidojuma diagnostika. Bet vienlaicīgi jāpievērš uzmanība apstarošanas laikam un jaudas blīvumam. Kā parādīja eksperimentālie pētījumi ar fotoizbalēšanas efektu – apstarošana destruktīvi ietekmē ādas šūnas, kā arī maina difūzo atstarošanas spektru, kas var radīt kļūdas mērījumos un novest pie neprecīzas diagnozes.

Aizstāvēšanai izvirzītās tēzes

1. Darbā piedāvātais AF fotoizbalēšanas ātruma parametrs ir izmantojams pigmentēto jaunveidojumu diagnostikā, ko apstiprina iespēja bazaliomas atšķirt no citiem pigmentētiem ādas jaunveidojumiem.
2. Fotoizbalēšanas process ietekmē ādas AF dzīves laikus un spektrālo sadalījumu. Ierosinot ar 405 nm un 470 nm pikosekunžu lāzeriem, AF fotoizbalēšanas procesā dzīves laika komponente τ_2 palielinās, bet τ_3 – samazinās. Apstrādājot datus ar TRES metodi, konstatētas AF spektrālā sadalījuma izmaiņas. kas liecina par fluoroforu sastāva izmaiņām fotoizbalēšanas procesā.
3. Salīdzinot ādas un intradermālā nēvusa dzīves laika komponentes un AF intensitātes dzišanas ātrumu fotoizbalēšanas laikā, novērota korelācija starp kinētiskajiem parametriem (AF dzīves laika starpībām un AF intensitātes izmaiņām pēc fotoizbalēšanas). Tas liecina par AF kinētisko parametru izmantošanas iespējām ādas klīniskajā diagnostikā.
4. Lāzeru drošības standartiem atbilstoša zema jaudas blīvuma (< 200 mW/cm2) apstarošana palielina ādas oksihemoglobīna koncentrāciju apstarotajā vietā. Šis pieaugums ir proporcionāls lāzera jaudas blīvumam un apgriezti proporcionāls lāzeru starojuma viļņa garumam.

Ar darbu saistīto publikāciju saraksts:

I. A. Dzerve, **I. Ferulova**, A. Lihachev, and J. Spigulis "Time of flight for photon in human skin", J of Biomedical Photonics & Eng 2(3), 030301-1, (2016)

II. A. Lihachev, A. Derjabo, **I. Ferulova**, M. Lange, I. Lihacova, J. Spigulis, "Autofluorescence imaging of basal cell carcinoma by smartphone RGB camera", J. Biomed. Opt. 20(12), 120502 (2015).

III. **I. Ferulova**, A. Lihachev, J. Spigulis, "Photobleaching effects on in vivo skin autofluorescence lifetime", J. Biomed. Opt. 20(5), 051031 (2015)

IV. A.Lihachev, **I. Ferulova**, J. Spigulis, D. Chorvat "Parallel measurements of *in vivo* skin autofluorescence lifetimes and photobleaching rates", IFMBE Proc. Volume 48, 2015, pp 78–81 (2015)

V. A.Lihachev, **I. Ferulova**, J. Spigulis, M. Tamosiunas "Simultaneous detection of tissue autofluorescence decay distribution and time-gated photo-bleaching rates", Proc. of SPIE, Vol. 9504 95040P-1 (2015)

VI. A Lihachev, **I Ferulova**, K Vasiljeva, J Spigulis, "Investigation of *in vivo* skin autofluorescence lifetimes under long-term cw optical excitation", Quantum Electron., 2014, 44 (8), 770–773 (2014)

VII. **I.Ferulova**, A.Lihachov, J.Spigulis. "Fluorescence life-time spectroscopy: potential for *in vivo* estimation of skin fluorophores changes after low power laser treatment" Proc. of SPIE, 9032, 90320B. (2013)

VIII. **I.Ferulova**, J.Lesins, A.Lihachev, D.Jakovels, J.Spigulis. "Influence of low power CW laser irradiation on skin hemoglobin changes". Proc.SPIE 8427, 84273I (2012).

IX. **I. Ferulova**, A.Rieba, J.Lesins, A.Berzina, A.Lihachev, J.Spigulis, "Portable device for skin autofluorescence photobleaching measurements", Lith. J. Phys, Vol. 52(1), pp. 55–58 (2012)

Promocijas darba rezultāti prezentēti 16 starptautiskās konferencēs:

1. **I. Ferulova**, K. Vasiļjeva, A. Lihachev, J. Spigulis "Multimodal time resolved fluorescence spectroscopy for characterization of *in vivo* skin auto-fluorescence" Advanced Optical Materials and Devices 2014 (AOMD-8) Riga, Latvia, 25–27 August 2014. Poster
2. **I. Ferulova**, A .Lihachov, J. Spigulis "Investigation of skin Auto-fluorescences life time during long term optical irradiation" International Conference on Laser Application in Life Sciences 2014, Ulm, Germany, 29 June – 2 July, Poster with oral presentation.
3. **I. Ferulova**, K. Vasiljeva, A. Lihachov, J. Spigulis. "Fluorescence life-time measurements of healthy skin", Lasers for Life, Laserlab Foresight Workshop, 2–4 June 2014, London, UK Poster
4. K. Vasiljeva, **I. Ferulova**, A. Lihachov, J. Spigulis. "Fluorescence life-time measurements of healthy skin" Development in Optics and Comunications (DOC'14) and Laserlab III Training School for Potential Users "Laser Applications in Spectroscopy, Industry and Medicine", Riga, Latvia, 9–12 April 2014. Poster.
5. I. Brice, **I. Ferulova**, J. Spigulis, J. Alnis. "Towards skin fluorescence diagnostics using femtosecond frequency comb laser" Biophotonic Riga 2013, Riga, Latvia, August 2013. Posters
6. **I. Ferulova**, A. Lihachov, J. Spigulis. "Fluorescence life-time spectroscopy: potential for *in vivo* estimation of skin fluorophores changes after low power laser treatment" Biophotonic Riga 2013, Riga, Latvia, 26–31 August 2013. Posters.
7. **I. Ferulova**, A. Lihachev, J. Spigulis "Picosecond laser-excited fluorescence lifetime measurements." Development in Optics and Comunications (DOC'13), Riga, Latvia, 10–12 April 2013. Poster.
8. **I. Ferulova**, A. Lihachev, D. Jakovels, J. Spigulis. "Diffuse reflectance changes in healthy skin due to low power cw laser irradiation" European Conferences on Biomedical Optics (ECBO) 12–16.05. 2013 Munich, Germany. Oral presentation.
9. J. Lesins, M. Rumaka, K. Rozniece, **I. Ferulova**, J. Spigulis, "Skin autofluorescence photobleaching synchronization with physiological state".

Biophotonics in Dermatology and Cardiology, Riga, Latvia, 30–31 March 2012. Poster

10. J. Lesins, M. Rumaka, K. Rozniece, **I. Ferulova**, J. Spigulis. Impact of physiological state on skin autofluoresce photobleaching. Development in Optics and Comunications (DOC'12), Riga, Latvia, 12–14 April 2012. Poster
11. J. Lesins, M. Rumaka, K. Rozniece, **I. Ferulova**, J. Spigulis. Physiological state influence to skin autofluorescence photobleaching. European Conferences on Biomedical Optics, Brussels, Belgium, 16–19 April 2012. Poster
12. **I. Ferulova**, J. Lesins, D. Jakovels, A. Lihachev, J. Spigulis. Skin optical density changes after low power laser irradiation. Development in Optics and Comunications (DOC'12), Riga, Latvia, 12–14 April 2012. Poster
13. **I. Ferulova**, J. Lesins, A. Lihachev, D. Jakovels, J. Spigulis. "Influence of low power CW laser irradiation on skin hemoglobin changes". European Conferences on Biomedical Optics, Brussels, Belgium, 16–19 April 2012. Poster
14. **I. Ferulova**, J. Lesins, A. Lihachev, D. Jakovels, J. Spigulis. "Signs of haemoglobin in low power CW-laser induced human skin detected by diffuse reflectance spectroscopy and multispectral imaging". Biophotonics in Dermatology and Cardiology, Riga, Latvia, 30–31 March 2012. Oral
15. **I. Ferulova**, A. Rieba, J. Lesins, A. Berzina, A. Lihachev, J. Spigulis. "Device for skin diagnostics by autofluorescence photobleaching". Biophotonics in Dermatology and Cardiology, Riga, Latvia, 30–31 March 2012. Poster
16. **I. Ferulova**, A. Rieba, J. Lesins, A. Berzina, A. Lihachev, J. Spigulis. "Portable device for skin autofluorescence photobleaching measurements". Advanced Optical Materials and Devices 2011 (AOMD-7) Vilnius, Lithuania, 28–31 August 2011. Poster

IZMANTOTĀ LITERATŪRA

[1] P. Apinis, Anatomija, fizioloģija, pataloģijas pamati, Rīga: Nacionālais Medicīnas apgāds & Apgāds Jāņa sēta, 1998, p. 113–139.

[2] P. S. Andersson, E. Kjellin, S. Montan, K. Svanberg, S. Svanberg, "Autofluorescence of Various Rodent Tissues and Human Skin Tumour Samples," Lasers Med. Sci.2:41, 1987.

[3] E. Borisova, E. Pavlova, T. Kundurjiev, P. Troyanova, T. Genova, and L. Avramov, "Light-induced autofluorescence and diffuse reflectance spectroscopy in clinical diagnosis of skin cancer," Proc. SPIE 9129, p. 91291O, 2014.

[4] J. Spigulis, A. Lihachev, and R. Erts, "Imaging of laser-excited tissue autofluorescence bleaching rates," Appl. Opt. 48(10), p. D163–D168, 2009.

[5] Y. Pu, S. Achilefu, R. R. Alfano, Cancer detection/fluorescence imaging: 'Smart beacons' target cancer tumors, [Online] BioOptics world, http://www.biooptics-world.com.

[6] A. C. Rueck, C. Hauser, S. Mosch, S. Kalinina, "Spectrally resolved fluorescence lifetime imaging to investigate cell metabolism in malignant and nonmalignant oral mucosa cells," J. Biomed. Opt. 19(9) 096005, 2014.

[7] J. Horilova, H. Studier, Z. Nadova, P. Miskovsky, D. Chorvat Jr., A. Marcek Chorvatova, "Time-Resolved Spectrometry of Mitochondrial NAD(P)H Fluorescence and Its Applications for Evaluating the Oxidative State in Living Cells," in Mitochondrial Medicine Volume I, Probing Mitochondrial Function, New York Heidelberg Dordrecht London, Springer, 2015.

[8] K. Konig, H. Meyer, H. Schneckenburger, A. Ruck, "The study of endogenous porphyrins in human skin and their potential for photodynamic therapy by laser induced fluorescence spectroscopy," Lasers Med. Sci, vol. 8, pp. 127–132, 1993.

[9] H. Zengs, C. MacAulay, Dl. McLean, B. Palcic, H. Lui, "The dynamics of laser-induced changes in human skin autofluorescence – experimental measurements and theoretical modeling," Photochem. Photobiol., vol. 68(2), pp. 227–236, 1998.

[10] A. Lihachev, J. Spigulis, "Skin autofluorescence fading at 405/532 nm laser exitation," Northem Optics, pp. 63–65, 2006.

[11] J. Lesiņš, "Dzīvas ādas "foto atmiņas" efekts un tā spektrālās īpatnības," in Maģistra darbs, Riga, Latvijas Universitātes, 2011.

[12] A. A. Stratonnikov, V. S. Polikarpov, V. B. Loschenov, "Photobleaching of Endogenous Fluorochroms in Tissues in vivo during Laser Irradiation," Proc. SPIE, vol. 4241, 2001.

[13] A. Lihachev, K. Rozniece, J. Lesins, J. Spigulis, "Photobleaching measurements of pigmented and vascular skin lesions: results of a clinical trial," in SPIE-OSA Biomedical Optics, 2011.

[14] H. Zeng, "Human skin optical properties and autofluorescences decay Dynamics," in PhD Thesis, Vancouver, BC, University of Columbia, 1993, p. 222.

[15] David J. Gawkrodger, in Dermatology 4th ed, Churchill Livingstone Elsevier, 2008, pp. 92–100.

[16] K. Wolf, R. A. Johnson, Fitzpatrick's color atlas & synopsis of clinical dermatology 6th ed., New York: McGraw-Hill. ISBN-10: 0071599754, 2009.

[17] E. N. Marieb, K. Hoehn, "Pearson International Edition, Ch.5," in Human Anatomy & Physiology (7th Edition), 2006, pp. 152–170.

[18] I. Ļihačova, "Ādas onkoloģisko pataloģiju novērtējums ar multispektrālās attēlošanas metodēm," in Promocijas darba kopsavilkums, Riga, Latvijas universitāte, 2015.

[19] D. S. Rigel, R. J. Friedman, L. M. Dzubow, D. S. Reintgen, J-C. Bystryn, R. Marks, Cancer of the skin, Elsevier Inc., 2005.

[20] I. Kuzmina, "Kontakta un bezkontakta difūzās refleksijas spektrometrija ādas patoloģiju novērtējumam," in Promocijas darba kopsavilkums, Riga, Latvijas Universitāte, 2011.

[21] В. В. Тучин, Лазеры и волоконная оптика в биомедицинских Исследованиях, Физико-математическая литература, 2010, pp. 10–46.

[22] G. J. Muller, D. H. Sliney, Dosimetry of Laser Radiation in Medicine and Biology, Bellingham: WA, SPIE Inst. Advanced Opt. Techn., V. IS5, 1989.

[23] G. Yoon, A. J. Welch, M. Motamedi, "Development and application of three-dimensional light distribution model for laser irradiated tissue," IEEE J. Quantum Electr., Vols. 23, № 10., p. 1721–1733, 1987.

[24] М. А. Ельяшевич, Атомная и молекулярная спектроскопия, Москва: Физико-математическая литература, 1962, pp. 17,81,755.

[25] Reseapro, Fluorescence spectroscopy, [Online] Reseapro Scientific Services. http://blog.reseapro.com/tag/jablonski-diagram/, 2017.

[26] L. Marcu, P. M. W. French, D. S. Elson, Fluorescence lifitime spectroscopy and imaging, CRC Precc, 2015, pp. 47–85, 333.

[27] Cortassa, Aon, Marban, Winslow, O'Rourke, The CellML Project, [Online], https://models.cellml.org/exposure/e5ba9ba5ee28a2b107c2dd0f8343cea2/view.

[28] H. Stanley, J. Botas, V. Malhotra, "The mechanism of Golgi segregation during mitosis is cell type-specific," in Proc. Natl. Acad. Sci. U.S.A., 1997.

[29] B. Chance, B. Thorell, "Localization and kinetics of reduced pyridine nucleotide in living cells by microfluorometry," J Biol Chem., vol. Nov; 234, pp. 3044–50, 1959.

[30] B. Chance, H. Sies, A. Boveris, "Hydroperoxide metabolism in mammalian organs," Physiol Rev, vol. Jul; 59(3), pp. 527–605, 1979.

[31] K. Nakayama, T. Nakamura, M. Taniguchi, T. Tanaka, "Irreversible deacylation of plasma membrane phospholipids by the combined action of Mg2+ and a long-chain acyl-CoA synthetase inhibitor in Saccharomyces cerevisiae," J Biosci Bioeng, vol. 94(3), pp. 258–63, 2002.

[32] H. Schneckenburger, K. Koenig, "Fluorescence decay kinetics and imaging of NAD(P)H and flavins as metabolic indicators," Opt. Eng., vol. 31, p. 1447–1451, 1992.

[33] L. Huang, CP. Kirschke, J. Gitschier, "Functional characterization of a novel mammalian zinc transporter, ZnT6," J Biol Chem, vol. 277(29), pp. 26389–95, 2002.

[34] K. Nakayama, T. Yamaguchi, T. Doi, Y. Usuki, M. Taniguchi, T. Tanaka, "Synergistic combination of direct plasma membrane damage and oxidative stress as a cause of antifungal activity of polyol macrolide antibiotic niphimycin," J Biosci Bioeng., vol. 94(3), pp. 207–11, 2002.

[35] D. N. Romashko, E. Marban, B. O'Rourke, "Subcellular metabolic transients and mitochondrial redox waves in heart cells," in Natl. Acad. Sci., USA, 1998.

[36] Alcohol deshidrogenasa, [on-line]: http://alcoholdeshidrogenasa.weebly.com/apuntes.html.

[37] S. E. Forest, J. D. Simon, "Wavelength-dependent photoacoustic calorimetry study of melanin," Photochem Photobiol, vol. Sep; 68(3), pp. 296–8, 1998.

[38] K. Konig, I. Riemann, "High-resolution multiphoton tomography of human skin with subcellular spatial resolution and picosecond time resolution," J. Biom. Opt, vol. 8, pp. 432–439, 2003.

[39] A. N. Bashkatov, E. A. Genina, V. I. Kochubey, and V. V. Tuchin, "Optical properties of human skin, subcutaneous and mucous tissues in the wavelength range from 400 to 2000 nm, " J. Phys. D: Appl. Phys., vol. 38, p. 2543–2555, 2005.

[40] G. Zonios, J. Bykowski, N. Kollias, "Skin Melanin, Hemoglobin, and Light Scattering Properties can be Quantitatively Assessed In Vivo Using Diffuse Reflectance Spectroscopy," The Journal Of Investigative Dermatology, vol. 117 (6), 2001.

[41] J. Allen, A. Murray, "Modelling the relationship between peripheral blood pressure and blood volume pulses using linear and neural networksystem identification techniques," Physiol Meas, vol. 20, p. 287–301, 1999.

[42] M. A. Ansari, R. Massudi, "Study of light propagation in Asian and Caucasian skins by means of the Boundary Element Method," Opt. Lasers Eng., vol. 47 (9), pp. 965–970, 2009.

[43] S. L. Jacques, D. J. McAuliffe, "The melanosome: threshold temperature for explosive vaporization and internal absorption coefficient during pulsed laser irradiation," Photochem. Photobiol, vol. 53, pp. 769–775, 1991.

[44] E. Claridge, D. Hidović-Rowe, P. Taniere, T. Ismail, "Quantifying mucosal blood volume fraction from multispectral images of the colon," 2007.

[45] R. Yip, "Significance of an abnormally low or high hemoglobin concentration during pregnancy: special consideration of iron nutrition1,2,3," Am. J. Clin Nutr, vol. 72, pp.272S–9S, 2000.

[46] OMCL, Optical properties spectra, [Online]: Oregon Med. Laser Cent. http://omlc.org/spectra/melanin/, 2017.

[47] OMCL, Optical properties spectra, [Online]: Oregon Med. Laser Cent. http://omlc.org/spectra/hemoglobin/, 2017.

[48] M. E. Darvin, N. N. Brandt, and J. Lademann, "Photobleaching as a Method of Increasing the Accuracyin Measuring Carotenoid Concentration in Human Skinby Raman Spectroscopy," Optics and Spectroscopy, vol. 109(2), p. 205–210, 2010.

[49] T. Johansson, M. S. Thompson, M. Stenberg, C. Klinteberg, S. Andersson-Engels, S. Svanberg, and K. Svanberg, "Feasibility Study of a System for Combined Light Dosimetry and Interstitial Photodynamic Treatment of Massive Tumors," Applied Optics, vol. 41(7), p. 1462–1468, 2002.

[50] M. S. Thompson, A. Johansson, T. Johansson, S. Andersson-Engels, S. Svanberg, N. Bendsoe, and K. Svanberg, "Clinical system for interstitial photodynamic therapy with combined on-line dosimetry measurements," Applied Optics, vol. 44(19), p.4023–4031, 2005.

[51] T. Bernas, M. Zarebski, R. R. Cook, J. W. Dobrucki, "Minimizing photobleaching during confocal microscopy of fluorescent probes bound to chromatin, role of anoxia and photon flux," J. Microsc, vol. 215, pp. 281–296, 2004.

[52] P.S. Dittrich, P. Schwille, "Photobleaching and stabilization of fluorophores used for single-molecule analysis with one- and two-photon excitation," Appl. Phys, sēj. B 73, pp. 829–837, 2001.

[53] B. Hoffmann, T.Zimmer, N. Klöcker, L. Kelbauskas, K. König, K. Benndorf, C. Biskup, "Prolonged irradiation of enhanced cyan fluorescent protein or Cerulean can invalidate Förster resonance energy transfer measurements," J. Biomed. Opt., vol. 13(3), pp. 031250–1, 2008.

[54] A. Hopt, E. Neher, "Highly nonlinear Photodamage in two-photon fluorescence microscopy," Biophys. J., vol. 80, pp. 2029–2036, 2002.

[55] K. Konig, P. T. C. So, W. W. Mantulin, B. J. Tromberg, E. Gratton, "Two-Photon excited lifetime imaging of autofluorescence in cells during UVA and NIR photo-stress," J. Microsc., vol. 183, pp. 197–204, 1996.

[56] G. H. Patterson, D. W. Piston, "Photobleaching in two-photon excitation microscopy," Biophys. J, vol. 78, pp. 2159–2162, 2000.

[57] D. Axelrod, D. E. Koppel, J. Schlessinger, E. Elson, and W. W. Webb, "Mobility measurement by analysis of fluorescence photobleaching recovery kinetics," Biophys J., vol. Sep; 16(9), p. 1055–1069, 1976.

[58] B. L. Sprague, R. L. Pego, D. A. Stavreva, J. G. McNally, "Analysis of binding reactions by fluorescence recovery after photobleaching," Biophys J., vol. Jun; 86(6), p. 3473–3495, 2004.

[59] A. B. Houtsmuller, "Fluorescence recovery after photobleaching: application to nuclear proteins," Adv. Biochem. Eng. Biotechnol., vol. 95, pp. 177–199, 2005.

[60] K. S. Zadeh, H. J. Montas, A. Shirmohammadi, "Identification of biomolecule mass transport and binding rate parameters in living cells by inverse modeling," Theor Biol Med Model, 2006.

[61] L. J. Krafta, A. K. Kenworthy, "Imaging protein complex formation in the autophagy pathway: analysis of the interaction of LC3 and Atg4BC74A in live cells using Förster resonance energy transfer and fluorescence recovery after photobleaching," J Biomed Opt., vol. Jan; 17(1), p. 011008, 2012.

[62] J. Schleusener, J. Lademann, M. E. Darvin, "Depth-dependent autofluorescence photobleaching using 325, 473, 633, and 785 nm of porcine ear skin ex vivo," J Biomed Opt, vol. 22(9), p. 091503, 2017.

[63] Velscope, [Online]: http://www.velscope.com/.

[64] fotofinder, [Online]: https://www.fotofinder.de/en/applications/fluorescence-diagnostics/.

[65] Dermnetnz, [Online]: https://www.dermnetnz.org/topics/wood-lamp-skin-examination/.

[66] Observ, [Online]: http://www.observ.uk.com.

[67] European standard, Safety of Laser Products—Part 1: Equipment Classification and Requirements, CENELEC, EN 60825–1, 2007.

[68] Projekta, Inovatīvas ādas diagnostiskās attēlošanas tehnoloģijas (#2014/0041/2DP/2.1.1.1.0/14/APIAA/VIAA/015), 3. posma zinātniskā atskaite, [Online]: http://www.lu.lv/fileadmin/user_upload/lu_portal/projekti/es/2007-2013/eraf/adasdiagnostika/Zin-atsk_3.pdf.

[69] MathWorks, 1994–2017 The MathWorks, Inc., MATLAB, [Online]: https://www.mathworks.com/products/matlab.html, 2017.

[70] R. Cubeddu, P. Taroni, G. Valentini, and G. Canti, Photobiol, vol. B 12, p. 109, 1992.

[71] Q. Fang, T. Papaioannou, J. A. Jo, R. Vaitha, K. Shastry,and L. Marcu, "Time-domain laser-induced fluorescence spectroscopy apparatus for clinical diagnostics," Rev. Sci. Instrum, vol. 75, no. 1, pp. 151–162, 2004.

[72] L. H. Laiho, T. M. Hancewicz, P. D. Kaplan, P. T. C. So, "Two-photon 3-D mapping of ex-vivo human skin endogenous fluorescence species based on fluorescence emission spectra," J. Biomed. Opt, vol. 10, pp. 024016–1, 2005.

[73] R. Richards-Kortum, R. Drezek, K. Sokolov, I. Pavlova, M. Follen, "Survey of endogenous biological fluorophores," in Handbook of Biomedical Fluorescence, New York, Basel, Marcel Dek-ker Inc, 2003, pp. 237–264.

[74] D. Schweitzer, M. Hammer, F. Schweitzer, R. Anders, T. Doebbecke, S. Schenke, E. R. Gaillard, "In vivo measurement of time-resolved autofluorescence at the human fundus," J. Biomed. Opt, vol. 9, pp. 1214–1222, 2004.

[75] J. R. Lakowicz, H. Szmacinski, K. Nowaczyk, M. L. Johnson, "Fluorescence lifetime imaging of free and protein-bound NADH," PNAS, vol. 89, pp. 1271–1275, 1992.

[76] D. K. Bird, L. Yan, K. M. Vrotsos, K. E. Eliceiri, E. M. Vaughan, "Metabolic mapping of MCF10A human breast cells via multiphoton fluorescence lifetime imaging of coenzyme NADH," Cancer Res, vol. 65, p. 8766–8773, 2005.

[77] T. H. Chia, A. Williamson, D. D. Spencer, M. J. Levene, "Multiphoton fluorescence lifetime imaging of intrinsic fluorescence in human and rat brain tissue reveals spatially distinct NADH binding," Optics Express, vol. 16, pp. 4237–4249, 2008.

[78] D. Chorvat, A. Chorvatova, "Spectrally resolved time-correlated single photon counting: a novel approach for characterization of endogenous fluorescence in isolated cardiac myocytes," Eur. Biophys. J., Vols. 36:73-83, pp. 40–47, 2006.

[79] O. Warburg, "On the origin of cancer cells," Science, vol. 123, pp. 309–314, 1956.

[80] O. Warburg, "On respiratory impairment in cancer cells," Science, vol. 124, pp. 269–270, 1956.

[81] D. Chorvat Jr. and A. Chorvatova, "Multi-wavelength fluorescence lifetime spectroscopy: a new approach to the study of endogenous fluorescence in living cells and tissues," Laser Phys. Lett., vol. 6, 2008.

[82] J. R. Lakowicz, Principles of Fluorescence Spectroscopy, 3rd edn, Springer, 2006.

[83] R. J. Paul, H. Schneckenburger, "Oxygen concentration and the oxidation-reduction state of yeast: Determination of free/bound NADH and flavins by time-resolved spectroscopy," Naturwissenschaften, vol. 83, pp. 32–35, 1996.

[84] D. Schweitzer, M. Hammer, F. Schweitzer, S. Schenke, E. Birckner, W. Becker, A. Bergmann, "In vivo autofluorescence lifetime imaging at the fundus of the human eye," in Proc. SPIE 6138, 2006.

[85] D. Schweitzer, S. Schenke, M. Hammer, F. Schweitzer, S. Jentsch, E. Birckner, W. Becker, "Towards Metabolic Mapping of the Human Retina," Micr. Res. Tech, vol. 70, pp. 403–409, 2007.

[86] M. C. Skala, K. M. Riching, D. K. Bird, A. Dendron-Fitzpatrick, J. Eickhoff, K. W. Eliceiri, P. J. Keely, N. Ramanujam, "In vivo multiphoton fluorescence lifetime imaging of protein-bound and free nicotinamide adenine dinucleotide in normal and precancerous epithelia," J. Biomed. Opt., vol. 12, pp. 02401–1, 2007.

[87] M. C. Skala, K. M. Riching, A. Gendron-Fitzpatrick, J. Eickhoff, K. W. Eliceiri, J. G. White, N. Ramanujam, "In vivo multiphoton microscopy of NADH and FAD redox states, fluorescence lifetimes, and cellular morphology in precancerous epithelia," PNAS, vol. 104, pp. 19494–19499, 2007.

[88] M. Szaszak, P. Steven, K. Shima, R. Orzekowsky-Schröder, Gereon Hüttmann, I. R. König, W. Solbach, J. Rupp, "Fluorescence Lifetime Imaging Unravels C. trachomatis Metabolism and Its Crosstalk with the Host Cell," PLOS Pathogens, vol. 7, pp. e1002108–1, 2011.

[89] H. D. Vishwasrao, A. A. Heikal, K. A. Kasischke, W. W. Webb, "Conformational Dependence of Intracellular NADH on Metabolic State Revealed by Associated Fluorescence Anisotropy," J. Biol. Chem., vol. 280, pp. 25119–25126, 2005.

[90] W. Becker, Advanced time-correlated single-photon counting techniques, Berlin, Heidelberg, New York: Springer, 2005.

[91] D. V. O'Connor, D. Phillips, Time-correlated single photon counting, London: Academic Press, 1984.

[92] J. Yguerabide, "Nanosecond fluorescence spectroscopy of macromolecules," Meth. Enzymol, vol. 26, pp. 498–578, 1972.

[93] W. Becker, The bh TCSPC Handbook, 5th edition, 2012.

[94] A. S. R.Koti, M. M. G.Krishna, N. Periasamy, "Time-Resolved Area-Normalized Emission Spectroscopy (TRANES): A Novel Method for Confirming Emission from Two Excited States," J. Phys. Chem., vol. 105, pp. 1767–1771, 2001.

[95] P. P. Provenzano, D. R. Inman, K. W. Eliceiri, J. G. Knittel, L. Yan, C. T. Rueden, J. G. White and P. J. Keely, Collagen density promotes mammary tumor initiation and progression, BMC Medicine, 2008.

[96] Z. Xu, M. Reilley, R. Li, M. Xu, "Mapping absolute tissue endogenous fluorophore concentrations with chemometric wide-field fluorescence microscopy," J. Biomed. Opt., vol. 22(6), 2017.

[97] J. Lesins, A. Lihachev, R. Rudys, S. Bagdonas, J. Spigulis, "Skin autofluorescence photobleaching and photo-memory," Proc. of SPIE-OSA Biomedical Optics, vol. 8092, p. 80920N, 2011.

[98] I. A. Nakhaeva, M. R. Mohammed, O. A. Zyuryukina, and Yu. P. Sinichkin, "The Effect of an External Mechanical Compression on in vivo Optical Properties of Human Skin," Optics and Spectroscopy, vol. 117, no. 3, p. 506–512, 2014.

[99] T. Svensson, E. Alerstam, D. Khoptyar, J. Johansson, S. Folestad, and S. Andersson-Engels, "Near-infrared photon time-of-flight spectroscopy of turbid materials up to 1400 nm," Rev. Sci. Instrum., vol. 80(6), p. 063105, 2009.

[100] D. Khoptyar, A. A. Subash, S. Johansson, M. Saleem, A. Sparén, J. Johansson, and S. Andersson-Engels, "Broadband photon time-of-flight spectroscopy of pharmaceuticals and highly scattering plastics in the VIS and close NIR spectral ranges," Optics Express, vol. 21(18), pp. 20941–20953, 2013.

[101] Virtual Beauty Corporation, [Online]: http://www.virtualbeauty.co.nz/posters/.

[102] J. Fitzpatrick and A. Eisen, Dermatology in General Medicine, New York: McGraw-Hill, 1993.

PATEICĪBAS

Izsaku pateicību darba vadītājam profesoram Jānim Spīgulim par iespēju izstrādāt promocijas darbu, par iedvesmu un atbalstu visos darba posmos. Paldies kolēģiem Aleksejam Ļihačovam, Ilonai Kuzminai, Ilzei Ošiņai, Edgaram Kviesim-Kripgem, Ilzei Ļihačovai, Uldim Rubīnam, Ērikam un Jānim Zaharanam par palīdzību un iesaistīšanos darba procesā. Paldies dermatoonkologam Aleksandram Derjabo un dermatologam Annai Bērziņai par palīdzību klīnisko mērījumu veikšanā, kas notika Latvijas Onkoloģijas centrā un Lāzerplastiskas klīnikā.

Vēlreiz paldies visiem LU Atomfizikas un spektroskopijas institūta darbiniekiem par sniegto atbalstu.

PIELIKUMS

Publikāciju saraksts:

I. A.Dzerve, **I.Ferulova**, A.Lihachev, and J.Spigulis “Time of flight for photon in human skin”, J of Biomedical Photonics & Eng 2(3), 030301-1, (2016).

II. A.Lihachev, A.Derjabo, **I. Ferulova**, M.Lange, I.Lihacova, J.Spigulis, "Autofluorescence imaging of basal cell carcinoma by smartphone RGB camera," J. Biomed. Opt. 20(12), 120502 (2015).

III. **I.Ferulova**, A.Lihachev, J.Spigulis, “Photobleaching effects on in vivo skin autofluorescence lifetime”, J. Biomed. Opt. 20(5), 051031 (2015).

IV. A.Lihachev, **I. Ferulova**, J. Spigulis, D. Chorvat "Parallel measurements of *in vivo* skin autofluorescence lifetimes and photobleaching rates", IFMBE Proc. Volume 48, 2015, pp 78-81 (2015).

V. A.Lihachev, **I. Ferulova**, J. Spigulis, M. Tamosiunas ”Simultaneous detection of tissue autofluorescence decay distribution and time-gated photo-bleaching rates”, Proc. of SPIE, Vol. 9504 95040P-1 (2015)

VI. A Lihachev, **I Ferulova**, K Vasiljeva, J Spigulis, "Investigation of *in vivo* skin autofluorescence lifetimes under long-term cw optical excitation ", Quantum Electron., 2014, 44 (8), 770–773 (2014)

VII. **I.Ferulova**, A.Lihachov, J.Spigulis. "Fluorescence life-time spectroscopy: potential for *in vivo* estimation of skin fluorophores changes after low power laser treatment" Proc. of SPIE, 9032, 90320B. (2013)

VIII. **I.Ferulova**, J.Lesins, A.Lihachev, D.Jakovels, J.Spigulis. "Influence of low power CW laser irradiation on skin hemoglobin changes." Proc.SPIE 8427, 84273I (2012).

IX. **I. Ferulova**, A.Rieba, J.Lesins, A.Berzina, A.Lihachev, J.Spigulis, “Portable device for skin autofluorescence photobleaching measurements”, Lith. J. Phys, Vol. 52(1), pp. 55–58 (2012)

I.

Time of flight for photon in human skin

Antra Dzerve*, Inesa Ferulova, Alexey Lihachev, and Janis Spigulis
Institute of Atomic Physics and Spectroscopy, University of Latvia, 19 Rainis blvd., Riga, Latvia

* **e-mail**: antra_dzerve@inbox.lv

Abstract. The time of flight for photons in human skin was measured using picosecond diode laser. Two different wavelength lasers were used - 405 nm and 510 nm. A difference for time of flight in normal skin and in nevus was observed as well as a difference for different wavelength laser irradiation was observed. For 405 nm laser irradiation the difference was 41 ps while comparison of time of flights skin and nevi using 510 nm irradiation showed a result of 32 ps. Results allow to conclude that the time photon travels in skin might depend on the characteristics of the medium and wavelength of the irradiation. This can be related to known data for light penetration depth in human skin for different wavelengths. © 2016 Journal of Biomedical Photonics & Engineering.

Keywords: absorption, light impulse, biophotonics, medical physics.

Paper #2363 received 2016.05.18; revised manuscript received 2016.09.16; accepted for publication 2016.09.29; published online 2016.09.30. doi: 10.18287/JBPE16.02.030301

References

1. R. L. Siegel, K. D. Miller, and A. Jemal, "Cancer statistics, 2016," A cancer journal for clinicians 66(1), 7-30 (2016).
2. J. Lesins, A. Lihache, R. Rudys, S. Bagdonas, and J. Spigulis, "Skin autofluorescence photo-bleaching and photo-memory," Proc. SPIE-OSA 8092, 80920N (2011).
3. I. Ferulova, A. Lihachev, and J. Spigulis, "Photobleaching effects on in vivo skin autofluorescence lifetime," J. Biomed. Opt. 20(5), 051031 (2015).
4. T. Svensson, E. Alerstam, D. Khoptyar, J. Johansson, S. Folestad, and S. Andersson-Engels, "Near-infrared photon time-of-flight spectroscopy of turbid materials up to 1400 nm," Rev. Sci. Instrum. 80(6), 063105 (2009).
5. D. Khoptyar, A. A. Subash, S. Johansson, M. Saleem, A. Sparén, J. Johansson, and S. Andersson-Engels, "Broadband photon time-of-flight spectroscopy of pharmaceuticals and highly scattering plastics in the VIS and close NIR spectral ranges," Optics Express 21(18), 20941-20953 (2013).
6. J.-C. Bernengo, H. Adhoute, and D. Mougin, "Measurement of the time of flight of photons into the skin: influence of site, age and gender, correlation with other skin parameters," Skin Research and Technology 21(1), 25-34 (2014).
7. Safety of Laser Products - Part 1: Equipment Classification and Requirements IEC 60825-1 (2007).
8. R. R. Anderson, and J. A. Parrish, "The optics of human skin," Journal of Investigative Dermatology 77(1), 13-19 (1981).

1 Introduction

Skin is by far the largest organ for humans and it is also the one that comes in contact with many threats from outside world all the time – air pollution can clog pores and create rash or zits, too much time spent in the sun can result in sunburns, UV irradiation can be a cause of diseases. According to statistics, the number of diagnosed melanomas per year is growing [1]. Therefore optical diagnostics as a fast and relatively easy way for diagnosing skin diseases is getting more popular.

By time of flight one understands the time photon spends in skin before it is reflected back and exits the skin. When light enters the skin, part of it is reflected back from the surface, but part of it continues to penetrate deeper layers of skin. This light can be scattered, absorbed or reflected in many different directions. Time of flight for photon is affected by

characteristics of the medium it travels in. Information about photon behaviour under different types of skin and skin formations is a key element to understanding many different effects connected to research aimed at improving and developing new ways for skin disease diagnostics and other experimental uses. Finding unusual formations not noticeable to naked eye by comparing results of the time light spends in patients skin with data for normal, healthy skin without the need to use surgical intrusion – this is only one of possible uses for database with photon times of flight in human skin and not dangerous formations such as nevi. This type of database can help revolutionise skin diagnostics alongside other similar researches on other topics, such as photobleaching [2], skin autofluorescence lifetime [3] and others.

Researches about time of flight of photons in different mediums such as turbid materials [4] and pharmaceuticals, also highly scattering plastics have already been carried out [5]. But the usage of photon time of flight spectroscopy undoubtedly has a place in medical spectroscopy field for human skin. This kind of research has already been carried out in with specific wavelength lasers. For example, a research was done using 1064 nm laser irradiation and the authors themselves suggest that measurements using shorter wavelengths should be carried out for more extensive conclusions [6].

Investigation for time of flight for photons in human skin was conducted using picosecond diode laser of wavelengths 405 nm and 510 nm and results were acquired, comparing the time of flight for photon in healthy human skin and in a nevi. For 405 nm irradiation difference in flight time was found at 41 ps while for 510 nm laser the difference was found to be 32 ps.

2 Method and equipment

In order to determine the time spent under skin for photons of different wavelengths and compare data for normal, healthy skin and nevi, following experimental setup was created.

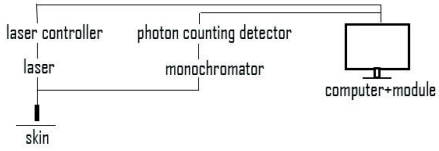

Fig. 1 Experimental setup scheme for measurements of photon time-of-flight in human skin.

The single-spot measurement setup scheme is shown in Fig. 1, it comprised a laser controller and a pico-second laser (PicoQuant: 405 nm, pulse half-width 59 ps, repetition rate 20 MHz mod. LDH-D-C-405, PicoQuant: 510 nm, pulse half-width 107 ps, repetition rate 20 MHz mod. LDH-D-C-510) with 200 micrometer silica core optical fibre output via the SMA-connector. The fibre connected to laser represented one leg of a Y-shaped optical fibre bundle while other leg contained additional 6 fibres to deliver the light via a monochromator to the photon counting detector (Becker&Hickl, PMC-100-4). Monochromator was set to allow thought the wavelength equal to the wavelength of the laser being used. This was done to eliminate possible fluorescence effects which may lead to extra emitted photons not ones that reflect inside the skin and travel through it. The laser controller and photon counting detector were connected to a PC with a data processing card (Becker&Hickl, TCSPC, mod. SPC-150). The fibre-optic probe was tightly fixed in a way that the skin surface and tip of the Y-shaped fibre bundle were in contact in such a way that skin surface and fibre create a ninety degree angle and the laser impulse goes directly into the skin straight down. That way the part of light that enters and gets reflected straight back can be observed and measured. Laser impulse was measured by using a highly reflective metal surface and measuring reflected signal to acquire the form of laser impulse. This impulse was used as a reference for comparison.

By comparing measured reflected signals to laser impulse signals from human skin visually, one can observe a shift in the peak and slight widening of the impulse. Using a time line connected to all measurements, and a signal can be properly compared to acquire peak shift in time units [6]. The error for any acquired measurement is set by time resolution of the experimental setup. For this specific case the error could be approximated as 6 ps.

Laser irradiation that was used was well below the skin laser safety limit (200 mW/ cm^2, exposure time up to 103 s [7]. The safety and well-being of the human subjects involved in all clinical measurements was assured through the supervision of the local ethics committee that authorized the studies.

Experiments were carried out on 10 volunteers aged from 22 to 30 with skin phototype II (classified by Fitzpatrick classification). The main goal was determining if the results show different tendencies for length of photon time of flight for healthy skin and nevi.

Data were acquired from volunteers' upper back and chest regions. Differentiation between healthy skin and nevi (or distinguishing nevus from any different type of skin abnormality) was performed with the help of volunteers themselves, who had previously on their personal occasions consulted with medical personnel.

3 Results

A difference in time of flight for healthy skin and nevi was observed. For 510 nm laser a difference of 19-39 ps between time of flight in healthy skin and in nevus was observed, healthy skin having a longer time of flight. Most of the differences were around the 19 ps mark. For 405 nm laser a difference of 19-58 ps was observed, mostly falling in the 39-58 ps diapason. With this

wavelength healthy skin had longer times of flight as nevi as well. Since the times of flight were measured from comparable regions of volunteers' skin, data does not give any more description for other parts of body at the moment. More research should be conducted to compare these results to possibly different ones from other parts of body.

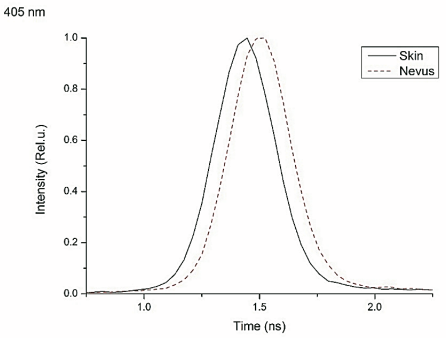

Fig. 2 Comparison of pulse from healthy skin and from nevus, using 405 nm laser.

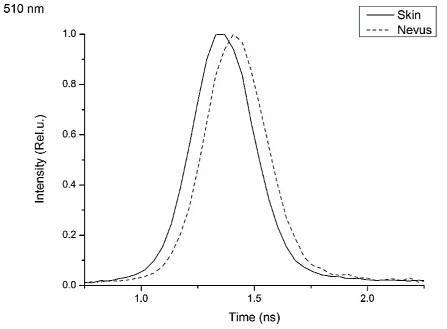

Fig. 3 Comparison of pulse from healthy skin and from nevus, using 510 nm laser.

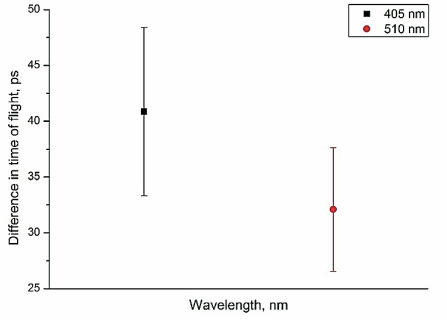

Fig. 4 Difference for time of flight in healthy skin and nevi for 405 nm and 510 nm lasers.

Examples for gathered data with 405 nm and 510 nm lasers are shown in Fig. 2 and Fig. 3. Average time of flight for both lasers is shown in Fig. 4.

Analysis of gathered data shows a tendency for length of time – times of flight for 510 nm laser impulses were longer than for 405 nm laser for healthy skin.

4 Discussion

As shown in previously mentioned results, it can be seen that for 510 nm laser times of flight are longer, compared to 405 nm laser irradiation times of flight. This can be attributed to penetration depth for different wavelengths of lasers. Other researches on skin and laser light interaction show this tendency with penetration depths for lasers of shorter wavelengths [8].

A constant difference in times of flight for healthy skin and nevi was observed. This is possibly connected with different characteristics of the medium the laser pulse travels in. Shorter times of flight in nevi can be attributed to higher density in tissue material. Photons that enter the skin have more points on which they can scatter - a different scattering coefficient describes nevi, compared to normal skin. This is backed up by practical measurements - those done on nevi had to have longer data acquisition times than healthy skin with no defects. Time of measurement was chosen basing on count of registered photons - it had to be the same for healthy skin and nevus to compare the data. Prolonged measurements for nevi can also be attributed to higher absorption coefficient for nevi.

This type of measurement allows to conduct diagnostics very quickly. One measurement can take from only one or two seconds up to thirty seconds, only for very specific cases it would take a minute. The shortness and specifics of one measurement is a huge advantage compared to other types of skin diagnostics – no surgical intrusion, short waiting time (the patient does not have to sit still for long periods of time, thus minimising the probability of error from a simple movement), a chance for creating an interface to acquire immediate visual and numerical results.

At the moment one of limitations is time resolution. For this specific set-up, as mentioned before, the error is close to being comparable with acquired results. This, though, could be fixed or at least improved by using lasers with a more suitable frequency.

5 Conclusions

As shown above, the chosen experimental setup can deliver reproducible data and be used with different wavelength lasers which allows to carry out the experiment to comparably easily gather diverse results in different spectral regions.

Acquired data show a constant difference in time of flight for healthy skin and nevi. As it can be seen in acquired results, the difference in photon time of flight for 405 nm irradiation was found at 41 ps while for 510 nm laser the difference was found to be 32 ps.

Using this as a guideline, a database for times of flight in different types of skin can be created. The database could be used as a reference in diagnostics. Database should not be limited to only healthy skin and nevi. By adding a specialist from medical staff, differentiation between other skin formations could be made and it would allow to widen the possible database.

Further research would require a more extensive data acquisition from a larger group of volunteers using more wavelengths, optionally, in optical diapason to create a large database that could be a reference point for this type of fast, relatively easy and not time consuming diagnostics. This would not only minimise the need for surgical intervention, it could in the future be used as a standard for optical diagnostics.

II.

Journal of Biomedical Optics

BiomedicalOptics.SPIEDigitalLibrary.org

Autofluorescence imaging of basal cell carcinoma by smartphone RGB camera

Alexey Lihachev
Alexander Derjabo
Inesa Ferulova
Marta Lange
Ilze Lihacova
Janis Spigulis

SPIE.

Autofluorescence imaging of basal cell carcinoma by smartphone RGB camera

Alexey Lihachev,[a,*] Alexander Derjabo,[b] Inesa Ferulova,[a] Marta Lange,[a] Ilze Lihacova,[a] and Janis Spigulis[a]
[a]University of Latvia, Institute of Atomic Physics and Spectroscopy, Biophotonics Laboratory, Raina Boulevard 19, Riga LV-1586, Latvia
[b]Riga East University Hospital, Oncology Centre of Latvia, Hipokrata Street 4, Riga LV-1079, Latvia

Abstract. The feasibility of smartphones for *in vivo* skin autofluorescence imaging has been investigated. Filtered autofluorescence images from the same tissue area were periodically captured by a smartphone RGB camera with subsequent detection of fluorescence intensity decreasing at each image pixel for further imaging the planar distribution of those values. The proposed methodology was tested clinically with 13 basal cell carcinoma and 1 atypical nevus. Several clinical cases and potential future applications of the smartphone-based technique are discussed.
 [DOI: 10.1117/1.JBO.20.12.120502]

Keywords: autofluorescence; photobleaching; RGB imaging; smartphone.

Paper 150558LRR received Aug. 20, 2015; accepted for publication Nov. 12, 2015; published online Dec. 11, 2015.

1 Introduction

Incidences and mortality from skin cancer are still increasing.[1] Depending on the melanin concentration, skin tumors are broadly classified into two types—malignant melanomas (MM) and nonmelanoma skin cancers (NMSC). MM is the most aggressive skin cancer modality with death rate ~80% of all fatal skin cancer cases.[1] The most common NMSC are basal cell carcinoma (BCC, about 80% of new cases) and squamous cell carcinoma (SCC, about 20% of new cases) derived from the basal and squamous cells of the epidermis, respectively.[2] BCC is characterized by very slow growth tendency, low mortality rate, and high risk of recurrence, while SCC is more aggressive and associated with the risk of metastasis.[3,4]

Early detection and removal of skin cancers can significantly increase the survival time. Noninvasive methods in primary oncological diagnostics of skin tumors are still topical for dermatologists and oncologists worldwide. One of those is skin autofluorescence (AF) imaging and spectroscopy, based on differences of AF specific information (intensity, spectral shape, and lifetime) in the tumor and surrounding normal skin.[5–8]

The feasibility of AF spectroscopy for BCC diagnostics and differentiation has been studied extensively over this most recent decade. AF spectra from BCC lesions excited in UV/blue region (337 to 450 nm) were broadly characterized by decreased fluorescence intensity in comparison with surrounding healthy skin,[8] most often attributed to the shift in the levels of NADH/NAD+ (reduced form and oxidized form of nicotinamide adenine dinucleotide) and reduced elastin and collagen, affected by malignant process. In some cases, especially in late tumor growing stages, a weak red fluorescence peak of the endogenous porphyrins has been observed.[8]

Tissue AF usually shows the photobleaching effect,[9] which may be helpful in biomedical applications.[10–14] Under continuous wave (cw) excitation, skin AF intensity mainly drops during the first 15 to 20 s, followed by a slow decrease. Photobleaching kinetics can be well described by empirical double-exponential function with subsequent extraction of time constants τ_1 and τ_2 that characterize the rate of fast and slow phases of the AF decrease.[9] Our previous research has demonstrated that each skin pathology as well as healthy skin has its own specific AF intensity decrease kinetics depending on excitation, localization, melanin content, and blood perfusion. Furthermore, the analysis of AF decrease kinetics during the first 15 to 20 s of cw laser excitation seems to be most suitable for clinical implementation.[15,16]

Currently available smartphones equipped with high-resolution RGB cameras in combination with good light sensitivity and color representation mainly satisfy the required technical properties for adequate image acquisition.[17] This technology may become a useful diagnostic tool for dermatologists and oncologists thanks to wide accessibility, convenient use, and low cost.[18,19] However, the ability to switch off the "embedded" automatized settings such as exposure time, white balance, and ISO is crucial for the skin parametric imaging. Our latest studies have shown that smartphones such as Galaxy and Nexus are suitable for mapping of skin chromophores.[17]

So far use of smartphones in skin pathology diagnostics has been mainly related to dermatoscopy—specifically magnified image acquisition under white or color illumination with subsequent analysis based on ABCD rules, fractal image analysis or other algorithms established in dermatoscopy.[20–24] In this paper, we present a smartphone-compatible technique for acquisition and analysis of 405 nm light-emitting diode (LED) excited skin autofluorescence images.

2 Materials and Methods

2.1 *Experimental Setup*

For parametric mapping of skin AF intensity decrease rates, a sequence of AF images under continuous 405 nm LED (model LED Engin LZ1-00UA00-U8, spectral band half-width 30 nm) excitation for 20 s at a power density of ~20 mW/cm^2 with a frame rate 0.5 fr/s was recorded and analyzed. Four battery-powered violet LEDs were placed within a cylindrical light-shielding wall that also ensured fixed distance (60 mm) between the smartphone camera and evenly irradiated a spot (diameter 40 mm) of the examined tissue. A long pass filter (>515 nm) was placed in front of smartphone camera to prevent detection of the LED emission. The recorded RGB images were further separated to exploit R- and G-images for imaging of skin tissue AF

*Address all correspondence to: Alexey Lihachev, E-mail: aleksejs.lihacovs@gmail.com

1083-3668/2015/$25.00 © 2015 SPIE

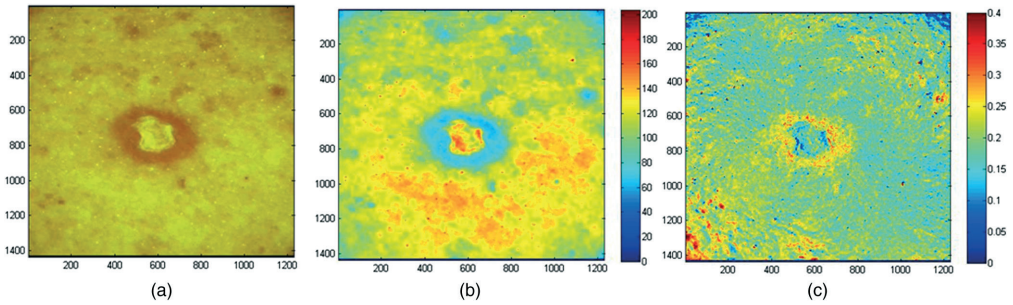

Fig. 1 Images of ulcerating basal cell carcinoma (BCC). Filtered AF color image (a) at excitation start moment, (b) the corresponding G-band image, and (c) normalized AF intensity decrease map. The pseudo color scale represents (b) the G-band intensity range and (c) the normalized AF intensity variation range.

in the red and green spectral bands, respectively. Due spectral cutoff by 515-nm long pass filter B band images in further calculations are not used. The Samsung Galaxy Note 3 smartphone comprising integrated CMOS RGB image sensor with resolution of 13 MP was used for image acquisition. All images were taken using the following settings: ISO—100, white balance—daylight, focus—manual, exposure time—fixed 200 ms.

2.2 *Image Processing*

In order to visualize the skin AF intensity decrease rates during the photobleaching, the following image processing expression was applied:

$$N(\mathrm{C}) = [I_{t0}(C) - I_t(C)]/I_{t0}(C), \quad (1)$$

where $N(C)$ represents normalized AF intensity decrease map for each pixel (or pixel group) during the excitation period, $I_{t0}[C]$—AF image at the excitation start moment, $I_t[C]$—AF image after 20 s of continuous excitation. C—color component of the RGB image—red (R), green (G), and blue (B), respectively. The values of RGB components were defined from the image data by a special program developed in MATLAB®.

Overall 50 patients with 150 different skin neoplasms (or suspicious) were inspected in the clinic. For the detailed image analysis 13 BCC and 1 atypical nevus were selected. This study was approved by the Ethics Committee of the Institute of Experimental and Clinical Medicine, University of Latvia. All involved volunteers were informed about the study and signed required consent.

3 Results and Discussion

A total of 10 solid and 3 ulcerating BCCs were selected for the study. In all BCC cases (confirmed by cytological examination) the AF images showed lowered AF intensity in malignant tissue as compared with the healthy surrounding skin, which may be attributed to decreased levels of fluorophores and increased blood perfusion caused by the malignancy process.[2,5,7] AF spectra from *in vivo* BCC under 405 nm excitation are characterized by broad (450 to 750 nm) emission spectrum with maximum in green spectral region (510 to 530 nm). In comparison with surrounding healthy skin, the intensity of AF from malignant tissue usually are lower, while the shape of the spectrum remains unchanged. Moreover, the intensity of AF is strictly correlated with the tumor pigmentation, specifically, the higher the pigmentation, the lower is the intensity of fluorescence.[2,8] In all BCC cases, the G-band (corresponding to the AF maximum) AF intensity images in comparison with R-band images showed the more pronounced intensity contrast within the tumor tissue

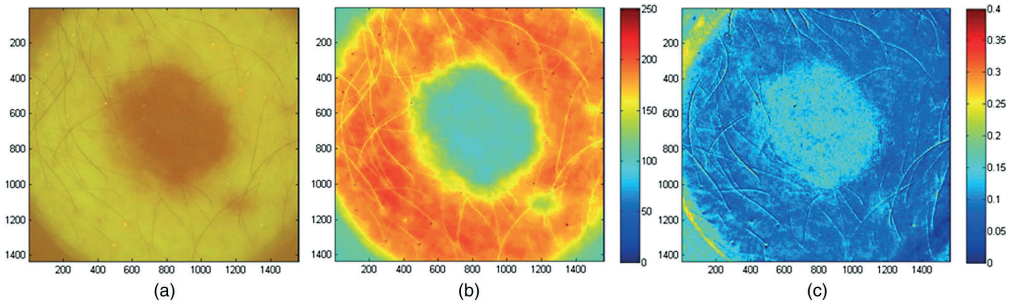

Fig. 2 Images of solid BCC. Filtered AF color image (a) at excitation start moment, (b) the corresponding G-band image, and (c) normalized AF intensity decrease map. The pseudo color scale represents (b) the G-band intensity range and (c) the normalized AF intensity variation range.

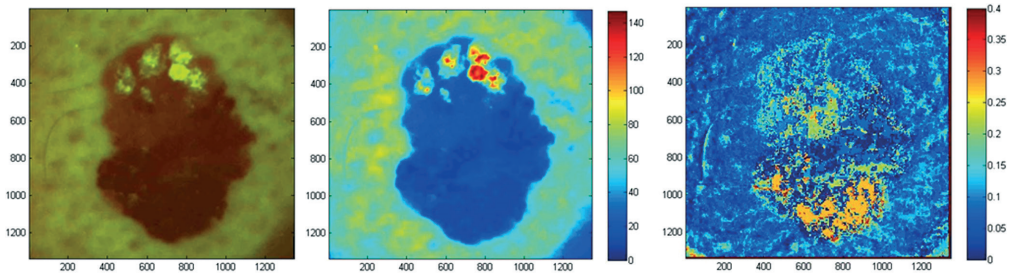

Fig. 3 Color filtered AF image of skin atypical nevus (a) at the excitation start moment, (b) the corresponding G-band image and (c) normalized AF intensity decrease map. The color scale at (b) image represents G-band intensity range and at (c) image—range of normalized AF intensity variations.

and surrounding healthy skin. Moreover, G-band AF decrease maps showed more structured compositions at tumor area in comparison with R-band AF decrease maps. In the cases of solid BCCs the AF images showed clearly bordered tumor areas with relatively low AF intensity in comparison with surrounding healthy skin. Whereas the ulcerating BCCs can be characterized by the high AF intensity in the ulcerating part surrounded by clearly bordered tissue emitting relatively low AF intensity. Furthermore, in all BCC cases the normalized AF intensity decrease maps showed high AF intensity decrease rates at the tumor areas with low AF intensity in comparison with the surrounding healthy skin and the internal ulcerating area.

Figure 1 represents images of ulcerating BCC: (a) filtered AF image at the excitation start moment, AF intensity G-band image (b), and parametric map of normalized AF intensity decrease rates in the green band (c). AF intensity image [Fig. 1(b)] shows high AF intensity in the ulcerating part (pathology center), surrounded by clearly bordered tissue emitting relatively low AF intensity. Furthermore, the AF intensity decreasing is more intensive at the external tumor area exposures in comparison with the surrounding healthy skin and the internal ulcerating area [Fig. 1(c)].

Another case of solid BCC is presented in Fig. 2. G-band AF intensity image [Fig. 2(b)] shows relatively low intensity within the tumor area with clear margins between tumor and surrounding healthy skin. The tumor area also shows higher AF intensity decrease rate [Fig. 2(c)] in comparison with the surrounding healthy skin. Besides, the images presented in Fig. 2 reveal a small area with lowered fluorescence located at "five o'clock" from the main tumor. The low AF intensity and high AF intensity decrease rate in that skin area similarly indicates to cancerous process, which is probably determined by multicentric tumor growing process.

In addition, one atypical nevus was selected for the study (Fig. 3). The nevus before surgical excision was suspected as melanoma; histological analysis of the removed tissue samples had confirmed three different types of tissue cells within the lesion area. Specifically, the upper part of the pathology mostly prevailed by intradermal nevus, the middle part by dysplastic nevus, and the lower part by junctional nevus. Normalized AF decrease distribution map [Fig. 3(c)], on the other hand, showed the fastest intensity decrease in the lower (junctional nevus) and upper side (intradermal nevus), while the middle part (dysplastic nevus) of lesion photobleached slower. The observed different AF photobleaching rates most probably are associated with different tissue fluorophore concentration, melanin content, localization, and metabolic state.

4 Conclusions

Smartphone AF imaging has shown potential for remote primary evaluation of cancerous or suspicious skin tissues. The proposed noninvasive technique and method adequately (with respect to the available literature data) represented planar distribution of AF intensities in malignant and healthy tissues. Moreover, the temporal analysis of AF intensity during the photobleaching showed a potential to be used as an additional indicator for demarcation of suspicious tissues. It may find clinical implementation, e.g., for primary evaluation of BCC, such as determination of precise excision margins prior to surgery, adequate selection of treatment method (in the case of multicentric growing process the nonsurgical methods are more desirable for the patients), as well as in selective application of immune response modulators for BCC therapy. The proposed excitation band around 405 nm covers the absorption maxima of several porphyrines and may find applications in photodynamic diagnostics of superficial nonmelanoma lesions. The most intriguing result of this research was the fact that AF photobleaching rate map showed quantitative correlation with the histology tests in the case of atypical dysplastic nevus. To explain, one can assume that specific tissue fluorophores might have individual bleaching kinetics features, which eventually could provide information on fluorophore concentration and environmental factors. The increased photobleaching rates in the tumor area most probably indicate different fluorophore content composition affected by the tumor growing process, e.g., destruction of collagen elastin cross-links along with decrease in NADH levels. Undoubtedly, this phenomenon requires additional studies to clarify the exact mechanism of uneven photobleaching of skin fluorophores under continuous optical excitation.

Acknowledgments

This work was supported by the European Regional Development Fund project "Innovative technologies for optical skin diagnostics" (No. 2014/0041/2DP/2.1.1.1.0/14/APIA/VIAA/015).

References

1. American Cancer Society, "Cancer facts & figures," (2009), http://www.cancer.org.
2. E. Drakaki et al., "Spectroscopic methods for the photodiagnosis of nonmelanoma skin cancer," *J. Biomed. Opt.* **18**(6), 061221 (2013).
3. E. N. Marieb and K. Hoehn, *Human Anatomy & Physiology*, 7th ed., Pearson International Edition, San Francisco, pp. 152–170 (2006).
4. S. D. Rigel et al., *Cancer of the Skin: Expert Consult*, 2nd ed., pp. 99–123, Elsevier Saunders, China (2011).
5. M. Panjehpour et al., "Laser-induced fluorescence spectroscopy for in vivo diagnosis of non-melanoma skin cancers," *Lasers Surg. Med.* **31**(5), 367–373 (2002).
6. N. P. Galletly et al., "Fluorescence lifetime imaging distinguishes basal cell carcinoma from surrounding uninvolved skin," *Br. J. Dermatol.* **159**(1) 152–161 (2008).
7. D. Chorvat and A. Chorvatova, "Multi-wavelength fluorescence lifetime spectroscopy: a new approach to the study of endogenous fluorescence in living cells and tissues," *Laser Phys. Lett.* **6**(3), 175–193 (2009).
8. E. G. Borisova, L. P. Angelova, and E. P. Pavlova, "Endogenous and exogenous fluorescence skin cancer diagnostics for clinical applications," *IEEE J. Quantum Electron.* **20**(2), 7100412 (2014).
9. H. Zeng et al., "The dynamics of laser-induced changes in human skin autofluorescence experimental measurements and theoretical modeling," *Photochem. Photobiol.* **68**(2), 227–236 (1998).
10. M. E. Darvin et al., "Optical methods for noninvasive determination of carotenoids in human and animal skin," *J. Biomed. Opt.* **18**(6), 061230 (2013).
11. H. Wang et al., "Improving skin Raman spectral quality by fluorescence photobleaching," *Photodiagn. Photodyn.* **9**(4), 299–302 (2012).
12. J. S. Goodwin and A. K. Kenworthy, "Photobleaching approaches to investigate diffusional mobility and trafficking of Ras in living cells," *Methods* **37**(2), 154–164 (2005).
13. G. Hennig, H. Stepp, and A. Johansson, "Photobleaching-based method to individualize irradiation time during interstitial 5-aminolevulinic acid photodynamic therapy," *Photodiagn. Photodyn. Ther.* **8**(3), 275–281 (2011).
14. C. Jayyosi et al., "Photobleaching as a tool to measure the local strain field in fibrous membranes of connective tissues," *Acta Biomater.* **10**(6), 2591–2601 (2014).
15. J. Spigulis, A. Lihachev, and R. Erts, "Imaging of laser-excited tissue autofluorescence bleaching rates," *Appl. Opt.* **48**(10), D163–D168 (2009).
16. A. Lihachev et al., "Investigation of in-vivo skin autofluorescence lifetimes under long-term cw optical excitation," *Quantum Electron.* **44**(8), 770–773 (2014).
17. I. Kuzmina et al., "Study of smartphone suitability for mapping of skin chromophores," *J. Biomed. Opt.* **20**(9), 090503 (2015).
18. Statista GmbH, "Number of smartphone users* worldwide from 2014 to 2019 (in millions)," (2015), http://www.statista.com/statistics/330695/number-of-smartphone-users-worldwide/ (26 November 2015).
19. S. A. Lamel et al., "Application of mobile teledermatology for skin cancer screening," *J. Am. Acad. Dermatol.* **67**(4), 576–581 (2012).
20. S. Kroemer et al., "Mobile teledermatology for skin tumour screening: diagnostic accuracy of clinical and dermoscopic image tele-evaluation using cellular phones," *Br. J. Dermatol.* **164**(5), 973–979 (2011).
21. J. Robert et al., "Early detection of malignant melanoma: the role of physician examination and self-examination of the skin," *CA Cancer J. Clin.* **35**, 130–151 (1985).
22. T. Maier et al., "Accuracy of a smartphone application using fractal image analysis of pigmented moles compared to clinical diagnosis and histological result," *J. Eur. Acad. Dermatol. Venereol.* **29**(4), 663–667 (2015).
23. S. Dreiseitl et al., "Computer versus human diagnosis of melanoma: evaluation of the feasibility of an automated diagnostic system in a prospective clinical trial," *Melanoma Res.* **19**(3), 180–184 (2009).
24. C. Massone et al., "Melanoma screening with cellular phones," *PLoS ONE* **2**(5), e483 (2007).

III.

Journal of Biomedical Optics

SPIEDigitalLibrary.org/jbo

Photobleaching effects on *in vivo* skin autofluorescence lifetime

Inesa Ferulova
Alexey Lihachev
Janis Spigulis

SPIE

Journal of Biomedical Optics 20(5), 051031 (May 2015)

Photobleaching effects on *in vivo* skin autofluorescence lifetime

Inesa Ferulova,* Alexey Lihachev, and Janis Spigulis
University of Latvia, 19 Raina Boulevard, Riga 1586, Latvia

Abstract. The autofluorescence lifetime of healthy human skin was measured using excitation provided by a picosecond diode laser operating at a wavelength of 405 nm and with fluorescence emission collected at 475 and 560 nm. In addition, spectral and temporal responses of healthy human skin and intradermal nevus in the spectral range 460 to 610 nm were studied before and after photobleaching. A decrease in the autofluorescences lifetimes changes was observed after photobleaching of human skin. A three-exponential model was used to fit the signals, and under this model, the most significant photoinduced changes were observed for the slowest lifetime component in healthy skin at the spectral range 520 to 610 nm and intradermal nevus at the spectral range 460 to 610 nm. [DOI: 10.1117/1.JBO.20.5.051031]

Keywords: lifetime; skin autofluorescence; autofluorescences photobleaching.

Paper 140560SSRR received Sep. 1, 2014; accepted for publication Jan. 7, 2015; published online Jan. 30, 2015.

1 Introduction

The intensity of the photobleaching of skin autofluorescence decreases during temporally stable irradiation,[1] which indicates photoinduced structural changes in the skin. The mechanism of this effect has not been explained in detail so far, and only a few hypotheses have been examined experimentally. One of these hypotheses suggests that the mechanism involves the irreversible destruction of a fluorophore in its excited state due to its interactions with molecular oxygen or other surrounding molecules; the chemically modified fluorophore then returns to the ground state as a new molecule that no longer absorbs light at the excitation wavelength.[2] Skin autofluorescence photobleaching was previously investigated for healthy and pathological skin under 405-, 473-, and 532-nm laser excitation.[3,4] The specific distribution of photobleaching parameters in healthy and pathological skin had been examined earlier.[5] Our previous studies showed that the restoration of autofluorescence intensity after photobleaching is a long-term process and lasts for hours.[4] The influence of continuous wave (cw) laser irradiation on skin diffuse reflectance in the spectral range 500 to 600 nm was also demonstrated;[6] this study confirmed that the low-power cw laser irradiation increased the skin's oxy-hemoglobin content.

In this study, a 405-nm picosecond laser was used for fluorescence lifetime measurements, and a cw 405-nm laser initiated the photobleaching. Radiation with wavelength 405 nm is absorbed by a number of fluorophores: keratin (absorption maximum at 380 to 400 nm and 450 to 470 nm, emission maximum at 500 to 550 nm), reduced nicotinamide adenine dinucleotide (absorption maxima at 290 nm and 350 to 370 nm, emission maximum at 440 and 460 nm), flavin adenine dinucleotide (FAD) (absorption maximum at 420 to 450 nm, emission maximum at 520 to 550 nm), phospholipids (absorption maximum at 430 nm, emission maximum at 500 and 540 nm), and lipofuscin (absorption maximum at 340 to 395 nm, emission maximum at 430 to 460 nm and 540 nm).[7,8]

The influence of photobleaching on autofluorescence lifetimes of healthy skin and intradermal nevus is studied in this work. Autofluorescence decay curves were approximated by three exponential decay functions, and spectral responses of fluorescence lifetimes before and after photobleaching were recorded and displayed on a plot. The three-exponential model was chosen because it was more informative[9,10] and achieved a better fit. This model shows that the fluorophores with emission in the spectral range from 520 to 610 nm are more sensitive to photobleaching. Time-resolved emission spectra were plotted as time-resolved area-normalized emission spectra (TRANES).[11] Changes in lifetimes and peak shifts in TRANES can be related to photoinduced changes of specific skin fluorophore or chromophore concentrations.

2 Methods and Materials

The single-spot measurement setup scheme is shown in Fig. 1, and it comprised a laser controller and a picosecond/cw laser (PicoQuant: 405 nm, pulse half-width 59 ps, repetition rate 20 MHz, mod. LDH-D-C-405) with 200-μm silica core optical fiber output via the SMA-connector. The excitation fiber represented one leg of a Y-shaped optical fiber bundle that contained an additional six fibers to deliver the fluorescent light via a monochromator to the photon counting detector (Becker&Hickl, PMC-100-4). The laser controller and photon counting detector were connected to a PC with a data processing card (Becker&Hickl, TCSPC, mod. SPC-150). The fiber-optic probe was tightly fixed such that the distance between the skin surface and tip of the Y-shaped fiber bundle was 3 mm. The diameter of the irradiated skin spot was ~3 mm. The same probe was used for lifetime measurements under pulsed excitation as well as for inducing photobleaching by cw laser irradiation.

First, the measurements were taken from 10 different spots of healthy skin on the inner part of the forearm and from 10 different spots of the back of the hand of 10 volunteers ranging in age from 24 to 48 years and having skin types II and III according to

*Address all correspondence to: Inesa Ferulova, E-mail: inesa.ferulova@gmail.com

0091-3286/2015/$25.00

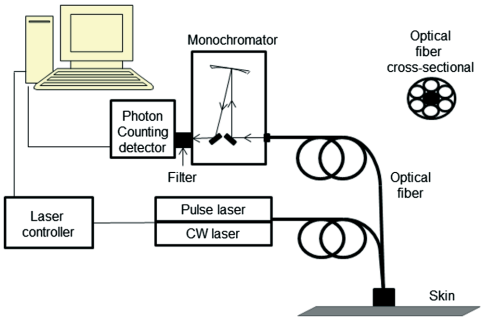

Fig. 1 Experimental setup for skin autofluorescence lifetime measurements.

the Fitzpatrick classification.[12] Data were collected at 475- and 560-nm emission wavelengths using a monochromator and interference filters.

Next, measurements of autofluorescence lifetimes of healthy *in vivo* skin and intradermal nevus before optical provocation (photobleaching) and immediately afterward were taken. Autofluorescence lifetimes were determined within the spectral range 460 to 610 nm with a step size of 10 nm via the monochromator (Fig. 2). Then, the laser was switched to cw mode and the same area was irradiated for 3 min at a laser power density of 40 mW/cm^2, well below the skin laser safety limit [200 mW/cm^2, exposure time up to 10^3 s (Ref. 13)]. Immediately after optical provocation, the laser was again switched to the pulsed mode and autofluorescence lifetime data were collected (which took ~10 s). The same procedure was applied during measurements of the intradermal nevus. The measurements were repeated three times for healthy skin on the inner part of the forearm of three volunteers and three times for the intradermal nevus of one volunteer. The safety and well-being of the human subjects involved in all clinical measurements were assured through the supervision of the local ethics committee that authorized the studies.

The obtained results were automatically processed using the Becker&Hickl SPCImage program. The results were approximated by a three-exponential decay function:

$$I = a_1 e^{-T/\tau_1} + a_2 e^{-T/\tau_2} + a_3 e^{-T/\tau_3}, \quad (1)$$

where I is the decaying intensity after pulsed laser excitation, T is the time, τ_i is the lifetime of the i'th component, and a_i is its amplitude ($i = 1$, 2, or 3).[9,10]

3 Results

The obtained average values of τ_1, τ_2, τ_3, and X_r^2 with standard deviation (SD) for healthy skin are presented in Table 1. It summarizes the results of 200 autofluorescence lifetime measurements: for each of 10 volunteers, 10 different spots of healthy skin on the inner part of the forearm and 10 different spots of the back of the hand. In all cases, the healthy skin autofluorescence lifetimes for all volunteers were similar (within a range of ±20%), which is confirmed by relatively low deviations from the average values. The three-exponential fitting resulted in the relatively low amplitude of the third component: $\tau_3 = 7.6 \pm 1.1$ ns, $a_3 = 6.4 \pm 0.4\%$ at 475 nm and $\tau_3 = 9.1 \pm 1.0$ ns, $a_3 = 7.8 \pm 2.7\%$ at 560 nm.

The spectral dependencies of the time-resolved emission intensity before and after photobleaching of healthy skin and the intradermal nevus are presented in Figs. 2 and 3, plotted

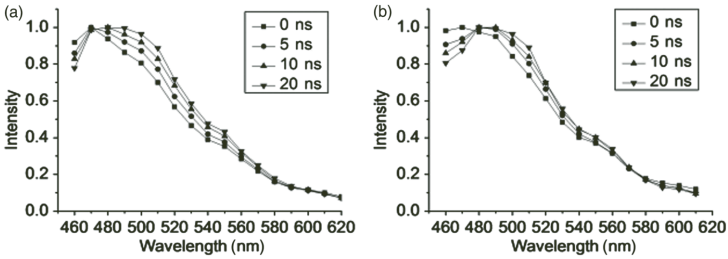

Fig. 2 Time-resolved area-normalized emission spectra (TRANES) of healthy skin before (a) and after (b) photobleaching.

Table 1 Averaged autofluorescence lifetime components based on *in vivo* measurements without photobleaching from the skin of 10 volunteers of second and third phototypes (SD—standard deviation).

	Triple-exponential decay						
	$\tau_1 \pm$ SD (ns)	$a_1 \pm$ SD (%)	$\tau_2 \pm$ SD (ns)	$a_2 \pm$ SD (%)	$\tau_3 \pm$ SD (ns)	$a_3 \pm$ SD (%)	$X_r^2 \pm$ SD
475 nm	1.2 ± 0.2	74.1 ± 1.1	4.4 ± 0.6	19.5 ± 0.8	7.6 ± 1.1	6.4 ± 0.4	1.3 ± 0.3
560 nm	1.1 ± 0.1	65.4 ± 4.1	4.3 ± 0.5	26.8 ± 1.6	9.1 ± 1.0	7.8 ± 2.7	1.1 ± 0.1

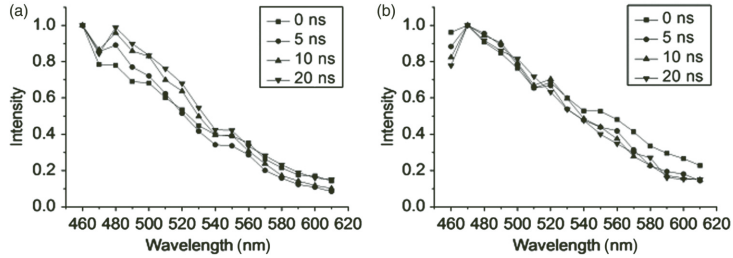

Fig. 3 TRANES of intradermal nevus before (a) and after (b) photobleaching.

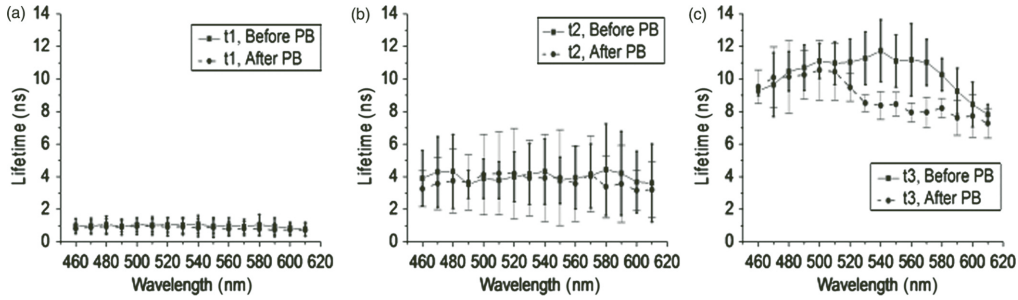

Fig. 4 Autofluorescence lifetimes of healthy skin before and after photobleaching. The parameters t1 (a), t2 (b), and t3 (c) are the averaged fluorescence lifetime components with error bars indicating the standard deviation (SD).

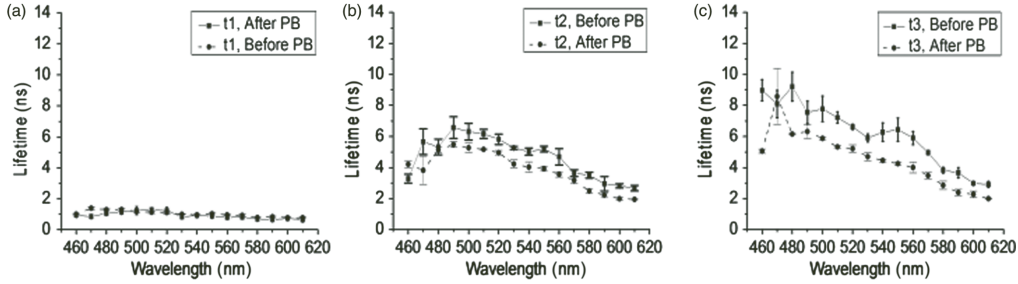

Fig. 5 Autofluorescence lifetimes of intradermal nevus before and after photobleaching. The parameters t1 (a), t2 (b), and t3 (c) are the averaged fluorescence lifetime components with error bars indicating the SD.

as TRANES; Figs. 4 and 5 show the spectral changes of the three lifetime components as a result of photobleaching. The typical numbers were: ~300,000 photons at the maximum and 19,500 photons at the minimum of healthy skin spectra before photobleaching, and 82,000 photons at the maximum and 11,000 at the minimum after photobleaching. In the cases of the intradermal nevus, about 50,000 photons were recorded at the maximum and 7000 photons at the minimum before photobleaching, and 30,000 photons at the maximum and 5000 at the minimum after photobleaching.

The third lifetime component appeared to be spectrally sensitive to photobleaching; it notably decreased in the spectral range 520 to 610 nm. In the case of the intradermal nevus, the third lifetime component decreased over the whole spectral range. The photobleaching-caused spectral changes were observed in the area-normalized emission spectra as well (Figs. 2 and 3). Figure 6 illustrates the spectral variations of the amplitude values.

4 Discussion

The reported results demonstrate that the three-exponential fitting of the obtained skin autofluorescence decay distribution is informative, and the third component with a relatively high lifetime and a low amplitude is spectrally sensitive. This decay component was observed by several authors under violet excitation.[9,10]

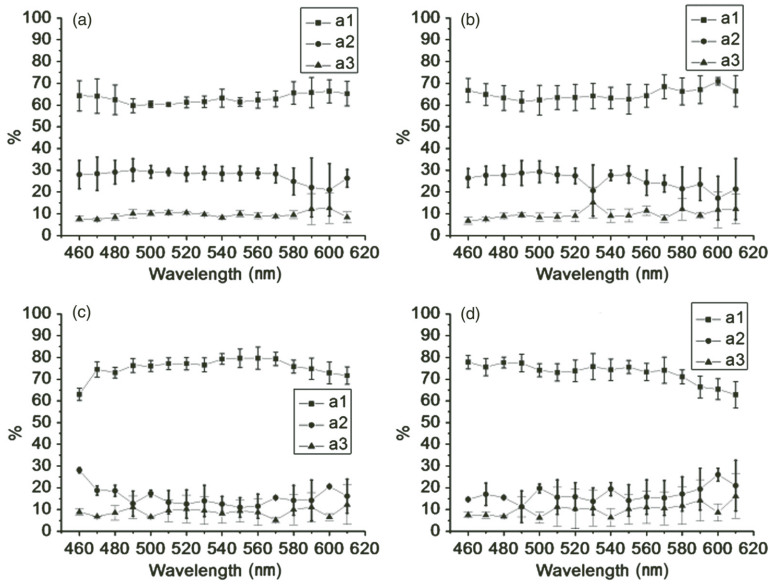

Fig. 6 Autofluorescence lifetime amplitudes of healthy skin and intradermal nevus before and after photobleaching. The parameters a1, a2, and a3 are the averaged fluorescence lifetime amplitude components with error bars indicating the SD. (a) Healthy skin before photobleaching; (b) healthy skin after photobleaching; (c) intradermal nevus before photobleaching; and (d) intradermal nevus after photobleaching.

Under normal conditions, the lifetime components for different subjects were similar (within ±20%, see Table 1). The results were obtained from 10 volunteers with second and third skin phototypes without extraillumination to induce photobleaching.

However, cw low-power laser irradiation caused notable changes in the lifetime components (especially τ_3) as well as in their spectral distributions (Figs. 4 and 5). The results of the experiment show a notable decrease of the third lifetime component in the spectral range 520 to 610 nm after photobleaching. TRANES show the emission intensity changes in the same spectral range; consequently, the decay becomes faster. The shift of the emission maxima in TRANES might be the result of changes in the composition and/or concentration of fluorophores (Figs. 2 and 3). In all cases, the corresponding amplitudes were unchanged.

Skin contains a number of different fluorophores, so it is still difficult to determine exactly which fluorophore(s) are most involved in the photobleaching phenomenon. The main fluorophores emitting in this spectral range are FAD, flavins, lipofuscin, and phospholipids. On the other hand, the 405-nm cw irradiation increases the oxy-hemoglobin content in the skin (perhaps as the result of photoinflammation),[6] which results in increased absorption and decreased lifetime. This phenomenon might be the major factor in our experimental conditions.

5 Conclusions

To the authors' knowledge, this investigation was the first attempt to study how external cw irradiation affects skin autofluorescence lifetimes. The observed variations in spectral responses of the three fluorescence lifetime components after photobleaching of healthy skin and the intradermal nevus may lead to a better understanding of the photobleaching mechanism. The results show the influence of photobleaching on FAD, flavins, and/or lipid fluorophores. The results point to changes in the composition and/or concentration of fluorophores as a result of photobleaching. Also, different lifetime spectral responses of healthy skin and the intradermal nevus were observed. The different responses of healthy and pigmented skin may provide additional information for skin diagnostics. More detailed clinical studies involving a larger number of volunteers of different ages, skin phototypes, and pathological structures have to be performed in the future.

Acknowledgments

Financial support of the EC FP7program (projects "Fotonika-LV," "FP7-REGPOT-CT-2011-285912," ERA-NET BiophotonicsPlus "BI-TRE," and "LaserLab Europe," EU-FP7 284464) is highly appreciated.

References

1. A. A. Stratonnikov, V. S. Polikarpov, and V. B. Loschenov, "Photobleaching of endogenous fluorochromes in tissues *in vivo* during laser irradiation," *Proc. SPIE* **4241**, 13–24 (2001).
2. P. Hinterdorfer and A. van Oijen, *Handbook of Single-Molecule Biophysics*, p. 50, Springer, Dordrecht, Heidelberg, London, New York (2009).
3. A. Lihachev and J. Spigulis, "Skin autofluorescence fading at 405/532 nm laser excitation," in *IEEE Xplore*, pp. 63–65 (2006).

4. A. Lihachev et al., "Low power cw—laser signatures on human skin," *Quantum Electron.* **40**(12), 1077–1080 (2011).
5. J. Spigulis, A. Lihachev, and R. Erts, "Imaging of laser-excited tissue autofluorescence bleaching rates," *Appl. Opt.* **48**(10), 163–168 (2009).
6. I. Ferulova et al., "Influence of low power CW laser irradiation on skin hemoglobin changes," *Proc. SPIE* **8427**, 84273I (2012).
7. D. Chorvat, Jr. and A. Chorvatova, "Multi-wavelength fluorescence lifetime spectroscopy: a new approach to the study of endogenous fluorescence in living cells and tissues," *Laser Phys. Lett.* **6**(3), 175–193 (2009).
8. E. G. Borisova, L. P. Angelova, and E. P. Pavlova, "Endogenous and exogenous fluorescence skin cancer diagnostics for clinical applications," *IEEE J. Quantum Electron.* **20**(2), 7100412 (2014).
9. H. E. Ediger et al., "Noninvasive, optical detection of diabetes: model studies with porcine skin," *Opt. Express* **12**(19), 4496 (2004).
10. J. Blackwell et al., "*In vivo* time-resolved autofluorescence measurements to test for glycation of human skin," *J. Biomed. Opt.* **13**(1), 014004 (2008).
11. A. S. R. Koti and M. M. Krishna, "Time-resolved area-normalized emission spectroscopy (TRANES): a novel method for confirming emission from two excited states," *J. Phys. Chem. A* **105**, 1767–1771 (2001).
12. J. Fitzpatrick and A. Eisen, *Dermatology in General Medicine*, p. 1694, McGraw-Hill, New York (1993).
13. European standard, *Safety of Laser Products—Part 1: Equipment Classification and Requirements*, pp. 60, CENELEC, EN 60825–1 (2007).

Inesa Ferulova is a scientific assistant and a PhD student in the Institute of Atomic Physics and Spectroscopy at the University of Latvia. Her main research interests are autofluorescence photobleaching, skin spectral imaging, and fluorescence lifetime.

Alexey Lihachev is a leading researcher in Institute of Atomic Physics and Spectroscopy in University of Latvia. His research interests focus on time- and spectral-resolved laser-excited skin autofluorescence.

Janis Spigulis is a professor at the University of Latvia and head of the Biophotonics Laboratory at the Institute of Atomic Physics and Spectroscopy. He has been active in biomedical optics since 1995.

IV.

Parallel Measurements of in-vivo Skin Autofluorescence Lifetimes and Photobleaching Rates

A. Lihachev[1], I. Ferulova[1], J. Spigulis[1], and D. Chorvat[2]

[1] Institute of Atomic Physics and Spectroscopy/ Biophotonics Laboratory, University of Latvia, Riga, Latvia
[2] International Laser Center/ Bratislava, Slovakia

Abstract— **Experimental methodology for parallel measurements of *in-vivo* skin autofluorescence (AF) lifetimes and photo-bleaching dynamic has been developed and tested. The AF lifetime decay distributions were periodically collected from fixed tissue area with subsequent detection of the fluorescence intensity decrease dynamic at different time shifts after the pulse excitation. Temporal distributions of skin AF lifetimes and bleaching dynamic were collected and analyzed by means of commercial time-correlated single photon counting system. Details of the equipment and data processing are described as well as some measurement results that confirm the feasibility of the proposed technology.**

Keywords— ***in-vivo*** **skin, autofluorescence, lifetime, photobleaching.**

I. INTRODUCTION

Laser induced time-resolved autofluorescence (AF) spectroscopy represents a promising adjunctive technique for in-vivo tissue diagnostics. Biological and biomedical applications of the autofluorescence spectroscopy have been successfully applied in cell biology and clinical diagnostics for detection of abnormal tissues [1-5]. The most important endogenous fluorophores are molecules widely distributed in cells and tissues, like proteins containing aromatic amino-acids, NAD(P)H, flavins and lipo-pigments [6,7]. The radiative lifetime of each fluorophore is unique, so fluorescence lifetime measurements can provide specific information on fluorphore content and distribution in the tissue. Tissue fluorescence lifetime value depends on environmental factors e.g. experimental setup, fluorophore localization, skin pH balance, viscosity, temperature etc. [8-10]. Selective analysis and separation of individual fluorophores underlying multi-exponential decays of *in-vivo* skin autofluorescence still is challenging problem.

In addition, tissue autoflurescence usually shows the photo-bleaching effect which is caused by chemical modification of the fluorochrome due to repeated excitation/emission states [11]. Due to mechanism of photo-bleaching is unclear, the purposeful use of photo-bleaching in biomedical applications are used very rarely. However, some of the authors successfully applied bleaching effect in Raman spectroscopy for improving the Raman spectra quality by decreasing of tissue fluorescence background [12, 13]. Temporal decrease of skin autofluorescence (AF) intensity can be well described by a double exponential function (1). Under long-term continuous/pulse excitation, the main decrease of the intensity I occur within the first 10–15 seconds, followed by relatively slow decrease which strives to a constant intensity level A:

$$I(t) = a_1 exp^{-t/T_1} + a_2 exp^{-t/T_2} + A \quad (1);$$

T_1 represents the fast phase of AFPB, T_2, the slow phase; a_1, a_2, and A are constants, and t is time [13,14]. The tissue AF photo-bleaching mechanism is still under discussion; however, one can assume that each tissue fluorophore might have its own specific AF bleaching rate, and any changes in the surface fluorophore composition would induce corresponding changes in the AF decay distribution and bleaching rates.

II. MATERIALS AND METHODS

The main focus of this study is to assess the possibility and potential of a combined time-resolved fluorescence spectroscopy method including parallel analysis of tissue autofluorescence lifetimes and photo-bleaching rates. For this purpose an experimental setup of parallel point measurements of skin AF lifetimes and photo-bleaching rates was assembled (Fig.1). The setup comprises a pico-second excitation laser (PicoQuant: pulse half-width 59 ps, 405nm, mean power density ~2mW/cm^2, mod. LDH-D-C-405) laser controller, monochromator, photon counting detector with temporal resolution of 180ps (mod. Becker&Hickl, PMC-100-4), data processing system "time-correlated single photon counting" with time resolution 6.6 ps, (TCSPC, mod. Becker&Hickl SPC-150), and a fiber optic probe. AF lifetimes of position stabilized healthy skin were measured during 3 minutes.

H. Mindedal and M. Persson (eds.), *16th Nordic-Baltic Conference on Biomedical Engineering*,
IFMBE Proceedings 48, DOI: 10.1007/978-3-319-12967-9_21

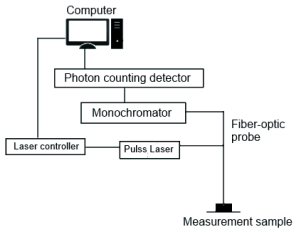

Fig. 1 Experimental setup for parallel point measurements of skin autofluorescence lifetimes and photo-bleaching dynamic.

Skin AF lifetimes were collected every 10 seconds. Totally during the 3 minute cycle 18 measurements (Fig.2) of tissue AF decay distributions were registered. Each measurement contained temporal distribution of AF decay and a number of registered photons collected during the 10 seconds. Due to the AF photo-bleaching process, the number of collected photons for each subsequent measurement decreases, thereby giving the opportunity to construct the AF photo-bleaching curves. Autofluorescence lifetimes were collected at 480 nm wavelength using Becker&Hickl software SPCM. For the analysis of AF lifetimes obtained, the multi-exponential fluorescence decay distribution model was applied:

$$f(t) = \sum_{i=0}^{n} a_i exp^{-t/\tau_i} + c \quad (2),$$

were f(t) is AF intensity at time moment t after the excitation pulse, n is number of decaying species in the exponential sum, and c is a background level of light in each particular case. The applied model comprises the lifetimes of the exponential components, τ_i, and the amplitudes of the exponential components, a_i.

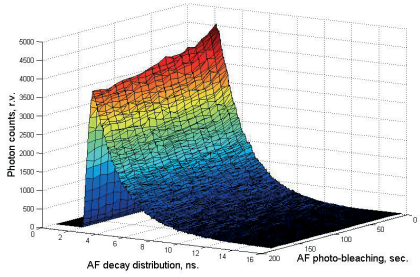

Fig. 2 *In-vivo* skin autofluorescence lifetime decay distributions during 3 minutes of pulse 405 nm excitation with mean power density 2mW/cm^2.

The program uses a deconvolution technique in conjunction with the measured instrumental response to function to obtain corrected autofluorescence decay curve in respect to instrument response. Thus, the set-up allows measuring the lifetimes up to 0.5 ns. The measurements were taken from 3 different spots of healthy skin at the inner part of forearm. For further analysis, the obtained AF decay distributions were approximated applying three-exponential decay model (n=3 (2)). Totally 5 volunteers with different skin photo types were involved into the study.

III. RESULTS

Table 1 represents the measured averaged values of healthy in-vivo skin AF lifetimes and their relative amplitudes. In all cases the healthy skin AF lifetimes and their relative distributions for all volunteers were nearly equal. The standard deviations (SD) show relatively low deviations from the average values.

Table 1. The averaged autofluorescence lifetime components τ_i, and, their relative amplitudes a_i of healthy skin for different volunteers

	a_1	τ_1	a_2	τ_2	a_3	τ_3
Average	69,26	1,52	22,12	6,02	8,6	8,10
Standard deviation (SD)	3,40	0,13	1,33	1,03	2,47	1,68

Each measurement can be also characterized by decreased number of collected photons during the 3 minute measurement cycle. Figure 3 demonstrates such decrease at different time shifts from the exiting pulse. As shown, the dynamics of collected AF photons in the ranges from 1… 2 ns, 5…6 ns and 8…9 ns are very similar and the mean photo-bleaching rate can be determined.

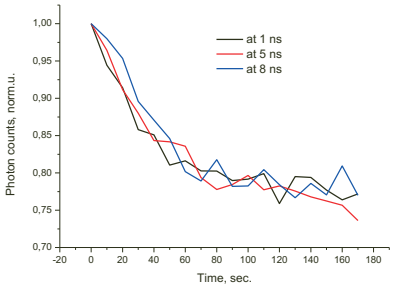

Fig. 3 Autofluorescence intensity decrease at different time shifts after pulse excitation with mean power 2 mw/cm^2.

However, in the case of ten time's stronger (20 mw/cm^2) excitation, the bleaching process becomes more intensive, and less homogeneous. In particular, during the 6 minutes of excitation the number of collected photons in the time gate 1…2 ns decreased approximately by 60%, in the time gate 5…6 ns by~ 55%, and in the time gate 8…9 ns - by~45% (Fig.4).

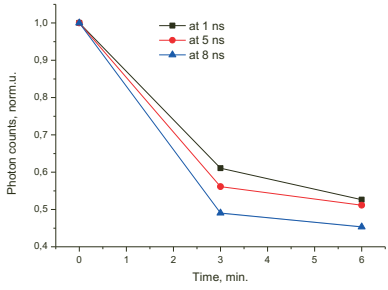

Fig. 4 Autofluorescence intensity decrease at different time shifts after pulse excitation with mean power 20 mw/cm^2.

This result shows that the AF lifetime components during photo-bleaching are changing. The value of τ_1 decreased from 1.52 ± 0.13 to 1.13 ± 0.11 ns, τ_2 decreased from 6.02 ± 1.0 ns to 4.95 ±0.62 ns, and τ_3 decreased from 8.1 ±1.68 ns to 5.97 ± 1.03 ns.

IV. DISCUSSION

The main result of this study is demonstration of possibility to take for parallel measurements of tissue fluorescence lifetimes and photo-bleaching rates by means of a commercial system. Healthy in-vivo skin can be better characterized by two dynamic parameters -autofluorescence lifetime and photo-bleaching rate. Furthermore, photo-bleaching efficiency can be estimated at different time shifts after the pulsed excitation. The observed good agreement between the photo-bleaching curves related to different time shifts at the mean excitation power density of 2mW/cm^2 (Fig.3) may be associated with dominating contribution in the resulting distribution by one specific fluorophore. However, under higher excitation power densities (20 mW/cm^2) the bleaching process becomes inhomogeneous, showing different photo-bleaching rates at different time shifts – it apparently indicates to some skin fluorophore content changes during the photo-bleaching process.

V. CONCLUSIONS

The proposed method demonstrates good perspectives for selective analysis and separation of individual tissue fluorophores underlying FLT and bleaching analysis. The proposed method further can be developed from point measurements to the imaging mode allowing for parallel visualization of tissue fluorescence lifetimes and bleaching rates.

ACKNOWLEDGMENT

This work was funded by the FP-7 projects "LaserLab Europe" (grant agreement n° 284464) and "Fotonika-LV" (grant agreement n° FP7-REGPOT-CT-2011-285912).

REFERENCES

1. Leng-Chun C, William R. Lloyd III, Ching-Wei C, Dhruv S et al. (2013) Fluorescence Lifetime Imaging Microscopy for Quantitative Biological Imaging. Method Cell Biol 114:457-488.

2. Tadrous PJ, Siegel J, French PMW et al. (2006) Time-resolved optical imaging provides a molecular snapshot of altered metabolic function in living human cancer cell models. Opt Express 14:4412-4426.
3. Rinaldi AG, Desplancq FD, Sibler A-P et al. (2013) The use of fluorescent intrabodies to detect endogenous gankyrin in living cancer cells. Exp Cell Res 319, 6:838–849.
4. Stamp GWH. (2003) Fluorescence lifetime imaging of unstained tissues: early results in human breast cancer. J Pathol 199:309-317.
5. Galletly NP, McGinty J, Dunsby C et al. (2008) Fluorescence lifetime imaging distinguishes basal cell carcinoma from surrounding uninvolved skin. Brit J Dermatol 159:152-161.
6. Roberts M.S, Dancik Y, Prow T.W et al. (2011). Non-invasive imaging of skin physiology and percutaneous penetration using fluorescence spectral and lifetime imaging with multiphoton and confocal microscopy. Eur J Pharm Biopharm 77, 3:469-488.
7. Blackwell J, Katika KM, Pilon L et al. (2008) In vivo time-resolved autofluorescence measurements to test for glycation of human skin. J Biomed Opt 13(1):014004 DOI: 10.1117/1.2830658.
8. Chorvat D, Chorvatova A. (2009) Multi-wavelength fluorescence lifetime spectroscopy: A new approach to the study of endogenous fluorescence in living cells and tissues. Laser Phys Lett 6, 3: 178-179.
9. Islam M. S, Honma M, Nakabayashi T et al. (2013) pH Dependence of the Fluorescence Lifetime of FAD in Solution and in Cells. INT J Mol Sci 14:1952–63.
10. Dmitrovsky E, Mycek M. A, Pitts J. Fluorescence lifetime spectrometer (fls) and methods of detecting diseased tissues. World Patent: WO2002069784 A2. Issued date September 12, 2002.
11. Lippincott-Schwartz J, Altan-Bonnet N, Patterson GH. (2003) Photobleaching and photoactivation: following protein dynamics in living cells. Nat Cell Biol 5:S7–S14.
12. Darvin ME, Meinke MC, Sterry W, Lademann J. (2013) Optical methods for noninvasive determination of carotenoids in human and animal skin. J Biomed Opt 61230 DOI: 10.1117/1.JBO.18.6.061230.
13. Wanga H, Zhaoa J, Leea A M.D et al. (2012) Improving skin Raman spectral quality by fluorescence photobleaching. Photodiagn Photodyn 9,4:299-302.
14. Zeng H, MacAulay C, McLean DI, Palcic B et al. (1998) The dynamics of laser-induced changes in human skin autofluorescence--experimental measurements and theoretical modeling. Photochem Photobiol 68(2):227-36.

Author: Alexey Lihachev
Institute: Institute of Atomic physics and Spectroscopy, Biophotonics laboratory, University of Latvia
Street: Raina blvd.19
City: Riga
Country: Latvia
Email: lihachov@inbox.lv

V.

Simultaneous detection of tissue autofluorescence decay distribution and time-gated photo-bleaching rates

Alexey Lihachev*[a], Inesa Ferulova[a], Janis Spigulis[a], Mindaugas Tamosiunas[b]
[a]Biophotonics Laboratory, University of Latvia, 19 Raina Boulevard, Riga 1586, Latvia;
[b]Biophysical research group, Faculty of Natural Sciences, Vytautas Magnus University, Vileikos 8, Kaunas LT-44404, Lithuania

ABSTRACT

Experimental methodology for parallel measurements of in-vivo skin autofluorescence (AF) lifetimes and photo-bleaching dynamic has been developed and tested. The AF lifetime decay distributions were periodically collected from fixed tissue area with subsequent detection of the fluorescence intensity decrease dynamic at different time gates after the pulse excitation. Temporal distributions of human *in-vivo* skin AF lifetimes and bleaching kinetics were collected and analyzed by means of commercial time-correlated single photon counting system.
Keywords: TCSPC, skin autofluorescence, and photo-bleaching.

1. INTRODUCTION

Laser induced time-resolved autofluorescence (AF) spectroscopy represents a promising adjunctive technique for in-vivo tissue diagnostics. Biological and biomedical applications of the autofluorescence spectroscopy have been successfully applied in cell biology and clinical diagnostics for detection of abnormal tissues [1-5]. The most important endogenous fluorophores are molecules widely distributed in cells and tissues, like proteins containing aromatic amino-acids, NAD(P)H, flavins and lipo-pigments [6,7]. The radiative lifetime of each fluorophore is unique, so fluorescence lifetime measurements can provide specific information on fluorophore content and distribution in the tissue. However, in tissue experiments there are a number of de-excitation processes that decrease the characteristic lifetime. Also, tissue fluorescence lifetime value depends on environmental factors e.g. experimental setup, fluorophore localization, skin pH balance, viscosity, temperature etc. [7,8]. Taking into account the aforementioned circumstances, the selective analysis and separation of individual fluorophores underlying multi-exponential decays of in-vivo skin autofluorescence still is challenging problem.

Moreover, tissue autoflurescence usually shows the photo-bleaching effect which is caused by chemical modification of the fluorophore due to repeated excitation/emission states. Temporal behavior of skin autofluorescence photo-bleaching can be well described by double exponential function [9]. The mechanism of photo-bleaching effect has not been explained in detail so far; however many studies have focused on purposeful use of photo-bleaching in biomedical applications. Some of the authors successfully applied bleaching effect in Raman spectroscopy for improving the Raman spectra quality by decreasing of tissue fluorescence background [10,11]. In photodynamic therapy, photo-bleaching of exogenous fluorophores was used as tool for tracking the concentration changes of light sensitizing agents and for individualization of irradiation time during the therapy [12]. In fluorescence microscopy the photo-bleaching widely used to investigate diffusional mobility of fluorescing proteins in living cells [13]. Also some of authors propose the use photo-bleaching as a tool to measure the local strain field in fibrous membranes of connective tissues [14].

In spite the fact that the mechanism of photo-bleaching is still unclear one can assume that tissue fluorophore might have its own specific bleaching kinetic, which can provide information on fluorophore concentration and environmental factors. Thus, the photo-bleaching at different time gates after the pulse excitation might provide additional information for selective analysis and separation of individual tissue fluorophores in combination with fluorescence lifetime spectroscopy.

The correlations between tissue AF lifetimes and photo-bleaching rates are studied in this work. The measurements were collected from different parts of healthy skin, nail and benign nevus. Autofluorescence decay temporal distributions were approximated by three exponential decay functions, and AF intensity decrease at different time gates after the pulse excitation during the repeated excitation were recorded and displayed on a plot.

Photon Counting Applications 2015, edited by Ivan Prochazka, Roman Sobolewski, Ralph B. James,
Proc. of SPIE Vol. 9504, 95040P · © 2015 SPIE · CCC code: 0277-786X/15/$18 · doi: 10.1117/12.2178827

2. MATERIALS AND METHODS

The measurement setup scheme for simultaneous detection of tissue AF lifetimes and photo-bleaching rates is shown in Fig. 1. The measurement setup comprised a pico-second excitation laser (PicoQuant: pulse half-width 59 ps, 405nm, mean power density ~2mW/cm^2, mod. LDH-D-C-405) laser controller, monochromator, photon counting detector with temporal resolution of 180ps (mod. Becker&Hickl, PMC-100-4), data processing system "time-correlated single photon counting" with time resolution 6.6 ps, (TCSPC, mod. Becker&Hickl SPC-150), and a fiber optic probe. The fiber optic probe was tightly fixed such to provide the distance between the skin surface and tip of the Y-shaped fiber bundle was 3 mm. The diameter of the irradiated skin spot was ~3 mm.

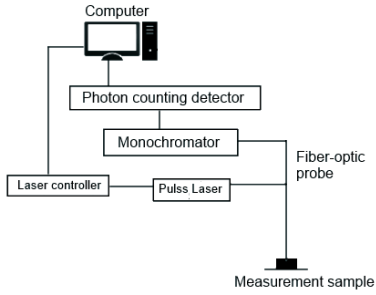

Figure 1. Experimental setup for simultaneous detection of autofluorescence decay distribution and photo-bleaching rates.

Skin AF decay distributions were collected every 10 seconds during 3 minutes. Totally 18 measurements (Fig.2) of tissue AF decay distributions were registered.

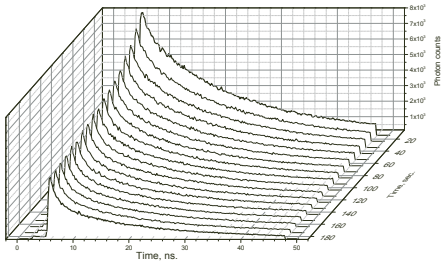

Figure 2. *In-vivo* human skin AF decay distributions collected during 3 minute cycle. Each distribution was collected at 490 nm wavelength during 10 seconds, power density 2mW/cm^2.

Each measurement contained temporal distribution of AF decay and a number of registered photons collected during the 10 seconds. Due to the AF photo-bleaching process, the number of collected photons for each subsequent measurement decreases, thereby giving the opportunity to construct the AF photo-bleaching kinetics at different time gates after the pulse excitation. Autofluorescence lifetimes were collected at 490 nm emission wavelength using monochromator and interference filters. The obtained AF decay distributions were automatically processed using the Becker&Hickl SPCImage program. The results were approximated by a multi-exponential decay function:

$$f(t) = \sum_{i=o}^{n} a_i \exp^{-t/\tau_i} + c \quad (1)$$

were *f(t)* is AF intensity at time moment t after the excitation pulse, *n* is number of decaying species in the exponential sum, and *c* is a background level of light in each particular case. The applied model comprises the lifetimes of the exponential components, τ_i, and the amplitudes of the exponential components, a_i.

3. RESULTS

Table 1 represents the AF lifetimes and their relative amplitudes collected form palm skin, forearm inner side skin, nail and intradermal nevus. The represented AF lifetimes obtained at two different time moments, at the beginning of the experiment and after 3 minutes of the repeated excitation with pulse 405 nm laser. The AF decay distribution of skin, nail and intradermal nevus can be characterized by three exponential decay components $\tau_{1,2,3}$ and their relatives amplitudes $a_{1,2,3}$. The vertical arrows have indicated on the direction of changes of obtained decay components and their amplitudes after 3 minutes of pulse excitation. As shown in Tab.1, AF lifetimes and their amplitudes after 3 minutes of pulse irradiation have slightly changed.

Table 1. The autofluorescence lifetime components τ_i, and, their relative amplitudes a_i collected from different parts of healthy skin, nail and intradermal nevus. AF lifetimes were obtained at two different time moments, before photo-bleaching (t=0 sec.), after 3 min of photo-bleaching (t=3min.).

Localization, measurement time moment	τ_1/ns, a_1(%)	τ_2/ns, a_2(%)	τ_3/ns, a_3(%)
Palm, t=0 sec.	1.0 ns, 55.8%	3.0 ns, 30.6%	8.9 ns, 13.6%
t=3 min.	0.8 ns ↓, 47.3% ↓	2.4 ns ↓, 37.1% ↑	8.9 ns, 15.5% ↑
Forearm inner side, t=0 sec.	1.0 ns, 54.2%	3.0 ns, 32.1%	9.0 ns, 13.6%
t=3 min.	1.0 ns, 57.5% ↑	3.1 ns, 29% ↓	9.1 ns, 13.5%
Nail, t=0 sec.	1.0 ns, 57.8%	3.2 ns, 34.4%	8.4 ns, 7.9%
t=3 min.	1.0 ns, 55.9% ↓	3.0 ns ↓, 35.1% ↑	8.1 ns ↑, 9% ↑
Intradermal nevus, t=0 sec.	0.9 ns, 60.3%	2.7 ns, 26.6%	8.1 ns, 13.1%
t=3 min.	0.9 ns, 62.7% ↑	2.7 ns, 26.1% ↓	8.7 ns ↑, 11.2% ↓

The more pronounced changes have occurred in the case of the palm skin. The value of τ_1 decreased from 1.0 to 0.8 ns, τ_2 decreased from 3.0 ns to 2.4 ns. At the same time, their amplitudes a_1 decreased from 55.8% to 47.3%, a_2 increased from 30.6% to 37.1% and a_3 increased from 13.6% to 15.5%. Furthermore, in the case of palm skin the photo-bleaching kinetics at different time gates have shown different decrease rates (Fig.3). In particular, during the 3 minutes the number of collected photons in the 6 ns time gate decreased approximately by 30%, in the 11 ns gate by 25%, and in the 21 ns gate by 20%. This result demonstrates that the fluorophores with higher lifetime bleach slower than fluorophores with short lifetime. Also, photo-bleaching kinetic at 6 ns gate can be well described by double-exponential fitting.

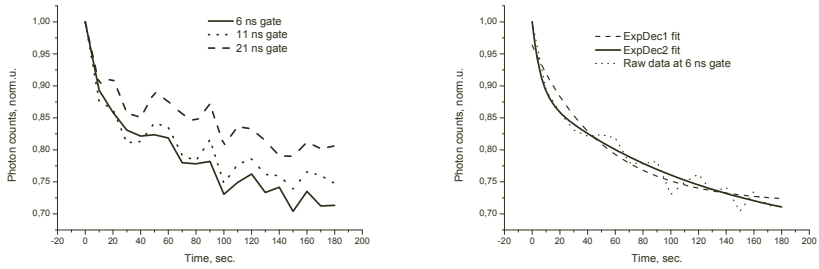

Figure 3. Palm skin AF photo-bleaching kinetics (left) at different time gates during 3 minutes of pulse excitation. Raw data (right) for the bleaching kinetic at 6 ns gate approximated by mono and double exponential functions.

Fig. 4 represents a photo-bleaching kinetics collected for forearm inner side skin and nail. As shown, in both cases the kinetics of collected AF photons in the different time gates is very similar, and can be well described by mono-exponential fitting.

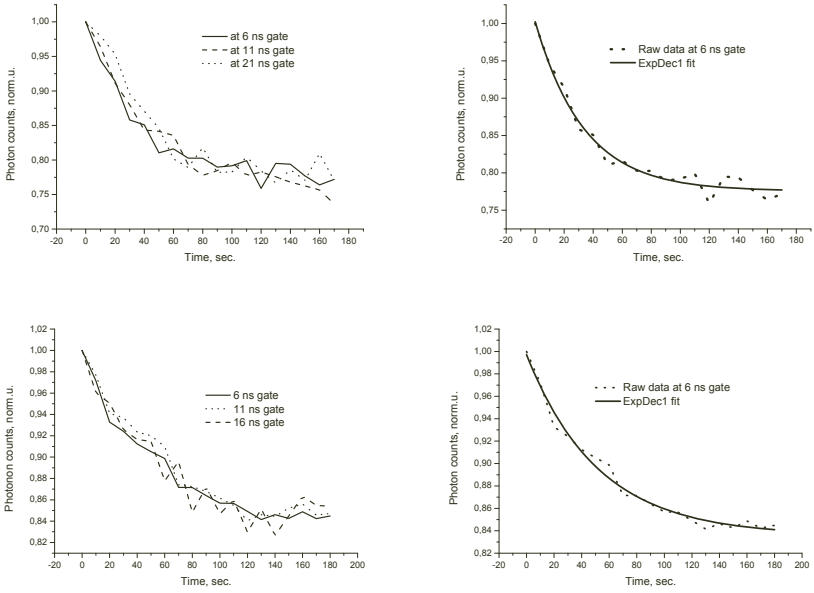

Figure 4. Forearm inner side skin and nail AF photo-bleaching kinetics at different time gates during 3 minutes of pulse excitation (left). Raw data (right) for the bleaching kinetic at 6 ns gate approximated by mono exponential function.

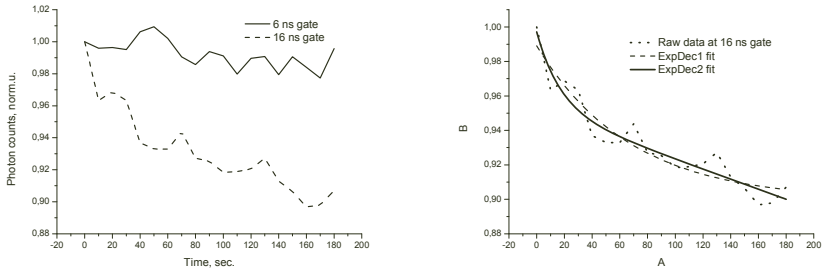

Figure 5. Intradermal nevus AF photo-bleaching kinetics at different time gates during 3 minutes of pulse excitation (left). Raw data (right) for the bleaching kinetic at 16 ns gate approximated by mono and double exponential functions.

In the case of intradermal nevus (Fig.5) kinetics of time gated photo-bleaching is completely different, showing the fastest bleaching in higher time gate. In particular, the number of collected photons at 6 ns gate remains virtually unchanged during the 3 minutes of pulse excitation, while the number of collected photons at 16 ns gate has decreased approximately by 10%. Moreover, the photo-bleaching kinetics obtained at 16 ns time gate can be better described by double-exponential fitting in comparison with mono-exponential fitting (Fig.6 right).

4. CONCLUSSIONS

The main result of this study is demonstration of possibility to take for parallel measurements of tissue fluorescence lifetimes and photo-bleaching rates at different time gates after the pulse excitation by means of a commercial system. *In-vivo* tissues can be characterized by AF lifetimes and time gated photo-bleaching rates. In all cases observed significant decrease in the number of collected photons in the nanosecond time scale range indicates on noticeable contribution photo-bleaching process during the 3 minutes of pulse excitation by 405 nm laser. The obtained results demonstrate that in the case of forearm inner side skin and nail (Fig.4) the photo-bleaching at different time gates are homogenous. In the case of palm skin (Fig.3) and intradermal nevus (Fig.5) observed inhomogeneous photo-bleaching at different time gates. The homogeneous intensity decreasing at different time gates, most probably associated with dominating of one specific fluorophore in resulting decay distribution. While, the uneven photo-bleaching at different time gates presumably indicates on the presence in resulting AF decay distribution at least two different fluorophores, moreover these fluorophores have own bleaching rate.

The proposed method demonstrates good perspectives for selective analysis and separation of individual tissue fluorophores underlying FLT and time-gated bleaching analysis.

ACKNOWLEDGMENT

Financial support of the EC FP7program (projects “ Fotonika-LV, ” “ FP7-REGPOT-CT-2011-285912, ” ERA-NET BiophotonicsPlus “ BI-TRE, ” and “ LaserLab Europe, ” EU-FP7 284464), and European Regional Development Fund (2014/0041/2DP/2.1.1.1.0/14/APIA/VIAA/015) is highly appreciated.

REFERENCES

[1] Sud, D., Zhong, W., Beer, D. and Mycek, A., "Time-resolved optical imaging provides a molecular snapshot of altered metabolic function in living human cancer cell models," Opt Express. 14(10), 4412-4426 (2006).

[2] Rinaldi, AS., Freund, G., Desplancq, D., Sibler, AP., Baltzinger, M., Rochel, N., Mely, Y., Didier, P., Weiss, E., "The use of fluorescent intrabodies to detect endogenous gankyrin in living cancer cells," Exp Cell Res. 1:319(6), 838-49 (2013).

[3] Tadrous, PJ.,, Siegel, J., French, PM., Shousha, S., Lalani, el-N., Stamp, GW., "Fluorescence lifetime imaging of unstained tissues: early results in human breast cancer," J Pathol. 199(3), 309-17 (2003).
[4] Galletly, NP.,, McGinty, J., Dunsby, C., Teixeira, F., Requejo-Isidro, J., Munro, I., Elson, DS., Neil, MA., Chu, AC., French, PM., Stamp, GW., "Fluorescence lifetime imaging distinguishes basal cell carcinoma from surrounding uninvolved skin," Br J Dermatol. 159(1), 152-61 (2008).
[5] Pires, L., Nogueira, MS., Pratavieira, S., Moriyama, LT., Kurachi, C., "Time-resolved fluorescence lifetime for cutaneous melanoma detection," Biomed Opt Express. 5(9), 3080-9 (2014).
[6] Borisova, E.G., Angelova, L.P., Pavlova, E.P., "Endogenous and Exogenous Fluorescence Skin Cancer Diagnostics for Clinical Applications," IEEE J. Quantum Electron. 20 (2), 7100412 (2014).
[7] Chorvat, D., and Chorvatova, A., "A new approach to the study of endogenous fluorescence in living cells and tissues," Laser Phys Lett. 6(3), 178-179 (2009).
[8] Serajul, I., Masato, H., Takakazu, N., Masataka K., Nobuhiro, O., "pH Dependence of the Fluorescence Lifetime of FAD in Solution and in Cells," Int J Mol Sci. 14(1), 1952–1963 (2013).
[9] Zeng, H., MacAulay, C., McLean DI., Palcic, B., Lui, H., "The dynamics of laser-induced changes in human skin autofluorescence experimental measurements and theoretical modeling," Photochem Photobiol. 68(2), 227-36 (1998).
[10] Darvin, ME., Meinke, MC., Sterry, W., Lademann, J., "Optical methods for noninvasive determination of carotenoids in human and animal skin," J Biomed Opt. 18(6), 61230 (2013).
[11] Wang, H., Zhao, J., Lee, AM., Lui, H., Zeng, H., "Improving skin Raman spectral quality by fluorescence photobleaching," Photodiagn Photodyn. 9(4), 299-302 (2012).
[12] Goodwin, JS., Kenworthy, AK., "Photobleaching approaches to investigate diffusional mobility and trafficking of Ras in living cells," Methods. 37(2), 154–164 (2005).
[13] Hennig, G., Stepp, H., Johansson, A., "Photobleaching-based method to individualize irradiation time during interstitial 5-aminolevulinic acid photodynamic therapy," Photodiagnosis Photodyn Ther.8(3), 275-81 (2011).
[14] Jayyosi, C., Fargier, G., Coret, M., Bruyere-Garnier, K., "Photobleaching as a tool to measure the local strain field in fibrous membranes of connective tissues," Acta Biomater. 10(6), 2591-601 (2014).

VI.

PACS numbers: 87.50.W–; 87.64.Rv
DOI: 10.1070/QE2014v044n08ABEH015483

Investigation of *in-vivo* skin autofluorescence lifetimes under long-term cw optical excitation

A. Lihachev, I. Ferulova, K. Vasiljeva, J. Spigulis

Abstract. **The main results obtained during the last five years in the field of laser-excited *in-vivo* human skin photobleaching effects are presented. The main achievements and results obtained, as well as methods and experimental devices are briefly described. In addition, the impact of long-term 405-nm cw low-power laser excitation on the skin autofluorescence lifetime is experimentally investigated.**

Keywords: *skin autofluorescence, photobleaching, lifetime spectroscopy.*

1. Introduction

A decrease in the fluorescence intensity as a result of long-term optical excitation is known as photobleaching. Laser-excited tissue autofluorescence photobleaching (AFPB) has been studied extensively over the last few decades. Most of the authors observed that a decrease in the skin autofluorescence (AF) intensity can be well described empirically by a double exponential function [1–6]. Under cw excitation, the autofluorescence intensity I mainly decreases during the first 10–15 s, followed by a slow-down. In this case, there is a residual intensity, which asymptotically strives to a constant level A:

$$I(t) = a\exp(-t/\tau_1) + b\exp(-t/\tau_2) + A. \quad (1)$$

Here, τ_1 and τ_2 characterise the fast and slow phase of AFPB, respectively; a, b and A are the constants; and t is the time. Our previous research has shown that the photobleaching effect was evident in all skin types and in some skin pathologies under UV/VIS laser excitation. The photobleaching effect can be approximated with a double exponential function for all skin types and most skin pathologies [7, 8]. The authors of [8, 9] demonstrated that the temporal analysis of AF photobleaching indices for different areas of the skin may vary, and the bleaching rates distribution over the skin surface is uneven. A subsequent study of laser-excited skin photobleaching has demonstrated that AF intensity recovery (Fig. 1) after 2-min cw excitation is a long-term process. The measurements of the recovery kinetics show that even after 125 hours of relaxation, the AF intensity of the skin recovered to only 80% of its initial value. And the consequence of the long-term recovery of intensity, the skin 'photo-memory' effect, has been experimentally demonstrated: low-power laser irradiation (below the standard skin safety limits) leaves traces in skin for several days [10, 11].

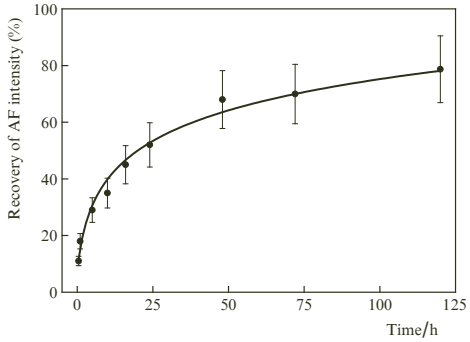

Figure 1. Kinetics of skin AF recovery after 2-min cw excitation by a 532-nm laser with a power density of 85 mW cm^{-2} [10].

Although the cause that gives rise to the photobleaching phenomenon remains unclear, it has become the focus of attention for its potential as a clinical diagnostic tool. In our previous clinical research we have focused on AFPB analysis of different pigmented, vascular and malignant skin pathologies. The analysis of dermatological pathologies showed that the most sensitive from the point of view of diagnosis are the parameters τ_1 and A. The pronounced difference in the A values (Fig. 2) for skin basal cell carcinomas appears to show the most promise for clinical implementation [12, 13].

In studying experimentally the AFPB of human skin we have found that under long-term cw irradiation the AF spectra as well as the diffuse reflectance spectra (Fig. 3) exhibit reabsorption peaks, which correspond to the absorption bands of oxy-haemoglobin. Thus, the appearance of the absorption peaks in the green (540 nm) and yellow (580 nm) regions of the visible spectrum during the experiment is an indication of a certain role of oxy-haemoglobin in the photobleaching process [14].

Although the mechanism of skin autofluorescence photobleaching has not been established in detail so far, we can assume that long-term cw laser irradiation most probably causes the photochemical process that leads to degradation of endogenous fluorophores. In turn, the degradation of skin fluorophores should affect the resulting skin autofluorescence lifetimes. The skin fluorophores that emit fluorescence under violet-blue excitation are NADH, flavins, porphyrins, localised

A. Lihachev, I. Ferulova, K. Vasiljeva, J. Spigulis Institute of Atomic Physics and Spectroscopy, University of Latvia, 19 Raina blvd, Riga, LV-1586, Latvia; e-mail: lihachov@inbox.lv, janispi@latnet.lv

Received 25 February 2014; revision received 15 June 2014
Kvantovaya Elektronika **44** (8) 770–773 (2014)
Submitted in English

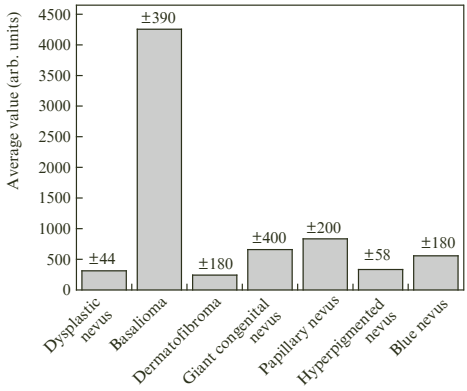

Figure 2. Average values of the photobleaching parameter A for different skin pathologies [12].

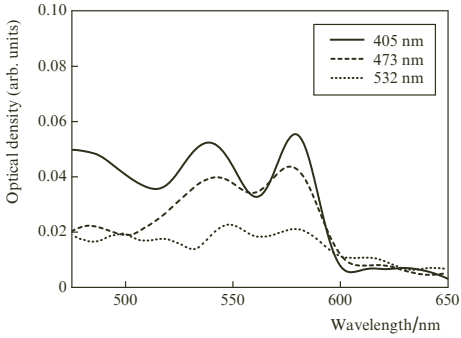

Figure 3. Typical oxy-haemoglobin absorption peaks in post-irradiated diffuse reflectance spectra of skin [14].

in the epidermis keratin as well as dermal elastin and collagen [5]. The radiative lifetime characteristics of each fluorophore are unique and can provide specific information for tissue identification. The fluorescence lifetimes for these skin fluorophores fall within range from 0.2 to 15 ns. However, in tissue experiments there are a number of de-excitation processes that decrease the characteristic lifetime. In addition, tissue fluorescence lifetime values are dependent on many environmental factors, such as the experimental setup, fluorophore localisation, skin pH balance, viscosity, temperature, etc. [15–17]. Taking into account the aforementioned circumstances, the selective analysis and separation of individual fluorophores underlying multi-exponential decays of *in-vivo* skin autofluorescence is still a challenging problem.

The goal of the experiment described in this paper is to investigate *in-vivo* skin AF lifetimes during long-term cw low-power laser excitation.

2. Experimental

The main focus of this study was to investigate *in-vivo* skin AF lifetimes under long-term optical excitation by a low-power laser at 405 nm. For this purpose an experimental setup to carry out parallel point measurements of skin AF lifetimes and photobleaching rates was assembled (Fig. 4). The setup comprises a picosecond/cw laser (PicoQuant LDH-D-C-405: pulse half-width 59 ps, 405nm), a laser controller, a monochromator, a photon counting detector with a temporal resolution of 180 ps (Becker&Hickl PMC-100-4), a data processing system for 'time-correlated single photon counting' with time resolution 6.6 ps (TCSPC, model SPC-150, Becker&Hickl GmbH), a fibre-optic probe, a CCD spectrometer (AvaSpec 2048) and a computer. The surface of healthy skin was excited via optical fibre by a pulsed laser for the lifetime measurements or by a cw laser for photobleaching measurements.

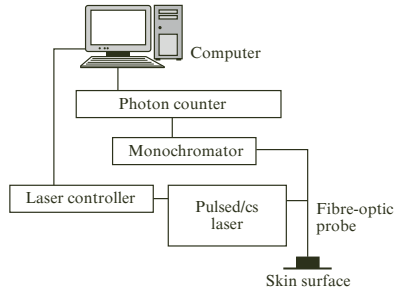

Figure 4. Experimental setup for parallel measurements of skin AF lifetime and photobleaching rate.

In order to avoid artefacts caused by the movements of the body, the arm was fixed during the measurements in a special position-stabilised holder. Autofluorescence was excited and measured on healthy, previously non-irradiated skin (at a distance of 6 mm from its surface) in the inner part of the forearm. Autofluorescence decay was measured on the same portions of skin prior to irradiation and immediately after 6-min cw excitation with the laser power density of 20 mW cm^{-2}. In all cases the time required for the collection of the AF lifetime data was 10 s at 480±10 nm. During 6 minutes of continuous cw excitation an AF intensity decrease was recorded by a spectrometer in the 450–800 nm spectral range. The autofluorescence intensity of skin was investigated using SPCM software (Becker&Hickl) by collecting photon counts during fixed time intervals. For the analysis of AF lifetimes, a multi-exponential fluorescence decay distribution model was applied:

$$f(t) = \sum_{i=0}^{n} a_i \exp(-t/\tau_i) + c, \tag{2}$$

where $f(t)$ is the AF intensity at time t after the excitation pulse, n is number of decaying species in the exponential sum and c is a background level of light in each particular case. The applied multi-exponential fitting model allowed us to obtain characteristic lifetimes of the exponential components, τ_i, and their amplitudes, a_i.

The program uses a deconvolution technique in conjunction with the measured instrumental response function to obtain an autofluorescence decay curve corrected for the instrument

Table 1. Averaged values and standard deviations (in brackets) of autofluorescence lifetime components, τ_i, and their relative amplitudes a_i.

Instant of time	Two-exponential fitting				Three-exponential fitting					
	a_1 (%)	τ_1/ns	a_2 (%)	τ_2/ns	a_1 (%)	τ_1/ns	a_2 (%)	τ_2/ns	a_3 (%)	τ_3/ns
Before photobleaching	72.48 (2.42)	1.63 (0.17)	27.52 (2.42)	7.15 (1.00)	69.26 (3.40)	1.52 (0.13)	22.12 (1.33)	6.02 (1.03)	8.6 (2.47)	8.10 (1.68)
After 3 min of photobleaching	71.66 (2.56)	1.29 (0.15)	28.34 (2.56)	6.22 (1.07)	72.14 (2.53)	1.31 (0.13)	20.94 (3.05)	6.25 (0.74)	6.94 (0.66)	6.81 (2.30)
After 6 min of photobleaching	70.9 (3.15)	1.13 (0.13)	29.1 (3.15)	5.37 (0.88)	71.32 (2.9)	1.13 (0.11)	21.22 (3.57)	4.95 (0.62)	7.46 (0.81)	5.97 (1.03)

response. Thus, the setup allows measurements of lifetime durations up to 0.5 ns. The measurements were collected from 3 different spots of healthy skin from the inner part of the forearm. For further analysis, the obtained AF decay time distributions were approximated with a two- and three exponential decay model. In total, ten volunteers with different skin photo types were involved in the study.

3. Results

Table 1 represents the averaged values of AF lifetimes and their relative amplitudes obtained from 10 different volunteers. Autofluorescence decay distributions were collected at three different time moments, before photobleaching, after 3 min of photobleaching and after 6 min of photobleaching. In all cases the healthy skin AF lifetimes and their contribution for all volunteers were virtually equal. The standard deviations (SD) show relatively low deviations from the average values.

The AF decay distribution of previously non-irradiated skin can be characterised by the parameters $\tau_{1,2}$ and $a_{1,2}$ or $\tau_{1,2,3}$ and $a_{1,2,3}$ (depending on the fitting model). In fitting one and the same AF decay distribution by two and three-exponential functions we obtain the same values of the parameters τ_1 and τ_2 within the standard deviation. However, with respect to three-exponential fitting an additional decay component with a relatively high lifetime $\tau_3 \sim 8.1$ ns and a low amplitude $a_3 \sim 8.6\%$ can be distinguished from the resulting decay distribution.

Figure 5 demonstrates *in-vivo* skin AF lifetime decay distributions before and after 6 min of cw excitation. As shown, AF lifetimes of skin after 6 min pre-irradiation have changed. Respectively, a significant decrease in τ_1 and τ_2 values

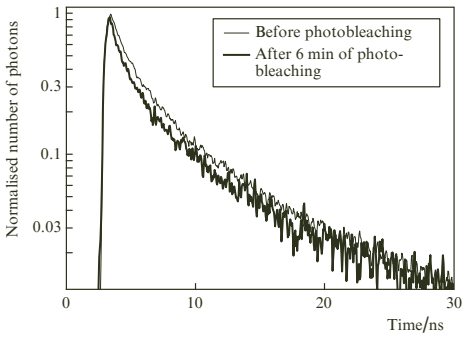

Figure 5. Skin AF lifetime decay curves before and immediately after 6 min of 405-nm cw laser irradiation.

is observed. The value of τ_1 decreased from 1.52±0.13 to 1.13±0.11 ns, τ_2 decreased from 6.02±1.0 ns to 4.95±0.62 ns and τ_3 – from 8.1±1.68 ns to 5.97±1.03 ns. At the same time, the amplitudes of the decay components demonstrate relatively insignificant changes. We have found that the changes in the AF decay distribution are a consequence of uneven bleaching of tissue fluorophores during long-term irradiation. The photon count at different instants of time after excitation shows a nonuniform decrease in the number of AF photons. Thus, the number of collected photons in the time range from 3 ns to 4 ns decreased approximately by 45%, in the range from 5 to 6 ns by 55% and photons collected in range from 8 ns to 9 ns decreased by 60%. Also after 6 min of cw irradiation, the quantile χ^2_r decreased from 1.4±0.2 to 1.1±0.1. At the same time we have found that the lifetime indices τ_2 and τ_3 become equal within the standard deviation after 6 min of optical excitation.

4. Discussion

The reported results demonstrate that three-exponential fitting of the obtained skin autofluorescnce decay distribution is more informative and reveals a third component with a relatively high lifetime and a low amplitude. This decay component was observed by several authors under violet excitation, and probably is associated with collagen cross links formed by advanced glycation end-products [18, 19]. At the same time, the components, τ_1 and τ_2, represent the averaged lifetimes of all emitting fluorophores (under 405-nm excitation), such as, collagen, elastin, keratin, NADH and flavines. The lifetimes of these fluorophores are characterised by short and long components. Moreover, the short components of these fluorophores lies in the picosecond range [15]. Thus, the precise estimation of the short AF decay component is impeded by system response time and serious contribution of laser excitation (scattering and reflection) [20, 21]. However, a significant decrease in the number of collected photons in the entire nanosecond time scale range during the bleaching process indicates a noticeable contribution of tissue fluorescence to the resulting decay distribution.

The main result of this work is an experimental demonstration of a decrease in the skin AF lifetime during the photobleaching process. The lifetime decrease indicates that the skin fluorophore content changes during the photobleaching process. This decrease is most probably caused by the equalisation of the fluorophore content of skin during this process. In addition, after photobleaching the tendency to equalisation of lifetime components $\tau_{2,3}$ suggests that the third component of the exponential expansion disappears, which may indicate that a certain fluorophore or group of fluorophores that had given rise to the parameter τ_3 has become extinct or changed concentration. Taking into account the long-term recovery of the AF intensity after photobleaching [10], a decrease in the

lifetimes is probably caused by a nonuniform degradation or photodamage of skin fluorophores after long-term optical excitation. We also should mention the fact that during the 7th or 8th minute of 15-min excitation the number of photons collected began to increase after a steady decrease, leading to a significant increase in the third decay component (τ_3) from 5.67 ns to 15.0 ns. An increase in the AF intensity and lifetimes indicates either heterogenous degradation of skin fluorophores or formation of their new compositions. Undoubtedly, this phenomenon requires additional study to determine the exact mechanism of photobleaching and its influence on the skin physiology.

5. Conclusions

This paper reviews the main achievements of cw laser-excited skin autofluorescence photobleaching and its potential applications in clinical diagnostics. In the experimental part of work we have demonstrated uneven bleaching of skin fluorophores under long-term optical excitation, which leads to a change in the autofluorescence decay distribution. This effect of uneven bleaching of autofluorescence requires additional studies to identify the fluorophores responsible for the change in the lifetime distribution. In addition, studies should involve more volunteers of different age with all skin photo types, and also include a variety of pathological structures.

Acknowledgements. This work was supported by FP-7 projects 'Fotonika-LV – FP7-REGPOT-CT-2011-285912' and 'LaserLab Europe' (Contract No. 284464).

References

1. Zeng H., MacAulay C.E., Palcic B., McLean D.I. *Proc. SPIE Int. Soc. Opt. Eng.*, **1882**, 278 (1993).
2. Salomatina E.V., Pravdin A.B. *Proc. SPIE Int. Soc. Opt. Eng.*, **5068**, 405 (2001).
3. Stratonnikov A.A., Polikarpov V.S., Loschenov V.B. *Proc. SPIE Int. Soc. Opt. Eng.*, **4241**, 13 (2001).
4. Wang H., Zhao J., Lee A.M.D., Lui H., Zeng H. *Photodiagn. Photodyn.*, **9** (4), 299 (2012).
5. Darvin M.E., Brandt N.N., Lademann J. *Opt. Spectrosc.*, **109** (2), 205 (2010).
6. Finlay J.C., Mitra S., Patterson M.S., Foster T.H. *Phys. Med. Biol.*, **49** (21), 4837 (2004).
7. Lihachev A., Spigulis J. *IEEE Xplore*, 10.1109/NO, 63 (2007).
8. Spigulis J., Lihachev A., Erts R. *Appl. Opt.*, **48** (10), D163 (2009).
9. Jakovels D., Spigulis J. *Proc. SPIE Int. Soc. Opt. Eng.*, **7376**, 737618 (2010).
10. Lihachev A., Lesins J., Jakovels D., Spigulis J. *Kvantovaya Elektron.*, **40** (12), 1077 (2010) [*Quantum Electron.*, **40** (12), 1077 (2010)].
11. Lesins J., Lihachev A., Rudys R., Bagdonas S., Spigulis J. *Proc. SPIE Int. Soc. Opt. Eng.*, **8092**, 80920N (2011).
12. Lihachev A., Rozniece K., Lesins J., Spigulis J. *Proc. SPIE Int. Soc. Opt. Eng.*, **8087**, 80872F (2011).
13. Spigulis J. *Latv. J. Phys.*, **49**, 5 (2012).
14. Ferulova I., Lesins J., Lihachev A., Jakovels D., Spigulis J. *Proc. SPIE Int. Soc. Opt. Eng.*, **8427**, 84273I (2012).
15. Chorvat D., Chorvatova A. *Laser Phys. Lett.*, **6** (3), 178 (2009).
16. Islam M.S., Honma M., Nakabayashi T., Kinjo M., Ohta N. *Int. J. Molec. Sci.*, **14**, 1952 (2013).
17. Dmitrovsky E., Mycek M.A., Pitts J. World Patent WO2002069784 A2, 2002.
18. Ediger H.E., Unione M., Deemer A., Stroman E., Baynes M., Korss J. *Opt. Express*, **12** (19), 4496 (2004).
19. Blackwell J., Katika K.M., Pilon L., Dipple K.M., Levin S.R., Nouvong A. *J. Biomed. Opt.*, **13** (1), 014004 (2008).
20. König K., Ehlers A., Stracke F., Riemann I. *Skin Pharmacol. Physiol.*, **19** (2), 78 (2006).
21. Bird D.K., Yan L., Vrotsos K.M., Eliceiri K.W., Vaughan E.M., Keely P.J., White J.G., Ramanujam N. *Cancer Res.*, **65** (19), 8766 (2005).

VII.

Fluorescence lifetime spectroscopy: potential for in-vivo estimation of skin fluorophores changes after low power laser treatment

Inesa Ferulova, Alexey Lihachev and Janis Spigulis

Institute of Atomic Physics and Spectroscopy, University of Latvia
Raina Blvd. 19, Riga, LV-1586, Latvia
e-mail: inesa.ferulova@gmail.com

ABSTRACT

The impact of visible cw laser irradiation on skin autofluorescence lifetimes was investigated in spectral range from 450 nm to 600 nm. Skin optical provocations were performed during 1 min by 405 nm low power cw laser with power density up to 20 mW/cm^2. Autofluorescence lifetimes were measured before and immediately after the optical provocation.

Key words: laser-skin interaction, skin, autofluorescence lifetime.

1. INTRODUCTION

Time and spectral dependencies of *in-vivo* skin autofluorescence and diffuse reflectance under continuous laser excitation have been studied in our previous works. Particular interest of our studies was related to the skin autofluorescence photobleaching. Skin autofluorescence photobleaching was investigated for healthy and pathological skin under 405 nm, 473 nm and 532 nm excitation [1, 2]. Specific distribution of bleaching parameters in healthy and pathological skin [3] was obtained. It was proved, that increased melanin content in the skin slows down the photobleaching process [4]. Our previous studies show that restoration of autofluorescence after photobleaching is a long-term process [2]. Influence of cw laser irradiation on skin diffuse reflectance in spectral range from 500 nm – 600 nm was also demonstrated [5]. Diffuse reflectance study showed that low power cw laser irradiation increases the skin oxy-hemoglobin absorption. However, the mechanism of skin autofluorescence photobleaching is still under discussion. Most probably, the photobleaching is caused by degradation of the skin fluorophore molecules. The fluorophores that emit under blue-green excitation are NAD, and keratin coferments (localized in epidermis), as well as the dermal collagen and elastin [6, 7, 8]. Thus, the degradation of skin fluorophores should affect the skin autofluorescence lifetime. Therefore, the aim of this study is to investigate the skin autofluorescence lifetimes before and after low power cw laser pre-irradiation.

2. EQUIPMENT AND METHODOLOGY

The set-up for fluorescence lifetime (FL) measurements presented in Fig.1. It comprises of a pico-second laser (PicoQuant: pulse half-width 59 ps, 405nm, model LDH-D-C-405), photon counting detector with temporal resolution of 180ps (mod. Becker&Hickl, PMC-100-4), data processing system “time-correlated single photon counting” with time resolution 6.6 ps, (TCSPC, mod. SPC-150), Y-shaped fiber-optic probe for

Biophotonics iga 2013, edited by Janis Spigulis, Ilona u ina, Proc. of SPIE Vol. 9032,
90320B · © 2013 SPIE · CCC code: 1605-7422/13/$18 · doi: 10.1117/12.2044688

delivering radiation to the skin surface and collecting excited autofluorescence, a monochromator and a computer. The set-up allows measure the lifetime duration 0.1 ns.

The fiber optic probe was designed to provide the optimal distance of 3 mm between the skin surface and the optical fiber tip for simultaneous fluorescence excitation and collecting. Skin autofluorescence lifetimes under 405 nm excitation were collected before and immediately after a 1 minute irradiation by 405 nm cw-laser light with power density of 20 mW/cm^2. Skin autofluorescence lifetimes were measured in the spectral range from 450 nm – 600 nm with 10 nm increment.

Obtained results automatically processed using programs from Becker&Hickl. Skin autofluorescence lifetime kinetics were approximated with double-exponential:

$$f(t) = a_1 e^{-\frac{t}{\tau_1}} + a_2 e^{-\frac{t}{\tau_2}} \quad (1),$$

where $\tau_{1,2}$ are lifetimes and $a_{1,2}$ are amplitudes.

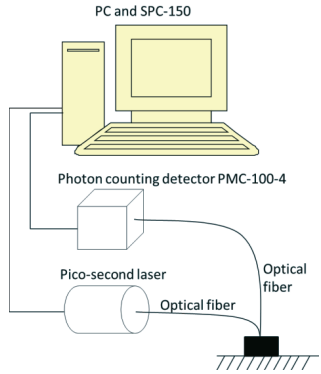

Fig.1. Experimental setup for in-vivo skin autoflurescence lifetime measurements.

3. RESULTS

Skin autofluorescence lifetimes before and after 1 minute of 405 nm laser irradiation were investigated in spectral region from 450 nm to 600 nm with 10 nm increment. In all cases, the number of collected photons was decreased, however lifetimes remain unchanged. The skin autofluorescence lifetime kinetics before and after 1 minute irradiation is presented in figure 2. The significant decreasing of collected autofluorescence photons was occurred. During 1 minute of optical provocation the total amount of collected photons decreased by 40% as compared to the “fresh” skin.

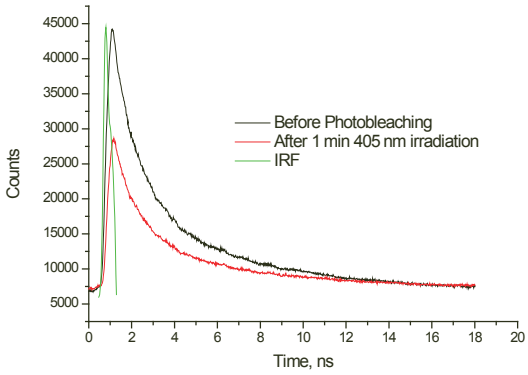

Fig.2 Skin autofluorescence lifetime kinetics before and after 1 min irradiation. 405 nm excitation, signal collected at 500 nm; IRF - Instrument response function.

Results presented in figure 3 illustrate skin autofluorescence lifetimes before (black line) and after 1 minute irradiation. As seen, skin autofluorescence lifetimes are nearly equal, respectively, before irradiation - 1.8 and 6.4 ns, after - 1.7 and 6.4 ns. Uncertainties are 0.1 ns.

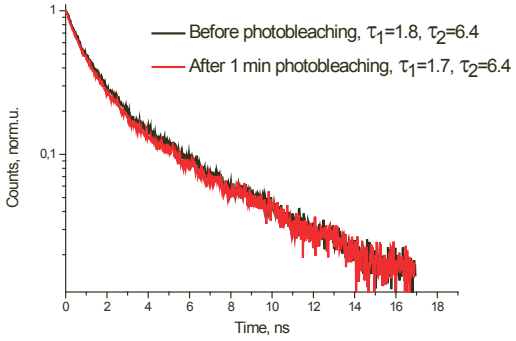

Fig.3 Normalized skin autofluorescence lifetime kinetics before and after 1 min irradiation. 405 nm excitation, signal collected at 500 nm.

4. CONCLUSIONS

Skin autofluorescence lifetime measurements before and after photobleaching show that the photobleaching process doesn't affect the skin autofluorescence lifetime. The unchanged skin autofluorescence lifetime after photobleaching most probably indicates on non photo-chemical intensity decreasing processes during long-

term optical excitation. Which in turn, can be associated with fluorescence mechanical quenching. However, the mechanism of skin photobleaching process is still under discussion and requires additional studies to determine the exact mechanism of this phenomenon.

Acknowledgments

This work was funded by financial support of Taiwan-Latvia-Lithuania research project “Combination of electroporation and sonoporation for efficient drug delivery into cells and tissues for tumor treatment“, “Fotonika-LV – FP7-REGPOT-CT-2011-285912” project and European FP7 project “LaserLab Europe”.

References

[1] Lihachev, A., Spigulis, J., "Skin autofluorescence fading at 405/532 nm laser excitation" IEEE Xplore 10.1109/NO, 63-65 (2007).

[2] Lihachev, A., Lesinsh, J., Jakovels, D., Spigulis, J., "Low power cw - laser signatures on human skin" Quantum Electronics. 40(12), 1077 - 1080 (2010).

[3] Spigulis, J., Lihachev, A., Erts, R., “Imaging of laser-excited tissue autofluorescence bleaching rates”, Applied Optics, 48(10), 163-168 (2009).

[4] Lihachev, A., Rozniece, K., Lesins, J., Spigulis, J., ”Photobleaching measurements of pigmented and vascular skin lesions: results of a clinical trial” Proc. SPIE 8087, 80872F (2011).

[5] Ferulova, I., Lesins, J., Lihachev, A., Jakovels, J., Spigulis, J. "Influence of low power CW laser irradiation on skin hemoglobin changes" Proc. SPIE 8427, 84273I (2012).

[6] Darvin, M.E., Brandt, N.N., Lademann, J., "Photobleaching as a method of increasing the accuracy in measuring carotenoid concentration in human skin by Raman spectroscopy" Opt.Spectr. 109 (2), 205 (2010).

[7] Tuchin, V.V., [Optical Biomedical Diagnostics] Fizmatlit, Moscow, 77 (2007).

[8] Chorvat, D., Jr., Chorvatova, A., "Multi-wavelength fluorescence lifetime spectroscopy: a new approach to the study of endogenous fluorescence in living cells and tissues" Laser Phys. Lett. 6(3), 175–193 (2009).

VIII.

Influence of low power CW laser irradiation on skin hemoglobin changes

Inesa Ferulova, Janis Lesins, Alexey Lihachev, Dainis Jakovels and Janis Spigulis

Institute of Atomic Physics and Spectroscopy, University of Latvia
Raina Blvd. 19, Riga, LV-1586, Latvia
e-mail: inesa.ferulova@gmail.com

ABSTRACT

Influence of low power laser irradiance on healthy skin using diffuse reflectance spectroscopy and multispectral imaging was studied. Changes of diffuse reflectance spectra in spectral range from 500 to 600 nm were observed after 405 nm, 473 nm and 532 nm laser provocation, leading to conclusion that the content of skin hemoglobin has changed. Peaks in spectral absorbance (optical density) curves corresponded to well-known oxy-hemoglobin absorbance peaks at 542 and 577 nm.

Key words: multispectral imaging, laser, diffuse reflectance spectra, optical density, normal skin, hemoglobin

1. INTRODUCTION

Laser irradiation is widely used for skin diagnostics and treatment. It is supposed that low power laser irradiation (<200 mW/cm^2, exposition time up to 10^3 s) is safe for the skin [1]. Higher power densities are used in surgery, dermatology and cosmetology to structurally change the skin [2].

Long-term impact of low-power laser irradiation on normal skin's autofluorescence photobleaching has been observed by means of multispectral imaging camera [3]. The autofluorescence recovery kinetics after preliminary laser irradiation was studied, and the skin autofluorescence images showed pronounced long-term changes –"signatures" of low power laser irradiation [3].

The multi-spectral imaging technique has been used for distant mapping of in-vivo skin chromophores by analyzing spectral data at each reflected image pixel and constructing 2-D maps of the optical density [4]. Point measurements of human skin diffuse reflectance spectra (DRS) contain both absorption and scattering characteristics of tissue and also could be useful for chromophore analysis.

Most probably, photobleaching is caused by degradation of the skin fluorophore molecules. The fluorophores that emit under blue-green excitation are NAD and keratin coferments (localized in epidermis), as well as the dermal collagen and elastin. The reconstructed (NAD-N) and bonded (NAD$^+$) forms of NAD co-ferments have different fluorescence spectra (band maximum at 460 nm and 435 nm, respectively), quantum yields (for NAD-N it is considerably higher), and different times of fluorescence decay (for NAD-N it is lower). However, the mechanism of skin autofluorescence photobleaching is still under study. It is not yet clear how exactly continuous excitation influences endogenous fluorophores of skin. We can assume that cw irradiation of the skin causes a photochemical process that leads to degradation of endogenous fluorophores. [1, 5, 6]. Role of hemoglobin in this process has not been studied so far.

2. EQUIPMENT AND METHODOLOGY

Two methods of skin diffuse reflectance spectra recording were used in the study: the single-spot irradiation/detection by means of fiber optic probe and spectrometer, and the non-contact method by means of multi-spectral imaging system.

Biophotonics: Photonic Solutions for Better Health Care III, edited by Jürgen Popp, Wolfgang Drexler, Valery V. Tuchin, Dennis L. Matthews, Proc. of SPIE Vol. 8427, 84273I
 · doi: 10.1117/12.922601

2.1 Contact method

The contact DRS set-up included light source (10 W halogen lamp, AvaLight-HAL, Avantes BV, NL), detector (the dual channel AvaSpec-2048-2 spectrometer with 2048 pixel CCD detector array, spectral range 200 to 1100 nm, resolution 2.1 nm, Avantes BV, NL), cw low power lasers with wavelengths of 532 nm, 473 nm, 405 nm and fiber optic contact probe.

The contact probe was designed to provide the optimal distance of 3 mm between the skin surface and the optical fiber tip for the sample illumination and signal detection. The optical fibers were connected to illuminating halogen lamp, irradiating laser and detecting spectrometer. DRS of the skin surface was registered as the reference before the irradiation of laser. During 5 second interval reflected spectrum was recorded at 0.5 second integration time calculating the average value. Then skin surface was irradiated for 60 second by a selected laser via the same fiber. The optical density (OD) spectrum of the skin surface was registered immediately after lasers irradiation. Measurements were taken at different laser power density levels ranging from 20 mW/cm^2 to 120 mW/cm^2 each time of another "fresh" skin area.

2.2 Non-contact method

The non-contact method comprised of multi-spectral imaging system Nuance 2.4 (Cambridge Research & Instrumentation, Inc., USA) for response detection, illumination light source, cw low power lasers and PC. Skin areas of the forearm were measured for spectral analysis of normal and provoked skin. A 100 W tungsten incandescent lamp (intensity fluctuations less than ±2% during the measurement time) with linear polarization filter was used as illumination source. The polarizer was oriented orthogonally to the built-in polarizer of the camera, so significantly reducing the influence of skin specular reflection [4, 7].

The system was adjusted for spatial resolution 0.75x0.75 mm (the pixel size) and spectral resolution 10 nm (bandwidth of the Nuance 2.4 liquid crystal tunable filter).

The data were collected in an image cube – a stack of intensity images at numerous wavelength bands. Typical time required for creation of the image cube in spectral interval 450–750 nm was 10 s. The back reflected light intensity (I) values at each pixel were transformed to the optical density OD as

$$\mathrm{OD} = -log_{10}\left(\frac{I}{I_0}\right) \quad (1),$$

where I_0 – reflection intensity of the skin before the laser irradiation, I – intensity after laser irradiation.

Multispectral camera and optical fiber for laser beam delivery to skin surface were set stationary. Measurement lasted about 2 minutes, during this time patient held forearm fixed. Diffuse reflectance spectra were registered before and after laser irradiation of 60 second period. For irradiation lasers of 405 nm and 473 nm wavelength were used. Laser power density was about 120 mW/cm^2 for wavelength of 405 nm and about 100 mW/cm^2 for wavelength of 473 nm.

3. RESULTS

Results of the contact method measurements are presented in Fig.1 – normal skin relative optical density changed immediately after laser irradiation at all exploited wavelengths. One can see that the green 532 nm irradiation does not influence much the DRS signals, but both 473 nm and 405 nm irradiations cause significant signal changes. The most pronounced spectral changes were observed after 405 nm irradiation.

Temporal behavior of optical density changes demonstrated a fast return to the reference level in about 3 minutes after 532 nm laser irradiation. The same tendency was observed if 405 nm and 473 nm lasers were used, but the return time was slightly longer.

Non-contact spectral imaging results of the measurements are presented in Fig.2. The laser irradiated skin areas have less intense DRS resulting in relative optical density changes, as expected.

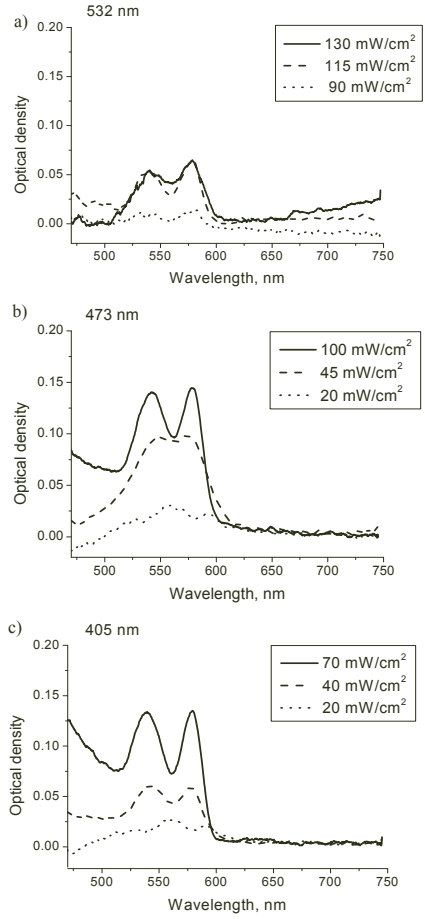

Fig.1. Changes of relative optical density depending on irradiation power density. a) skin was irradiated with cw laser of 532 nm, b) skin was irradiated with cw laser of 473 nm, c) skin was irradiated with cw laser of 405 nm

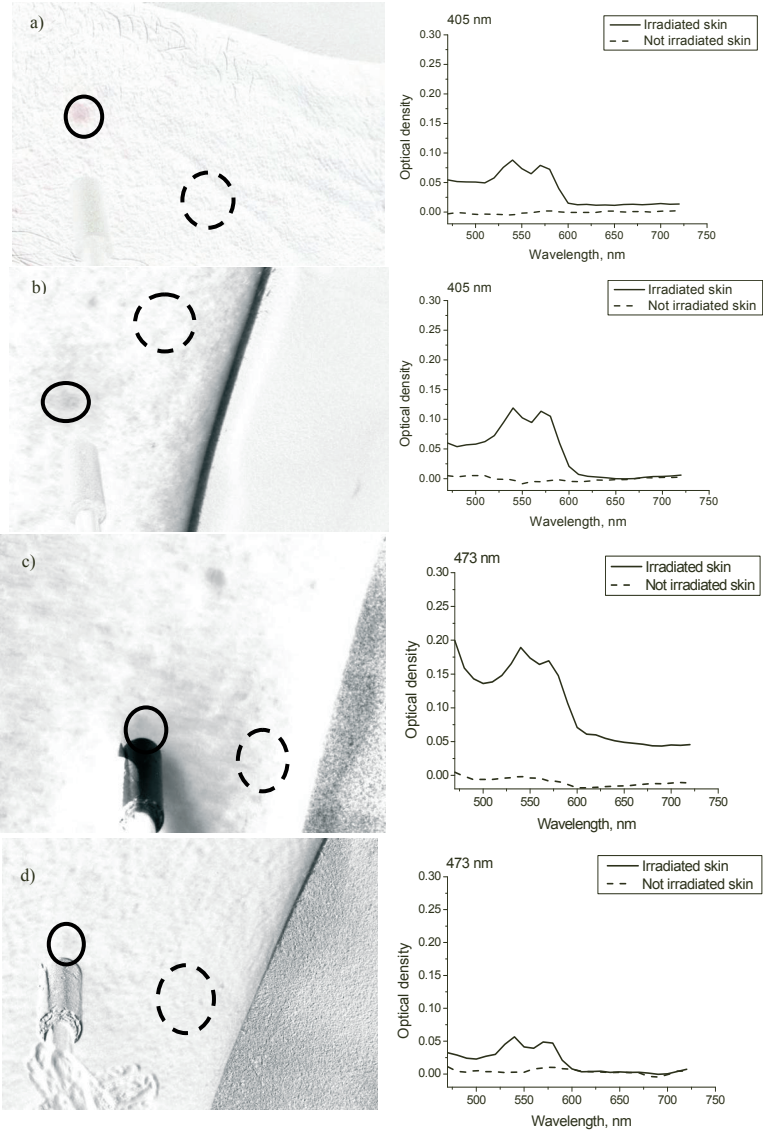

Fig.2. Left-side: multi-spectral images. Right-side: changes of relative optical density of selected areas in images. a), b) skin was irradiated with 405 nm laser; c), d) skin was irradiated with 473 nm laser.

4. DISCUSSION

Impact of low power laser irradiance on healthy skin shows up as dynamic changes of optical properties of tissue. This study provides insight into reflected optical information after AFPB effect, while our previous studies [3, 8] showed changes in optical properties of ongoing AFPB process in skin. The obtained results show that laser irradiation can affect the layers of human skin. Peaks at 542 nm and 577 nm in the relative optical density correspond to absorption of hemoglobin [9]. The same hemoglobin absorption impact were observed in previous study [8] indicating to some role of hemoglobin in the skin AFPB process at the 473 nm irradiation, and the 405 nm laser irradiation probably increases this role while 532 nm laser irradiation shows less significant spectral changes to autofluorescence spectra due to hemoglobin absorption (all laser output powers were adjusted to be approximately equal during the previous experiments).

Temporal behavior of relative OD shows that DRS absorption is a short-term effect – the DRS recovered to its initial level in a few minutes. Although the laser power densities per area unit were the same, for shorter laser wavelength the greater power density per volume unit were present, taking into account wavelength specific optical penetration depth into tissue. This resulted in longer return of OD values to the reference level after skin irradiation of 473 nm and 405 nm lasers. Our previous study [3] showed that autofluorescence recovery kinetics after laser irradiation is a long term effect. As relative restored intensity of autofluorescence after photobleaching is much less than fully restored DRS intensity in few minutes, this indicates to the DRS as a short-term coincidence with skin fluorophore degradation and as well as modification of skin absorption properties by laser irradiation.

Probably, complicate mechanisms of low power laser irradiation may cause direct skin fluorophore (for instance, porphyrin) degradation, as well as modification of absorption and quenching properties by both photo- and thermally-induced biophysical and biochemical processes inside the highly heterogeneous tissue structure. Appearance of hemoglobin absorption in the skin is caused by local fluorophore degradation during optical excitation, thereby increases the probability of light to penetrate to the deeper skin layers, where skin capillaries and vessels are located. Also it is assumed that laser irradiation causes inflammation by local heating and to this place comes more blood in regard to expanded capillaries, as an innate immune system defense of the organism to injurious stimulus. Increased blood volume fraction leads to intense optical absorption in oxyhemoglobin, after laser irradiation the skin locally cools down, so the capillaries narrow to initial size and oxyhemoglobin deoxygenates as the skin proceeds to heal itself.

The average change of the optical density depends on laser irradiation power and excitation laser wavelength. By contact method the change of the OD using laser with wavelength of 532 nm and power density of 120 mW/cm^2 is less than using laser with wavelength of 405 nm, 473 nm and power density of 70 mW/cm^2, 100 mW/cm^2.

Multispectral imaging camera was less sensitive to changes of OD due to spectral resolution of 10 nm and larger distance between skin surface and camera. However, non-contact methodology demonstrated the same features as OD peaks after low power laser-skin interaction compared to acquired results with single point methodology by using higher laser power densities for imaging than for contact method.

The obtained results coincide with the above postulated hypotheses. Fluorophore degradation might allow the light to penetrate the deeper layers of the skin as well as photochemical reactions can cause inflammation and locally increased blood volume as the immune defense.

5. CONCLUSIONS

Skin diffuse reflectance spectra showed increased hemoglobin level after 405nm, 473nm and 532nm cw laser irradiation at power densities around 100 mW/cm^2 (twice below the laser skin safety limit [3]). This indicates to some photo-inflammation; mechanism of erythema creation may be similar to that of sun-caused erythema. Accordingly to the obtained results, visible laser skin safety limits should be lowered at least for an order of magnitude to avoid any photo-biological effects.

Further studies are required to establish a general relationship between the mechanisms of the complex laser-skin interaction and the appearance of hemoglobin absorption after irradiation. Combined experiments involving parallel measurements of skin autofluorescence photo-bleaching and diffuse reflectance spectrometry are planned.

ACKNOWLEDGMENTS

This work was partially funded by the European Social Fund projects No.2009.0211/1DP/1.1.1.1.2.0/09/APIA/VIAA/077 and Nr. 2009/0138/1DP/1.1.2.1.2/09/IPIA/VIAA/004.

6. REFERENCES

[1] IEC 60825-1,"Safety of Laser Products", Part 1: Equipment Classification and Requirements, (2007)
[2] Laser Surgery and Medicine, Ed. A.Carmen, M.D.Puliafito, New York: John Wiley & Sons Inc., (1996).
[3]A.Lihachev, J.Lesinsh, D.Jakovels, J.Spigulis, "Low power cw - laser signatures on human skin", Quantum Electronics. 40(12), 1077 - 1080 (2010).
[4] D. Jakovels, J. Spigulis, "2-D mapping of skin chromophores in the spectral range 500-700 nm" J. Biophoton. 3(3), 125-129 (2010)
[5] M.E Darvin., N.N Brandt., J.Lademann, "Photobleaching as a method of increasing the accuracy in measuring carotenoid concentration in human skin by Raman spectroscopy", Opt.Spectr.. 109 (2), 205 (2010).
[6] V.V.Tuchin, „Optical Biomedical Diagnostics", Fizmatlit, Moscow, 77 (2007)
[7] S. G. Demos , R. R. Alfano, "Optical polarization imaging", App. Opt. 36(1), 150-155 (1997)
[8] J. Lesins, A. Lihachev, R. Rudys, S. Bagdonas, J. Spigulis, "Skin autofluorescence photo-bleaching and photo-memory", Proc. SPIE(8092), 80920N-1 (2011)
[9] http://omlc.ogi.edu/spectra/hemoglobin/

IX.

Lithuanian Journal of Physics, Vol. **52,** No. 1, pp. 55–58 (2012)

PHOTODIODE BASED PROTOTYPE DEVICE FOR SKIN AUTOFLUORESCENCE PHOTOBLEACHING DIAGNOSTICS IN DERMATOLOGY

I. Ferulova [a], A. Rieba [a], J. Lesins [a], A. Berzina [b], A. Lihachev [a], and J. Spigulis [a]

[a] *Institute of Atomic Physics and Spectroscopy, University of Latvia, Raina 19, LV-1586 Riga, Latvia*

E-mail: inesa.ferulova@gmail.com

[b] *Laserplastic Clinic, Baznīcas 31, LV-1010 Riga, Latvia*

Received 27 August 2011; revised 1 February 2012; accepted 1 March 2012

A new portable non-invasive prototype device for skin autofluorescence photobleaching measurements under a 532 nm laser excitation has been developed and clinically tested. The details of the equipment are described along with some measurement results illustrating the potentiality of the technology. Overall, 51 malformations of human skin were investigated by the device.

Keywords: skin, autofluorescence, photobleaching, prototype device, photodiode

PACS:87.64.kv

2. Introduction

Laser radiation is widely exploited in dermatology for diagnostics and treatment of skin diseases, using a wide range of laser wavelengths and radiation powers [1]. The potential of autofluorescence photobleaching (AFPB) for skin clinical diagnostics is of particular interest.

The AFPB is a decrease of fluorescent intensity during optical excitation [2, 3]. The AFPB of human skin has been studied at various pulsed and cw laser excitation wavelengths: ultraviolet (337 nm), violet (405 nm), blue (442 nm), green (532 nm), and red (632 nm) [4]. The temporal behaviour of the skin AFPB can be well described by the double exponential equation (1), where the parameters τ_1 and τ_2 characterise the fast and slow phases of AFPB, and A is a background level of intensity I [5, 6]:

$$I(t) = A + A_1\exp(-t/\tau_1) + A_2\exp(-t/\tau_2). \qquad (1)$$

The results of clinical studies showed that parameter τ_1 significantly differs between healthy skin and skin with pathologies of the same person. Our previous research proved that the increased content of melanin in the skin slows down the AFPB process under the green laser 532 nm excitation [4, 5, 7]. The AFPB might have a promising potential for skin clinical diagnostics.

In this paper a newly developed prototype device is described. It comprises a built-in photodiode for the skin autofluorescence (AF) detection instead of the previously used spectrometry set-up [4, 7]; such design simplifies detection and would reduce the costs of production.

2. Method and equipment

A continuous low power laser irradiation is used for the skin AF excitation at a visible wavelength of 532 nm. A set-up scheme of the prototype device is presented in Fig. 1. The skin AF is excited by a low power DPSS 532 nm laser (*Huanic* DD532-10-3) with output power density being 32 mW/cm^2. The intensity of AF is detected by a silicon photodiode (OPT101) with an amplifier registered by a 16-channel voltage data logger (PicoLog 1216) and saved at a laptop computer. A combination of 2 long pass filters

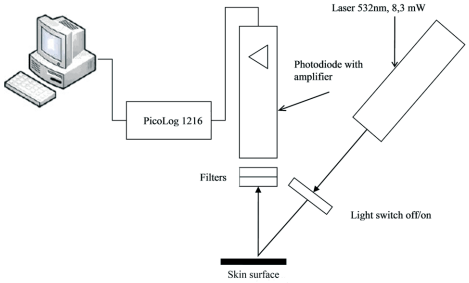

Fig. 1. A set-up scheme of the prototype device.

in front of the photodiode, *Semrock* BLP01-532R and *Eksma* OG570/KG3, is ensuring a transmission window between 550 and 650 nm in order to record the integral intensity of the laser induced skin AF of this wavelength range. The distance between the skin surface and the filters is 3 mm. The photodiode is installed orthogonally to the skin surface, and the exciting laser beam forms a 45° slope angle to the skin surface. The AFPB data of skin pathology is recorded for about 30 s (signal integration time is 1 ms), and then the AF of healthy skin near pathology is measured for comparison. The prototype device provides the ambient light isolation during the measurements, reducing the background noise.

3. Results

Overall, 51 patients in the Riga Laserplastic Clinic were investigated by means of the portable non-invasive prototype device (Fig. 2). The safety and well-being of patients involved in a clinical trial were provided according to permission of the local ethics committee. The initial AF intensity of healthy skin near pathology was always higher than AF intensity of pathological skin. The AF intensity of a healthy skin area was equally high in all cases, but the AF intensity for various pathologies was notably lower according to the degree of pigmentation. The pathologies were classified into two groups, of high and of low pigmentation. The ratio between the initial AF intensity of healthy skin and the AF intensity of high pigmentation pathologies was distributed within the interval of 2.3–4.8, and of low pigmentation pathologies within the interval of 1.2–1.7.

The recorded AFPB data were analysed and the parameters of Eq. (1) were calculated by fitting. For illustration, the AFPB time series taken from healthy skin, pigmented nevus and melanoma are presented in Fig. 3, along with photobleaching parameters. The AFPB effect was not observed on high pigmentation pathologies during 30 s of measurement. In case of pigmentation pathology the value of parameter τ_1 was always relatively higher than its value for healthy skin of the same person.

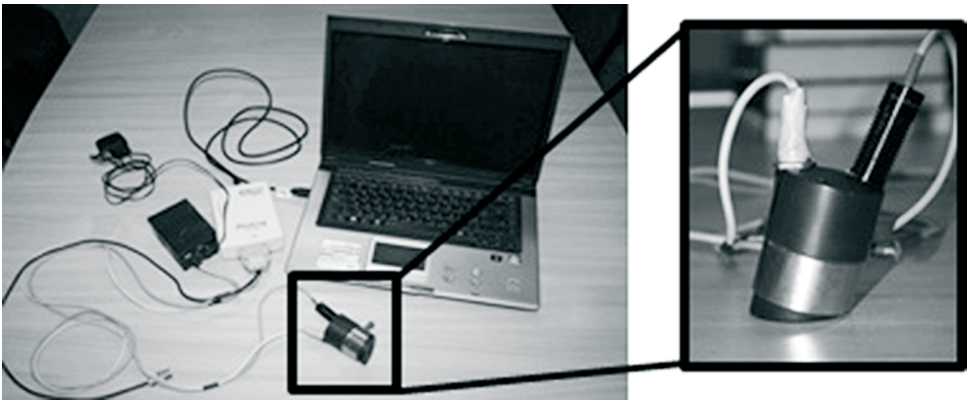

Fig. 2. View of the photodiode based prototype device set-up (left) and the zoomed prototype device (right).

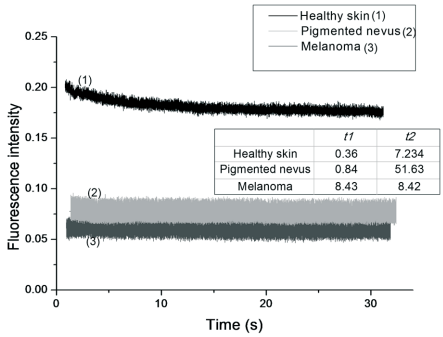

Fig. 3. AFPB time dependence taken from healthy skin and pigment nevus, with the corresponding photobleaching parameters (*t1, t2* correspond to τ_1 and τ_2)

The results obtained with the prototype device showed AF intensity bleaching by 8%, while previous studies with the spectrometry set-up proved AFPB up to 30% (in 30 seconds). The AFPB dependence on the equipment integration time was compared (Fig. 4) for the purpose of device testing. Significantly reducing the integration time of the spectrometer, the changes of AFPB dynamics were similar to the results of photodiode based device measurements.

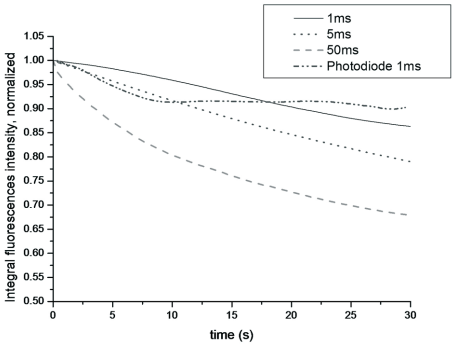

Fig. 4. AFPB at various integration times of the spectrometer and photodiode, taken from healthy skin.

4. Conclusions

A prototype device for skin AF recording was produced and clinically tested. Overall, 51 persons with pigmented skin pathologies were investigated by a new prototype device. AF intensity values and temporal changes of fluorescent intensity can be recorded by the prototype device, with subsequent calculation of relative changes and photobleaching parameters (τ_1, τ_2, A). Analysis of the clinical trial data showed that the device should be further improved in order to increase the signal-to-noise ratio and to fully avoid registration of the scattered laser radiation. Further investigations will focus on the device integration time adjustment based on changes in representation of AFPB dynamics.

Acknowledgments

This work was partially funded by the European Social Fund project No. 2009.0211/1DP/1.1.1.1. 2.0/09/APIA/VIAA/077FP7 and the EC FP7 project "Laserlab-Europe" (JRA4 OPTBIO), contract No. 228334.

References

[1] A. Carmen and M.D. Puliafito(eds.), *Laser Surgery and Medicine* (John Wiley & Sons Inc., New York, 1996).

[2] Y.P. Sinichkin, N. Kollias, G.I. Zonios, S.R. Utz, and V.V. Tuchin, Reflectance and fluorescence spectroscopy of human skin in-vivo, in: *Handbook of Optical Biomedical Diagnostics*, ed. V.V. Tuchin (SPIE Press, 2002) pp. 725–785.

[3] E.V. Salomatina and A.B. Pravdin, Fluorescence dynamics of human epidermis (*ex vivo*) and skin (*in vivo*), Proc. SPIE **506b**, 405–410 (2003).

[4] A. Lihachev and J. Spigulis, Skin autofluorescence fading at 405/532 nm laser excitation, IEEE Xplore **10.1109/NO**, 63–65 (2007).

[5] A. Lihachev, J. Spigulis, and R. Erts, Imaging of laser-excited tissue autofluorescence bleaching rates, Appl. Opt. **48**(10), D163–D168 (2009).

[6] A. Stratonnikov, V. Polikarpov, and V. Loschenov, Photobleaching of endogenous fluorochroms in tissues in vivo during laser irradiation, Proc. SPIE **4241**, 13–24(2001).

[7] A. Lihachev, J. Lesinsh, D. Jakovels, and J. Spigulis, Low power cw-laser signatures on skin, Quant. Electron. **40**(12), 1077–1080 (2010).

Fotodiodinio įtaiso prototipas odos autofluorescencinei fotoišbalinimo diagnostikai dermatologijoje

I. Ferulova [a], A. Rieba [a], J. Lesins [a], A. Berzina [b], A. Lihachev [a], J. Spigulis [a]

[a] *Latvijos universiteto Atominės fizikos ir spektroskopijos institutas, Ryga, Latvija*

[b] *Lazerinės plastikos klinika, Ryga, Latvija*

Santrauka

Sukurtas ir kliniškai išbandytas naujas prototipinis nešiojamas neinvazinis įrenginys, skirtas odos autofluorescenciniam fotoišbalinimui matuoti, naudojant 532 nm lazerio žadinimą. Pateiktas smulkus įrangos aprašas ir kai kurie matavimo rezultatai, iliustruojantys šio būdo galimybes. Iš viso šiuo prietaisu ištirtas 51 žmogaus odos probleminis darinys.